ISTITUTO NAZIONALE DI FISICA NUCLEARE

Sezione di Genova

W.M. Alberico, R. Cenni, A. Molinari:

PROBING THE NUCLEUS

PROBING THE NUCLEUS

W. M. ALBERICO[†], R. CENNI[‡], A. MOLINARI[†]

† – *Dipartimento di Fisica Teorica – Università di Torino
and I.N.F.N. – Sezione di Torino – Italy*
‡ – *I.N.F.N. – Sezione di Genova – Italy
Dipartimento di Fisica – Università di Genova*

ABSTRACT

A review is presented of the perturbative, variational and functional approaches to the nuclear response functions. The charge and spin (both transverse and longitudinal) responses to electromagnetic and hadronic probes are explored. The relativistic and subnucleonic aspects of the problem are also shortly addressed.

1. INTRODUCTION

In this report we shall be concerned with the response of the nucleus to an external probe. This topic "stricto sensu" would cover essentially the whole of nuclear physics and one is thus forced to make an "a priori" selection of the themes to be treated: our choice will be largely focussed on nuclear physics at intermediate energies.

Of course, even in this restricted sense, we have no pretence of offering a complete presentation of the subject; rather we shall deal with some aspects of the nuclear responses which, in our view, illustrate the richness of the field, what have we learned

in exploring it and where do the problems confronting us lie. Such an approach is obviously bound to reflect our own experience and also our general conceptual attitude toward this area of physics. This is reflected in the attempt of casting the formal treatment of the nuclear response functions not only in the frame of the old, but also of the modern Quantum Field Theory (QFT).

For the future developments of nuclear physics and for properly describing the data which will be supplied by the next generation of accelerators, it appears necessary to utilize a theoretical framework encompassing the structure of the nuclear constituents beyond the one of the nucleus itself. Indeed, by exploring the nucleus with larger and larger energies it has gradually been realized that, at the level of nuclear structure, nature works on a more microscopic basis of what it has been conventionally assumed in dealing with the low energy nuclear spectra. As a consequence the traditional distinction between particle and nuclear physics appears more and more obsolete.

Accordingly this report is organized as follows. In Section 2 the general formalism of the linear response theory is outlined in the functional framework.

In Section 3 we discuss the perturbative approach to the polarization propagator Π and, shortly, a few aspects of the variational one, both for infinite nuclear matter and for finite nuclei.

In Section 4 we shall deal with the nuclear response to an external electromagnetic field, considering the charge longitudinal as well as the transverse response. Also the role of the meson exchange currents (MEC) will be illustrated.

In Section 5 the nuclear responses to hadronic probes will be investigated, the emphasis being on the "surface RPA" (random phase approximation) approach.

In Section 6 we shall be concerned with the relativistic aspect of the nuclear response and we shall extend our investigation to the so–called EMC and cumulative effects. In this connection the relationship between the nuclear and the nucleon structure functions (the alternative name for the response functions) will be discussed.

Finally, in Section 7, we shall address the path integral formulation of the nuclear response theory. In our view this method offers the best perspectives to obtain a consistent description of how the nuclear system responds to an external probe, especially in order to fulfill general requirements as gauge invariance and relativistic covariance.

2. GENERAL FORMALISM OF THE LINEAR RESPONSE THEORY

In this section we shall treat the response of the nucleus to an external perturbation. If the latter is assumed to be weak then a linearized theory is both adequate and workable. To build the framework of such a theory let us start from a nuclear hamiltonian (without specifying whether it is relativistic or not, expressed in QFT or in potential theory) with the associated eigenvalues equation

$$\hat{H}|\psi_n >= E_n|\psi_n > \quad . \tag{2.1}$$

We now let the nucleus to be coupled with a "classical" external field $\phi(x)$ (or, in general, with a set of external fields) carrying some bosonic quantum numbers and vanishing sufficiently rapidly at infinite times. Then the time evolution of the system will be ruled by the new hamiltonian

$$\hat{H}'[\phi] = \hat{H} + \int dx \, \hat{j}(x)\phi(x) \tag{2.2}$$

where x is a four-vector and the nuclear degrees of freedom are embedded in the operator $\hat{j}(x)$, expressed in the Heisenberg picture.

The actual form of $\hat{j}(x)$ obviously depends upon the problem one deals with. Thus, e.g., for the response of the nucleus to an external pionic field, then $\phi(x)$ will just be a classical isovector field and the axial isovector density of the nucleon

$$\hat{j}_A(x) = i\bar{\psi}(x)\gamma_5\boldsymbol{\tau}\psi(x) \tag{2.3}$$

will be the one to be considered (eventually in the non–relativistic limit). For the response to an electromagnetic field then $\phi(x)$ will coincide with the standard four-potential $\mathcal{A}_\mu$ and $\hat{j}(x)$ with the nucleonic vector current, namely

$$\hat{j}_\mu(x) = \bar{\psi}(x)\gamma_\mu \frac{1+\tau_3}{2}\psi(x) \tag{2.4}$$

or with the corresponding non relativistic version. Note the use of a ˆ to indicate quantal operators in order to avoid confusion with classical quantities. For the Hamiltonian (2.2) the evolution operator is

$$U_\phi(t,t') = T \exp\left\{-i \int_{t'}^{t} dx_0 \int dx \, \hat{j}(x)\phi(x)\right\} \tag{2.5}$$

T being the chronological product and the subscript ϕ reminding the functional dependence of the evolution operator upon the external field.

Now, although $U_\phi(t, t')$ embodies the whole physics concerning the nucleus, including its interaction with an external probe, and its knowledge is sufficient in deriving the linear response theory, we prefer, for the same purpose, to utilize the generating functional

$$Z[\phi] = < \Psi_0|U_\phi(\infty, -\infty)|\Psi_0 > \ , \qquad (2.6)$$

the expectation value being taken in the exact nuclear ground state.

The physical content of $Z[\phi]$ is transparently displayed by its functional derivatives with respect to ϕ (more exactly, by the coefficients of its Volterra expansion), which read

$$Z[0] = < \Psi_0|\Psi_0 > \qquad (2.7)$$

$$\frac{\delta Z[\phi]}{\delta \phi(x)}\Big|_{\phi=0} = -i < \Psi_0|\hat{\jmath}(x)|\Psi_0 > \qquad (2.8)$$

$$\frac{\delta^2 Z[\phi]}{\delta \phi(x)\delta \phi(y)}\Big|_{\phi=0} = (-i)^2 < \Psi_0|T[\hat{\jmath}(x)\hat{\jmath}(y)]|\Psi_0 > \ . \qquad (2.9)$$

Thus the first functional derivative just yields the mean value of $\hat{\jmath}(x)$, the second is closely connected to the well–known polarization propagator and the third one is related to the three–particle Green's function.

Concerning the polarization propagator we remind that it is usually defined with the term $< \Psi_0|\Psi_0 >$ in the denominator, for the purpose of cancelling the disconnected (divergent) diagrams in the perturbative expansion. The same goal is achieved in the generating functional framework via the introduction of the new functional Z_c defined as

$$Z[\phi] = \exp\{iZ_c[\phi]\} \qquad (2.10)$$

which generates connected diagrams only (hence the subscript c) and obeys the relations

$$Z_c[0] = 0 \qquad (2.11)$$

$$\frac{\delta Z_c[\phi]}{\delta \phi(x)}\Big|_{\phi=0} = -\frac{< \Psi_0|\hat{\jmath}(x)|\Psi_0 >}{< \Psi_0|\Psi_0 >} \qquad (2.12)$$

$$\frac{\delta^2 Z_c[\phi]}{\delta \phi(x)\delta \phi(y)}\Big|_{\phi=0} = i\Bigg\{ \frac{< \Psi_0|T[\hat{\jmath}(x)\hat{\jmath}(y)]|\Psi_0 >}{< \Psi_0|\Psi_0 >}$$

$$- \frac{< \Psi_0|\hat{\jmath}(x)|\Psi_0 >}{< \Psi_0|\Psi_0 >}\frac{< \Psi_0|\hat{\jmath}(y)|\Psi_0 >}{< \Psi_0|\Psi_0 >} \Bigg\}. \qquad (2.13)$$

By introducing then the standard current deviation operator:

$$\tilde{\jmath}(x) = \hat{\jmath}(x) - \frac{< \Psi_0|\hat{\jmath}(x)|\Psi_0 >}{\Psi_0|\Psi_0 >} \qquad (2.14)$$

it is an easy matter to verify that (2.13) can be recast as to exactly reproduce the standard form of the polarization propagator, namely

$$\left.\frac{\delta^2 Z_c[\phi]}{\delta\phi(x)\delta\phi(y)}\right|_{\phi=0} = i\frac{<\Psi_0|T[\hat{\jmath}(x)\hat{\jmath}(y)]|\Psi_0>}{<\Psi_0|\Psi_0>} = -\Pi(x,y|j). \tag{2.15}$$

The physical meaning of Π, the fundamental theoretical tool to deal with the nuclear responses, is best illustrated by exploring how the average value of an operator (in the present case $\hat{\jmath}(x)$) is altered by the presence of an external classical field, which we assume to be weak. Then the expansion

$$\frac{<\Psi_0|\hat{\jmath}(x)|\Psi_0>}{<\Psi_0|\Psi_0>} = \left.\frac{<\Psi_0|\hat{\jmath}(x)|\Psi_0>}{<\Psi_0|\Psi_0>}\right|_{\phi=0}$$

$$+ \int dy \left.\frac{\delta}{\delta\phi(y)}\frac{<\Psi_0|\hat{\jmath}(x)|\Psi_0>}{<\Psi_0|\Psi_0>}\right|_{\phi=0}\phi(y) + \mathcal{O}(\phi^2) \tag{2.16}$$

$$= <\hat{\jmath}(x)>|_{\phi=0} + \int dy\, \Pi(x,y|j)\phi(y) + \mathcal{O}(\phi^2) \tag{2.17}$$

is justified and transparently shows that the small fluctuations of the expectation value of $\hat{\jmath}(x)$ around its unperturbed value are indeed described by Π.

Furthermore, once the latter is known, one can derive in the context of the linear response theory the inelastic inclusive cross section for the scattering of an external probe off the nuclear target. To illustrate this result, sometimes referred to as the fluctuation–dissipation theorem, let us consider as an example the case of the pion, assuming the following interaction Lagrangian

$$\mathcal{L}_I = ig\bar{\psi}(x)\gamma_5\tau\psi(x)\cdot\phi(x) = g\hat{\jmath}_A\cdot\phi. \tag{2.18}$$

Then the total inclusive cross section for absorbing a pion with momentum q on a nucleus, *at the lowest order* in the coupling constant g, reads

$$\sigma_{\text{incl}} = 2\pi g^2 \sum_n |<\Psi_0|\hat{\jmath}_A(q)|\Psi_n>|^2\delta(E_n - E_0 - \omega_q) \tag{2.19}$$

with $\omega_q = \sqrt{q^2 + m_\pi^2}$ (the occurrence of $\hat{\jmath}_A(q)$, instead of $\hat{\jmath}_A(q)$, the Fourier transform of (2.3), reflects the absence of elastic processes). Now Π, in momentum space, can be cast in the form

$$\Pi(q,\omega) = <\Psi_0|\hat{\jmath}_A(q)\frac{1}{\omega - \hat{H} + E_0 + i\eta}\hat{\jmath}_A(q)|\Psi_0>$$

$$+ <\Psi_0|\hat{\jmath}_A(q)\frac{1}{\omega + \hat{H} - E_0 - i\eta}\hat{\jmath}_A(q)|\Psi_0> \tag{2.20}$$

and the Lehmann representation of the first (retarded) term of the above equation reads

$$\Pi_{\text{ret}}(q,\omega) = \sum_n \frac{|<\Psi_0|\bar{j}_A(q)|\Psi_n>|^2}{\omega - E_n + E_0 + i\eta} \quad . \tag{2.21}$$

Hence, since the advanced part of (2.20) is purely real for $\omega > 0$, one immediately finds the connection

$$\sigma_{\text{incl}} = -\frac{g^2}{\pi}\text{Im}\Pi(q,\omega_q) \tag{2.22}$$

between Π and the cross section.

This procedure holds valid in general for absorbed particles on and off the mass shell (the latter case corresponding to a photon emitted by an electron or a pion emitted by a proton or a heavy ion). Obviously, for the situations corresponding to the exchange of a virtual particle, the amplitude $< \Psi_0|\bar{j}(q)|\Psi_n >$ should be implemented with the contribution arising from the vertex associated with the external probe and from the propagator of the exchanged quantum. This turns out to be basically disconnected from the nuclear dynamics in the non–relativistic regime and for not too strongly interacting probes. Accordingly, the formula

$$\sigma_{\text{incl}} = -\sigma_0(q,\omega_q)\frac{g^2}{\pi}\text{Im}\Pi(q,\omega_q) \tag{2.23}$$

can be used with σ_0, a real function in principle under control, embodying all the informations concerning the non–nuclear part of the cross section. Unfortunately relativity complicates such a picture and strongly interacting probes require as well a more elaborate treatment (these points will be more closely examined in the Sections 5 and 6).

In general the linear response theory can be safely applied to the cases where the nucleus absorbs one particle only: in this case the nuclear responses are fully engrained into the polarization propagator. If more than one particle is absorbed then linearity is lost and higher order Green's functions are needed to properly describe how the system has been perturbed by the coupling with the strongly interacting probe.

3. CALCULATION OF Π

In this section we address the problem of the actual calculation of the polarization propagator Π. First we consider nuclear matter whose simple geometry (reflected in the translational invariance of the system) substantially helps in simplifying the calculations. It becomes thus possible to reach a high degree of sophystication in the treatment of the polarization propagator Π, both in the perturbative as well as

in the variational framework, hardly obtainable in the case of finite nuclei. We shall deal with the latter in the second part of this section.

3.1 Nuclear Matter

To start with let us consider the Fermi gas, a system characterized by a single physical parameter, namely the Fermi momentum k_F. The associated polarization propagator reads (see for instance Fetter and Walecka, 1971)

$$\Pi^0(\mathbf{q}, \omega) = -\frac{i}{\hbar} \int d^4 k\, G_0(k+q) G_0(k) \tag{3.1}$$

and the non interacting single particle Green's function is

$$G_0(k) = \frac{\theta(|\mathbf{k}| - k_F)}{k_0 - \omega_\mathbf{k} + i\eta} + \frac{\theta(k_F - |\mathbf{k}|)}{k_0 - \omega_\mathbf{k} - i\eta} \tag{3.2}$$

where $\omega_\mathbf{k} = \hbar \mathbf{k}^2 / 2M$ (k stands for a four momentum and M is the nucleon mass). Upon integration one obtains for the imaginary part of (3.1) the expression (Alberico et al., 1989)

$$
\begin{aligned}
\mathrm{Im}\Pi^0(q, \omega) &= -\frac{M}{4\pi\hbar^2 q} \int_{k_F \psi_{nr}}^{\infty} dk\, k\, \theta(k_F - k)\theta(|\mathbf{q} + \mathbf{k}| - k_F) \\
&= -\frac{M k_F{}^2}{8\pi\hbar^2 q} \left\{ \frac{2M\omega}{\hbar k_F{}^2} \theta(\omega)\theta(1 - \psi_{nr} - \frac{q}{k_F}) + \right. \\
&\quad \left. + (1 - \psi_{nr}^2)\theta(1 - \psi_{nr}^2)\theta(\frac{q}{k_F} - 1 + \psi_{nr}) \right\}
\end{aligned}
\tag{3.3}
$$

where

$$\psi_{nr} = \frac{1}{k_F}\left(\frac{M\omega}{\hbar q} - \frac{q}{2} \right) = \frac{y}{k_F} \tag{3.3a}$$

will be later referred to as the non–relativistic *scaling* variable, constrained by the limits:[1])

$$-1 \le \frac{y}{k_F} \le 1. \tag{3.3b}$$

It thus appears that
  i) even for a non–interacting system like the Fermi gas, Π^0 embeds correlations of statistical nature among the nucleons (referred to as Pauli correlations),

---

[1]) The scaling variable has been originally introduced by West (1975) with the letter y, which we shall mantain in the non–relativistic responses.

ii) for $q \geq 2k_F$, the quantity $q \operatorname{Im}\Pi^0(q,\omega)$ is no longer a function of momentum and energy separately, but only of the single variable ψ_{nr},

iii) physically y corresponds to the minimum momentum a nucleon can have inside the system without violating the energy conservation.

By proceeding further, one faces two problems:
  a) which interaction should be switched on,
  b) which theoretical framework should be used.

In this paper we will not dwell on point a): we shall simply utilize effective or realistic (and meson carried) NN interactions whenever necessary, referring to the literature for critical discussions. Now, instead, we tackle point b) by considering perturbation theory.

The general perturbative scheme

In first order six Feynman diagrams (displayed in Fig. 3.1) are contributing to the polarization propagators. They correspond to the direct and exchange self–energy dressing (a,b,c and d) and to the direct and exchange first–order fermion-fermion interaction (e and f). When iterated up to infinite order these diagrams build up the Hartree–Fock (HF) mean field and the random phase approximation (RPA) correlations, respectively. Noteworthy, the seeds of these two key elements of the nuclear responses are the only ones appearing in the first order.
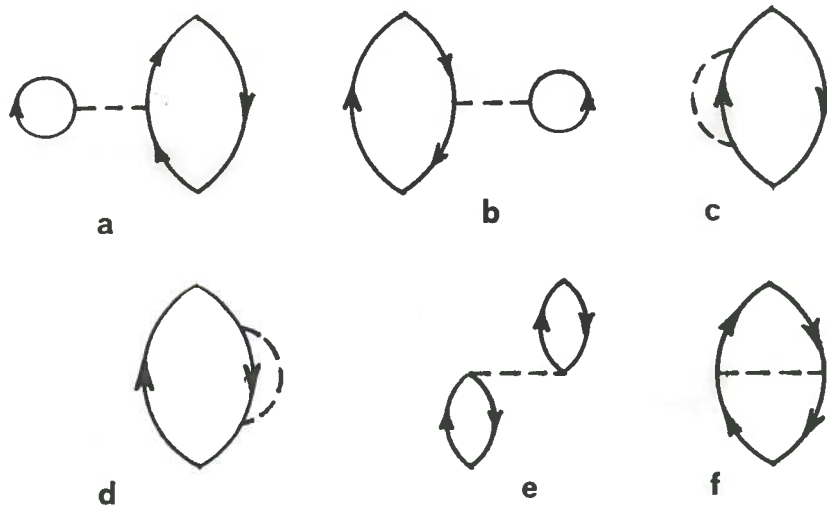

Fig. 3.1 – Diagrams representing the polarization propagator Π in the first–order perturbation theory.

Going to second order, the proliferation of diagrams becomes impressive as we shall see in the next subsection. Thus the perturbative approach, already on shaky ground since a small expansion parameter is missing for a dense strongly interacting many–body system, does also seriously challenge even the present days computational capabilities.

The idea is then to sum up infinite classes of diagrams and this is done for the already mentioned HF and RPA frameworks through the corresponding well-known equations, and for the ladder diagrams through the Bethe-Goldstone equation. Thus, given a two–body realistic nucleon-nucleon (NN) interaction, one could, in principle, account for the mean field (HF), long (RPA) and short (ladder) range correlations in the nuclear responses.

To illustrate the virtues and the limitations of these approximation schemes for the nuclear responses it is convenient to consider the particle–hole propagator

$$G_{\alpha\beta,\gamma\delta}^{\mathrm{ph}}(x_1, x_2; x_1', x_2') = \frac{< \Psi_0|T\{\hat{\psi}_{H\beta}^{\dagger}(x_2)\hat{\psi}_{H\alpha}(x_1)\hat{\psi}_{H\gamma}^{\dagger}(x_1')\hat{\psi}_{H\delta}(x_2')\}|\Psi_0 >}{< \Psi_0|\Psi_0 >}$$
$$- G_{\alpha\beta}(x_1, x_2)G_{\delta\gamma}(x_1', x_2'), \tag{3.4}$$

which is simply linked to the polarization propagator through the relation

$$\Pi(x, x') = \frac{i}{\hbar}G_{\alpha\alpha,\beta\beta}^{\mathrm{ph}}(x, x; x', x') \tag{3.5}$$

in coordinate space and

$$\Pi(q) = \frac{i}{\hbar} \int \frac{d^4p}{(2\pi)^4} \frac{d^4k}{(2\pi)^4} \, G_{\alpha\alpha,\beta\beta}^{\mathrm{ph}}(k+q, k; p+q, p), \tag{3.6}$$

in momentum space. Again the denominator in (3.4) is just for the purpose of cancelling disconnected diagrams and G is meant to be the *exact* single–particle propagator.

Now perturbation theory allows to write the following general expression for the polarization propagator

$$\Pi(q) = -\frac{i}{\hbar} \int \frac{d^4p}{(2\pi)^4} \Big\{ G_{\alpha\beta}(p+q)\, G_{\beta\alpha}(p) \tag{3.7}$$

$$- \frac{i}{\hbar} \int \frac{d^4k}{(2\pi)^4} G_{\alpha\lambda}(p+q)G_{\lambda'\alpha}(p)\Gamma_{\lambda\mu,\lambda'\mu'}(p+q, k; p, k+q)G_{\beta\mu}(k)G_{\mu'\beta}(k+q) \Big\},$$

in terms of the fully reducible four-points vertex function Γ and of the single–particle Green's function G (here and in the following indices denote spin–isospin variables).
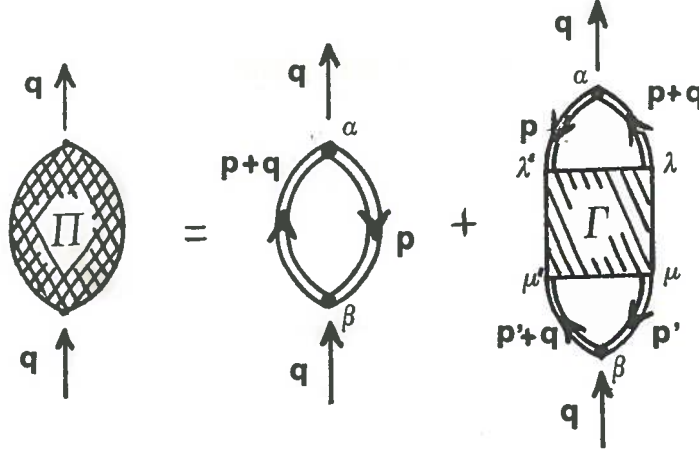
Fig. 3.2 - Graphical representation of eq. (3.7) for the polarization propagator in momentum space. The arrows show the four–momentum flow.

Equation (3.7) is diagrammatically illustrated in Fig. 3.2. Therefore the calculation of Π is based on the calculation of Γ and we shortly outline here how the evaluation of the latter can be achieved.

In lowest order Γ merely corresponds to the bare direct and exchange NN interaction according to the formula

$$\Gamma^0_{\lambda\lambda',\mu\mu'}(p,p_1;p_2,p+p_1-p_2) = \delta_{\lambda\lambda'}\,\delta_{\mu\mu'}\,U(p-p_2) - \delta_{\lambda\mu'}\,\delta_{\mu\lambda'}\,U(p_2-p_1) \quad (3.8)$$

where, for the sake of simplicity, a spin–isospin independent NN interaction U is assumed.

To proceed further it is important to realize that the four points of Γ identify in fact three different channels (see, e.g., Blaizot and Ripka, 1986), namely a particle–particle (Γ^{12}) and two particle–hole (Γ^{13} and Γ^{14}) ones. More precisely Γ^{12} corresponds, in lowest order, to the bare NN force, and, in general, it includes all the diagrams describing the NN interaction irreducible with respect to the cutting of two particle propagation lines. In other words a given diagram contributing to Γ^{12} is irreducible when it cannot be split into a part containing the lines $\{1,2\}$ and a part containing the lines $\{3,4\}$ only. Analogous definitions hold as well in the other two particle–hole (p–h) channels.

On the basis of this classification, in each channel an equation of the type

$$\Gamma = \Gamma^{ij} - \Gamma^{ij}GG\Gamma \quad (3.9)$$

can be shown to hold valid. The solution of (3.9), for a given perturbative approximation to Γ^{ij}, yields Π when inserted into (3.7). The Γ thus obtained turns out, however, to violate basic requirements of the theory, e.g. the antisymmetry.

To avoid such a shortcoming three coupled equations should be introduced, namely

$$\Gamma^{12} = \Gamma^N - \Gamma^{13}GG\Gamma - \Gamma^{14}GG\Gamma$$

$$\Gamma^{13} = \Gamma^N - \Gamma^{14}GG\Gamma - \frac{1}{2}\Gamma^{12}GG\Gamma \qquad (3.10)$$

$$\Gamma^{14} = \Gamma_N - \Gamma^{13}GG\Gamma - \frac{1}{2}\Gamma^{12}GG\Gamma,$$

Γ^N being the set of the diagrams irreducible with respect to all the three previously defined channels (in other words Γ^N represents the intersection of the ensembles of the diagrams Γ^{ij}). It can then be proved that the simultaneous solution of (3.9) and (3.10) (hard to obtain as it might be) would provide the correct, symmetry respecting, Γ. The latter, inserted into (3.10), would in turn yield the exact nuclear response.

But in addition one can prove that any perturbative approximation to the ensemble Γ^N leads to a Γ still preserving the basic symmetry requirements of the theory: the equations thus obtained are commonly referred to as "parquet equations" (Jackson et al., 1982).

An alternative path to the evaluation of the nuclear responses resorts directly to the integral equation, originally derived by Galitskii and Migdal (Galitskii and Migdal, 1958; Pines, 1962), for the p–h propagator

$$G^{\mathrm{ph}}_{\alpha\beta,\gamma\delta}(k+q,k;p+q,p) = -G_{\alpha\gamma}(p+q)G_{\delta\beta}(p)(2\pi)^4\delta(k-p) \qquad (3.11)$$

$$+ \frac{i}{\hbar}G_{\alpha\lambda}(k+q)G_{\lambda'\beta}(k)\int\frac{d^4t}{(2\pi)^4}\Gamma^{13}_{\lambda\lambda',\mu\mu'}(k+q,k;t+q,t)G^{\mathrm{ph}}_{\mu\mu',\gamma\delta}(t+q,t;p+q,p).$$

Note that Γ^{13} is precisely the same quantity appearing in the parquet equations (3.10) and that, beyond (3.11), two other integral equations can be established for the two–fermion Green's functions in the channels $\{12\}$ and $\{14\}$.

A common and simple approximation to (3.11) retains the lowest order for Γ^{13} only (i.e. the bare p–h interaction) and in addition neglects the exchange term. Utilizing then the single–particle Green's function G in the HF approximation, (3.11) reduces to:

$$G^{\mathrm{ph(r)}}_{\alpha\beta,\gamma\delta}(k+q,k;p+q,p) = -G^{\mathrm{HF}}_{\alpha\gamma}(p+q)G^{\mathrm{HF}}_{\delta\beta}(p)(2\pi)^4\delta(k-p)$$

$$+ \frac{i}{\hbar}G^{\mathrm{HF}}_{\alpha\lambda}(k+q)G^{\mathrm{HF}}_{\lambda'\beta}(k)U^{\mathrm{ph(d)}}_{\lambda\lambda',\mu\mu'}(q)\int\frac{d^4t}{(2\pi)^4}G^{\mathrm{ph(r)}}_{\mu\mu',\gamma\delta}(t+q,t;p+q,p)$$

$$(3.12)$$

where the superscript (r) reminds the *ring* structure of the diagrams summed up by the above equation.

By integrating over the variables k and p, according to (3.6), one finally arrives at

$$\Pi^{(r)}(q) = \Pi^{\mathrm{HF}}(q) + \Pi^{\mathrm{HF}}(q)\mathrm{U}(q)\Pi^{(r)}(q), \qquad (3.13)$$

Π^{HF} being the HF polarization propagator. The above (3.13) is the well–known algebraic (for nuclear matter) equation for the polarization propagator in the ring approximation, which is frequently exploited to get an orientation on the nuclear responses to external fields.

The second order polarization propagator

A comprehensive classification and treatment of the diagrams contributing to Π in the second order of perturbation theory has been recently carried out by De Pace and Drago (1989). Without entering in details, we simply illustrate here the second order contributions of relevance for the nuclear responses closely following the analysis of these authors. Indeed there is a growing consensus on the importance of such terms in shaping the nuclear response.
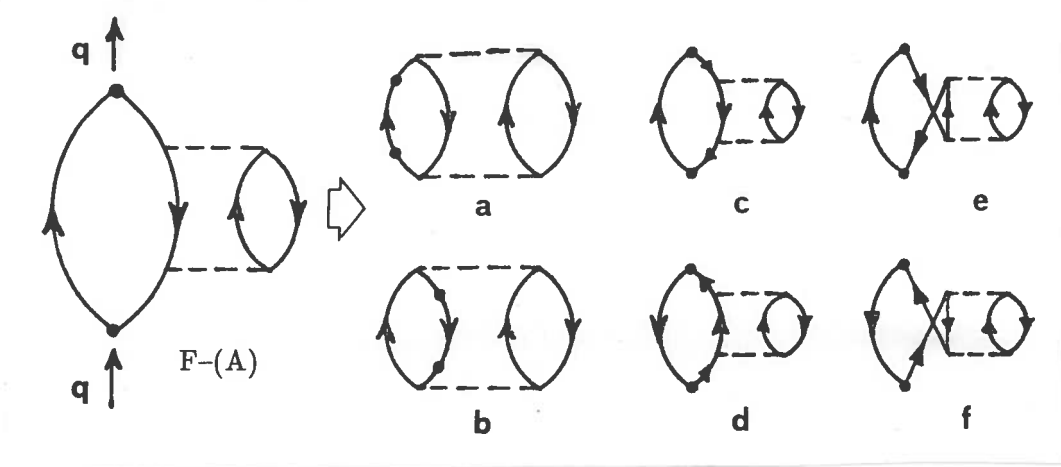

Fig. 3.3a - The Feynman diagram F–(A) generates the six topologically inequivalent Goldstone diagrams (a–f). In the latter the arrows indicate particles and holes.

Apart from the ones already included in the HF and RPA treatments, second order diagrams arise from the first term in the r.h.s. of eq.(3.7) via the insertion of

the second–order self–energy on the fermionic propagation line. One finds that six Goldstone diagrams are thus generated from the Feynman diagram F–(A): they are shown in Fig. 3.3a. Their physical significance is transparent: (a) and (b) describe NN correlations in nuclear matter, (c) [(d)] the second–order dressing of the particle [hole] propagator (which of course is not embodied in the HF framework) and (e) and (f) the influence of the correlations on the nucleon self–energy.

We consider next the second–order contributions stemming from the second term in the r.h.s. of (3.7). In order to classify them one should realize that five (and only five) diagrams (and as many exchange–ones) contribute to Γ in second–order. Some of them already enter in the antisymmetrized RPA, others account for the medium corrections to the πNN vertex (e.g. for an interaction carried by the pion). Those expected to play an important role in the many–body response functions are generated by the Feynman diagrams F–(B), F–(C) and F–(D) of Fig. 3.3b, 3.3c and 3.3d, respectively.
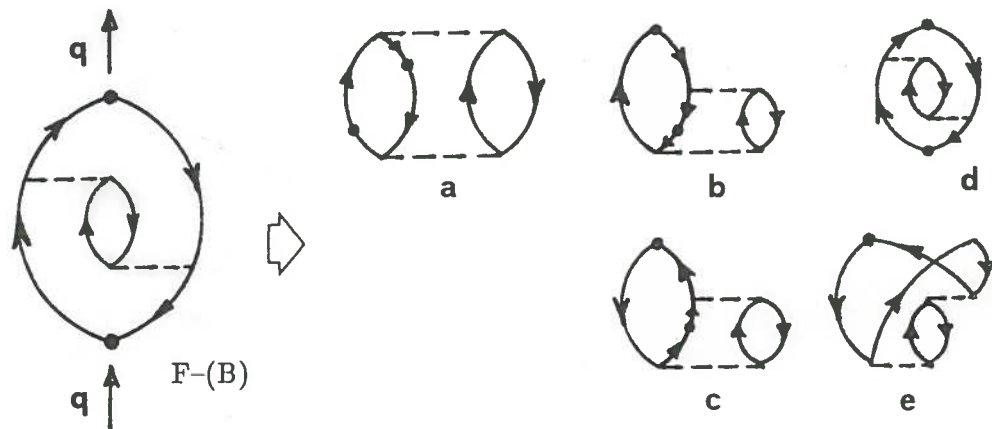

Fig. 3.3b - The Feynman diagram F–(B) generates the five topologically inequivalent Goldstone diagrams (a–e). In the latter the arrows indicate particles and holes.

Five Goldstone diagrams, displayed in Fig. 3.3b, stem from F–(B). Their physical significance is again transparent: (a) accounts for NN correlations with the probe linked to two different fermionic lines, whereas (b) and (c) strongly reflect the interference between the p–h and the 2p–2h sectors of the nuclear excited states; finally (d) and (e) are well–known to provide a screening of the p–h interaction.
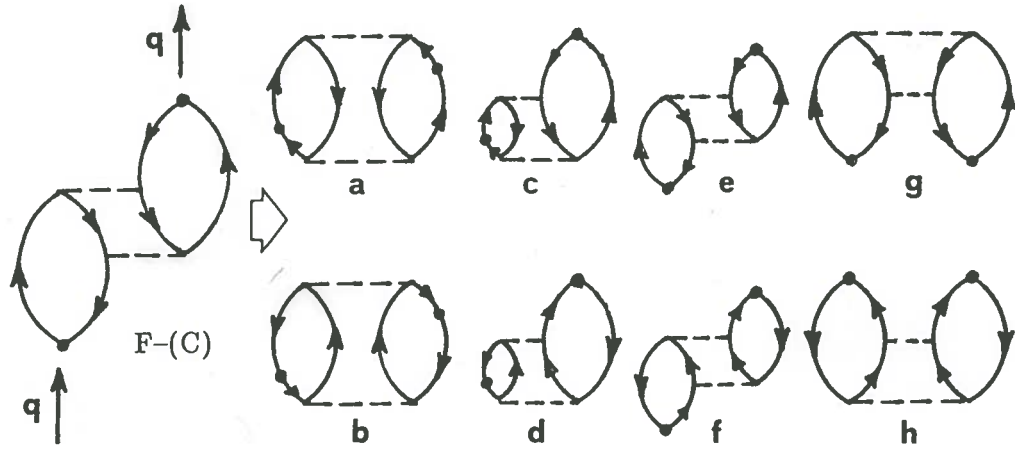
Fig. 3.3c - The Feynman diagram F–(C) generates the eight topologically in-
equivalent Goldstone diagrams (a–h). In the latter the arrows indicate
particles and holes.

The eight Goldstone diagrams (Fig. 3.3c) arising from F–(C) still describe NN
correlations [(a) and (b), but with the probe linked to different bubbles], and p–h,
2p–2h interference [(c) and (d)]. However new dynamical elements appear in the
diagram (e), (f), (g) and (h), which are known to play an important role in describing
the short range correlations in the electron theory of metals. Unfortunately the role
they play in the nuclear response has not yet been ascertained to our knowledge.
The same physics is essentially embodied in the five Goldstone diagrams associated
with F–(D), which are displayed in Fig. 3.3d.

It thus appears that the second–order perturbation theory brings into play new
important features of the nuclear responses, beyond the standard mean field and the
RPA correlations. As we shall see in Section 7, these new elements also naturally
arise in the loop expansion for the polarization propagator provided by the functional
approach. The latter has, however, the great merit of grouping them into classes
according to the prescriptions of the loop expansion, which thus provides a guide
for the diagrams one should keep in order to achieve a consistent treatment of the
nuclear responses. The conventional perturbative framework, instead, is obviously
untenable since it is based on the order dictated by the coupling constant of the
strong interactions.

Yet, as already mentioned, several calculations have demonstrated that second order
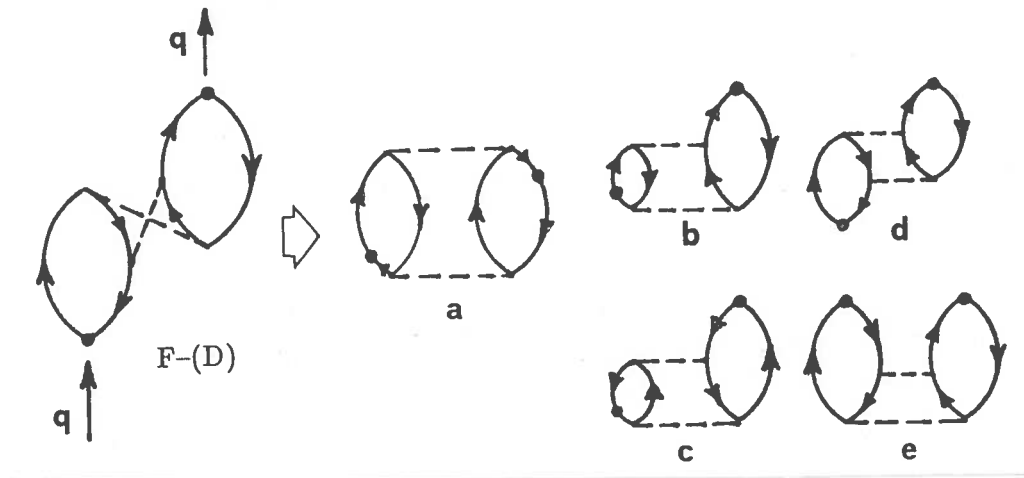
Fig. 3.3d - The Feynman diagram F–(D) generates the five topologically in-equivalent Goldstone diagrams (a–e). In the latter the arrows indicate particles and holes.

perturbative diagrams *do* play a most relevant role in the nuclear response, hence the necessity of accounting as accurately as possible for these type of contributions in a well–founded theoretical scheme.

The variational approach

As for the binding energy, also for the nuclear responses an alternative approach to the perturbative one has been developed with variational techniques. Its modern version relies on the so–called CBF (Correlated Basis Function) method (Feenberg, 1969; Clark *et al.*, 1979; Clark and Krotscheck, 1983; Fantoni, 1984; Manousakis and Pandharipande, 1986), which in fact attempts a linkage of the variational and of the perturbative theories. We briefly revisit here the method, closely following the presentation of Fantoni (1988).

The essence of the scheme lies in the use of the orthonormalized many–particle, many–hole correlated states (ONCS)

$$|p_1 \ldots p_n, h_1 \ldots h_n) = \frac{1}{\sqrt{\mathcal{N}}}(\mathcal{S} \prod F_{ij})|p_1 \ldots p_n, h_1 \ldots h_n >_{FG} \qquad (3.14)$$

where $|p_1 \ldots p_n, h_1 \ldots h_n >_{FG}$ is a n–particle, n–hole Fermi gas state, $\mathcal{N}$ a normal-ization constant and the two–particle correlation operator,

$$F_{ij} = \sum f^p(r_{ij})O^p(ij), \qquad (3.15)$$

is built out of the eigth two–body operators

$$O^{P=1,8}(ij) = 1; \quad \sigma_i \cdot \sigma_j; \quad \tau_i \cdot \tau_j; \quad (\sigma_i \cdot \sigma_j)(\tau_i \cdot \tau_j); \quad S_{ij};$$
$$S_{ij}(\tau_i \cdot \tau_j); \quad \mathbf{L} \cdot \mathbf{S}; \quad \mathbf{L} \cdot \mathbf{S}(\tau_i \cdot \tau_j) \qquad (3.16)$$

S_{ij} being the tensor operator and the $\mathcal{S}$ in (3.14) the symmetrizer of the product $\prod F_{ij}$.

Without entering into the heavy formal development of the theory, for which we refer the reader to the literature quoted by Fantoni (1988), we recall that, while the variational aspect of the latter is embodied in the function F_{ij}, chosen in such a way as to minimize the nuclear matter binding energy, the "perturbative" aspect of the method relies on the splitting of the hamiltonian into an unperturbed, H_0, and an interaction, H_I, term defined by the equations:

$$< m|H_0|n > = < m|H|m > \delta_{mn} = H_{mm}\delta_{mn} \qquad (3.17a)$$

$$< m|H_I|n > = < m|H|n > (1 - \delta_{mn}) = \bar{H}_{mn}, \qquad (3.17b)$$

$|m>$ being a generic ONCS and the matrix elements being calculated with the FHNC/SOC (Fermi Hypernetted Chain) technique (Rosati, 1981).

To calculate the imaginary part of the polarization propagator (here, for the sake of illustration, we shall consider the charge longitudinal channel) one starts from the formal expansion

$$\mathrm{Im}\Pi(q,\omega) = \sum_n (-1)^n < 0|\hat{\rho}_k^\dagger \frac{1}{H_0 - E_0 - \omega - i\eta} \Big(H_I \frac{1}{H_0 - E_0 - \omega - i\eta} \Big)^n \hat{\rho}_k|0 >$$
$$\qquad (3.18)$$

which, in the CBF framework, can be cast into the form:

$$\mathrm{Im}\Pi(q,\omega) = \sum_i X_0^*(i)G_0(i)X_0(i) - \sum_{ij} X_0^*(i)G_0(i)\bar{H}_{ij}G_0(j)X_0(j) + \ldots, \qquad (3.19)$$

$\hat{\rho}_k$ being the nuclear charge operator. In turn, (3.19) can be compactified by means of the following Dyson–type integral equation:

$$X(i) = X_0(i) - \sum_j \bar{H}_{ij}G_0(j)X(j) \qquad (3.20)$$

$$\mathrm{Im}\Pi(q,\omega) = \sum_i X_0^*(i)G_0(i)X(i). \qquad (3.21)$$

In the above $X_0^*(i) = < 0|\hat{\rho}_k^\dagger|i >$.

The various perturbative contributions are then obtained by including p–h, 2p–2h, etc. ONC states, derived by solving eqs. (3.17), in the sum over the intermediate states appearing in the expansion (3.19). It is clear that a variety of approximations are thus possible in dealing with this theoretical framework. For example, by setting $X(i) = X_0(i)$ and restricting the states $|i >$ to the p–h sector, one recovers the "zeroth–order" polarization propagator. The latter, however, has the great advantage of accounting, already at the level of zeroth–order perturbation theory, for the correlations embedded in the CBF states.
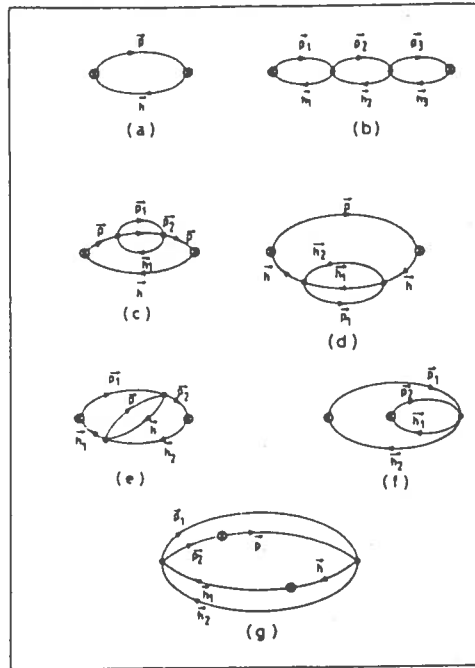

Fig. 3.4 - Correlated basis diagrams contributing to the response function. The circled crosses and the dots denote the vertices X_0 and the non–diagonal matrix elements $\bar{H}_{ij}$, respectively.

If, instead, the equations (3.20) and (3.21) are fully solved within the p–h sector, then one recovers a RPA–type (ring) polarization propagator, which again engraines the CBF correlations. Finally the inclusion of 2p–2h ONC states allows to account for more complex dynamical correlations (see Fig. 3.4) whose physical meaning is perhaps less transparent than for the corresponding diagrams of perturbation theory always because "correlations" enter here both at the variational and at the perturbative level. However, as already remarked in the previous section and as we shall

see in Section 4, these 2p–2h diagrams do appear to play an important role in the charge response.

On a general ground, for the variational approach it remains to be faced the problem of getting the binding energy of nuclear matter at the correct density, but this, of course, is also a problem for perturbation theory. What one would desire more is the extension of the method to treat interactions effectively carried by mesons, since they appear more in touch with the way nature works at the microscopic level.

3.2 Finite Nuclei

As a first step toward the evaluation of the polarization propagator in finite systems, we introduce here the semiclassical approximation (Schuck, 1984; Stroth *et al.*, 1984). Indeed it allows to account for the finite size of the nucleus and, in spite of its simplicity, is fairly accurate for not too low momentum transfers.

To start with, notice that one can write the independent particle Π in coordinate space as follows:

$$\Pi^0(\mathbf{r}_1, \mathbf{r}_2; \mathbf{r}_1', \mathbf{r}_2') = <\mathbf{r}_1 \mathbf{r}_2'|\Pi^0(H_1, H_2)|\mathbf{r}_1' \mathbf{r}_2 > \tag{3.22}$$

with

$$\Pi^0(H_1, H_2) = \frac{\theta(\mu_F - H_2)\theta(H_1 - \mu_F) - \theta(\mu_F - H_1)\theta(H_2 - \mu_F)}{\hbar\omega - H_1 + H_2 \pm i\eta}, \tag{3.23}$$

H_i being the single particle Hamiltonian within a chosen shell model and μ_F the chemical potential (Fermi energy) of the nucleus.

Now the Thomas–Fermi limit of the single–particle density operator $\hat{\rho} = \theta(\mu_F - H)$ is simply obtained by replacing the quantum hamiltonian H with its classical counterpart H^c. Accordingly the semiclassical version of (3.23) is obtained by the replacement:

$$H_i \Longrightarrow H_i^c = \frac{p_i^2}{2M} + V(R_i), \qquad (i = 1, 2), \tag{3.24}$$

R_i being the distance of the i–th particle from the center of the nucleus.

This leads to a Π^0 which corresponds to the Wigner transform of (3.22) with respect to the particle and hole variables. In practice one gets the semiclassical expression of Π^0 via the prescription:

$$\Omega\, \Pi(q, \omega, k_F) \longrightarrow 4\pi \int_0^{R_c} dR\, R^2 \Pi(q, \omega, k_F(R)), \tag{3.25}$$

Ω being the nuclear volume. Notably Π depends upon the radius R through the nuclear density (i.e., through k_F). The latter becomes position–dependent, according to the equation:

$$\frac{k_F{}^2(R)}{2M^*(R)} + V(R) = \frac{k_F{}^2(0)}{2M^*(0)} + V(0) \,, \tag{3.26}$$

which keeps the chemical potential constant at any point of the nucleus, and the normalization condition:

$$\int d^3R\,\theta(R_c - R)\rho(R) \equiv \int d^3R\,\theta(R_c - R)\frac{2k_F{}^2(R)}{3\pi^2} = A \,, \tag{3.27}$$

which fixes $k_F(0)$. In turn the upper limit of integration is set by the requirement

$$k_F(R_c) = 0. \tag{3.28}$$

It is worth pointing out that the non–linear problem associated with the set of eqs. (3.26)–(3.28) must be self–consistently solved.

Expression (3.25) for the polarization propagator is shown (Stroth *et al.*, 1984) to correspond to the lowest order in the $\hbar$ expansion of the Thomas–Fermi theory and it may also be referred to as a "local density approximation" to Π as far as the excitation operator (i.e. the external vertex) is a local one. Stroth *et al.* (1985) also proved that this approximation compares favourably with an exact calculation at least when, at sufficiently high momentum transfer, the shell effects are less relevant. We notice that $V(R)$ is a mean field which may be either deduced from a realistic Hartree–Fock calculation or somehow parametrized, e.g. by means of a Wood–Saxon well. Finally, in (3.26) an explicit R–dependence of the effective nucleon mass is usually introduced to account for the well–known density dependence of the latter.

In order to deal with an *exact* finite nucleus calculation, let us focus on the nuclear response to a pionic field [see eqs. (2.19) and (2.20)]. The corresponding polarization propagator in coordinate space (with explicit isospin indexes) will read:

$$\Pi_{a,b}(\mathbf{x}t, \mathbf{x}'t') = -\frac{i}{\hbar} < \Psi_0|T\{\hat{\jmath}^a_{A_H}(\mathbf{x}t)\hat{\jmath}^b_{A_H}(\mathbf{x}'t')\}|\Psi_0 > \tag{3.29}$$

where the second–quantized axial current operator is expressed in terms of the field operators (in Heisenberg representation) as follows:

$$\hat{\jmath}^a_{A_H}(\mathbf{x}t) = \int d\mathbf{y}\,\hat{\psi}^\dagger_H(\mathbf{y},t)j^a_A(\mathbf{x} - \mathbf{y})\hat{\psi}_H(\mathbf{y},t)$$

$$= \sum_{\alpha\beta} < \alpha|\hat{\jmath}^a_A(\mathbf{x})|\beta > \hat{a}^\dagger_{H\alpha}(t)\hat{a}_{H\beta}(t). \tag{3.30}$$

In the above

$$< \alpha | \hat{j}_A^a(\mathbf{x}) | \beta > = \int d\mathbf{y} \psi_\alpha^\dagger(\mathbf{y}) j_A^a(\mathbf{x} - \mathbf{y}) \psi_\beta(\mathbf{y}) \tag{3.31}$$

are the matrix elements of the current, evaluated in the first quantized scheme, between the single–particle states $\psi_\alpha(\mathbf{y})$, and $\hat{a}^\dagger$, $\hat{a}$ the anticommuting fermion operators.

Assuming now a pseudovector πNN coupling the current $\mathbf{j}_A$ (in coordinate space) will read:

$$j_A^a(\mathbf{x} - \mathbf{y}) = \tau^a \frac{i}{(2\pi)^3} \int d\mathbf{q} (\boldsymbol{\sigma} \cdot \mathbf{q}) e^{-i\mathbf{q} \cdot (\mathbf{x} - \mathbf{y})} \tag{3.32}$$

$\tau^a (a = x, y, z)$ being the Pauli isospin matrices of the nucleon. Furthermore the Fourier transform of (3.29) in momentum space can be written in the form:

$$\Pi_{a,b}(\mathbf{q}, \mathbf{q}'; \omega) = \frac{1}{\hbar} \sum_{\alpha\beta\gamma\delta} < \alpha | j_A^a(\mathbf{q}) | \beta > < \gamma | j_A^b(-\mathbf{q}') | \delta > \Lambda_{\beta\alpha,\gamma\delta}(\omega), \tag{3.33}$$

with

$$\Lambda_{\beta\alpha,\gamma\delta}(\omega) = \hbar \sum_{n \neq 0} \Big[\frac{< \Psi_0 | \hat{a}_\alpha^\dagger \hat{a}_\beta | \Psi_n > < \Psi_n | \hat{a}_\gamma^\dagger \hat{a}_\delta | \Psi_0 >}{\hbar\omega - (E_n - E_0) + i\eta}$$

$$- \frac{< \Psi_0 | \hat{a}_\gamma^\dagger \hat{a}_\delta | \Psi_n > < \Psi_n | \hat{a}_\alpha^\dagger \hat{a}_\beta | \Psi_0 >}{\hbar\omega + (E_n - E_0) - i\eta} \Big] \tag{3.34}$$

and

$$< \alpha | j_A^a(\mathbf{q}) | \beta > = i \int d\mathbf{y} \psi_\alpha^\dagger(\mathbf{y}) \tau^a (\boldsymbol{\sigma} \cdot \mathbf{q}) e^{i\mathbf{q} \cdot \mathbf{y}} \psi_\beta(\mathbf{y}). \tag{3.35}$$

The polarization propagator (3.33) can be now evaluated, e.g., in the independent particle approximation, which amounts to replacing $|\Psi_n >$ with Slater determinants of single–particle wave functions, denoted by $|\Phi_n >$. For the sake of illustration let us consider the harmonic oscillator (HO) basis for spin 1/2, isospin 1/2 particles:

$$\psi_\alpha^{HO}(\mathbf{r}) = R_{n_\alpha l_\alpha}(r) Y_{l_\alpha m_\alpha}(\Omega_r) \chi_{s_\alpha} \eta_{t_\alpha}, \tag{3.36}$$

with eigenvalues $\epsilon_{n_\alpha l_\alpha}$. The intermediate states $|\Phi_n >$ will be p–h states of definite angular momentum l, spin σ (coupled to a total angular momentum J) and isospin τ.

After some algebra one obtains:

$$\Pi_{a,b}^0(\mathbf{q}, \mathbf{q}'; \omega) = \delta_{a,b} \sum_J \frac{2J+1}{4\pi} P_J(\hat{\mathbf{q}} \cdot \hat{\mathbf{q}}') \sum_{ll'} a_{Jl} [\hat{\Pi}_J^0(q, q'; \omega)]_{ll'} a_{Jl'} \tag{3.37}$$

where

$$[\hat{\Pi}_J^0(q, q'; \omega)]_{ll'} = \sum_{ph} Q_{ph}^{Jl}(q) \left[\frac{1}{\hbar\omega - (\epsilon_p - \epsilon_h) + i\eta} - \frac{1}{\hbar\omega + (\epsilon_p - \epsilon_h) - i\eta} \right] Q_{ph}^{Jl'*}(q'),$$

$$(3.38)$$

$$Q_{ph}^{Jl}(q) = <j_p j_h; J|l\sigma; J> \delta_{\sigma,1}(-i)^{l+1}(-1)^{l_h} 4[\pi(2l_p + 1)(2l_h + 1)]^{1/2}$$

$$\times \mathcal{I}_{ln_p l_p n_h l_h}(q) \begin{pmatrix} l_p l_h l \\ 0 \ 0 \ 0 \end{pmatrix}, \qquad (3.39)$$

$$\mathcal{I}_{ln_p l_p n_h l_h}(q) = q \int dr r^2 j_l(qr) R_{n_p l_p}(r) R_{n_h l_h}(r) \qquad (3.40)$$

and

$$a_{Jl} \equiv (J010|l0) = (-1)^l \sqrt{2l+1} \begin{pmatrix} l_p l_h l \\ 0 \ 0 \ 0 \end{pmatrix}. \qquad (3.41)$$

In the above the P_J are Legendre polynomials and $j_l(z)$ the spherical Bessel functions. Notice that ph is a shortcut for $(n_p l_p j_p, n_h l_h j_h)$. The imaginary part of the propagator (3.37) is shown in Fig. 3.5 and compared with the same quantity in infinite nuclear matter.
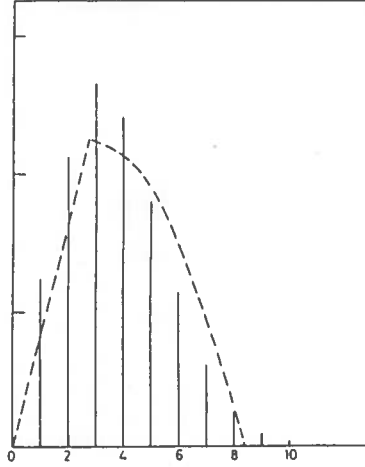

Fig. 3.5 - The quantity $-\mathrm{Im}\Pi_{3,3}^0(q, q; \omega)/A$, from eq.(3.37) at $q = 1.27\,\mathrm{fm}^{-1}$ is compared with the free nuclear matter propagator.

The RPA expression for the polarization propagator (3.33) can be naturally derived utilizing the random phase approximation for $\Lambda_{\beta\alpha,\gamma\delta}(\omega)$. The latter obeys the RPA equation

$$\Lambda_{\beta\alpha,\gamma\delta}^{RPA}(\omega) = \Lambda_{\beta\alpha,\gamma\delta}^{0}(\omega) + \frac{1}{\hbar} \sum_{\lambda\eta\sigma\rho} \Lambda_{\beta\alpha,\lambda\eta}^{0}(\omega) < \lambda\eta^{-1}|V|\sigma\rho^{-1} >_D \Lambda_{\sigma\rho,\gamma\delta}^{RPA}(\omega), \quad (3.42)$$

where $< \lambda\eta^{-1}|V|\sigma\rho^{-1} >_D$ is the direct p–h matrix element of the NN interaction (as in (3.13), we actually neglect, here, antisymmetrization) and

$$\Lambda_{\beta\alpha,\gamma\delta}^{0}(\omega) = \delta_{\alpha,\delta}\delta_{\beta,\gamma}\hbar \left[\frac{\theta(\gamma - F)\theta(F - \delta)}{\hbar\omega - (\epsilon_\gamma^0 - \epsilon_\delta^0) + i\eta} - \frac{\theta(F - \gamma)\theta(\delta - F)}{\hbar\omega + (\epsilon_\delta^0 - \epsilon_\gamma^0) - i\eta} \right], \quad (3.43)$$

F denoting the Fermi level.

By inserting (3.43) into (3.33) and performing the usual multipole decomposition, one ends up with the RPA equations for the quantity $[\hat{\Pi}_J]_{ll'}$, which enters into the full RPA propagator as in (3.37):

$$[\hat{\Pi}_J^{RPA}(q, q'; \omega)]_{ll'} = [\hat{\Pi}_J^0(q, q'; \omega)]_{ll'} \quad (3.44)$$
$$+ \frac{1}{(2\pi)^3} \int_0^\infty dk\, k^2 \sum_{l_1 l_2} [\hat{\Pi}_J^0(q, k; \omega)]_{ll_1} [U_J(k)]_{l_1 l_2} [\hat{\Pi}_J^{RPA}(k, q'; \omega)]_{l_2 l'},$$

where $[U_J(k)]_{l_1 l_2}$ is the corresponding multipolarity of the full p–h force entering into the channel selected by the external probe. We will come back to this point later, in dealing specifically with the spin–isospin responses.

Equations (3.44) are a set of integral equations, coupled or not depending upon the nature of the force U_J. The corresponding solution has been obtained both within a certain approximation scheme (Alberico *et al.*, 1986) which allows to find analytical expressions, and by numerical methods (Ichimura *et al.*, 1988; De Pace *et al.*, 1989). It has also been extended to account for the continuum of states above the Fermi level.

4. THE NUCLEAR RESPONSES TO AN EXTERNAL ELECTROMAGNETIC FIELD

The double differential cross section, in the laboratory system, for inclusive electron scattering from nuclei, is usually written in the form:

$$\frac{d^2\sigma}{d\Omega d\epsilon'} = \sigma_M \left\{ \left(\frac{Q^2}{q^2} \right)^2 R_L(q, \omega) + \left(\frac{1}{2} \left| \frac{Q^2}{q^2} \right| + \tan^2 \frac{\theta}{2} \right) R_T(q, \omega) \right\}. \quad (4.1)$$

Here an electron with incident 4–momentum $K^\mu = (\epsilon, \mathbf{k})$ is scattered through an angle θ to 4–momentum $K'^\mu = (\epsilon', \mathbf{k}')$ and $Q^\mu = (K - K')^\mu = (\omega, \mathbf{q})$ is the 4–momentum transferred to the nucleus and hence carried by the spacelike $(Q^2 \leq 0)$ virtual photon exchanged in the process. Furthermore, $L(T)$ refers to responses with longitudinal (transverse) projections of the nuclear currents and the Mott cross section is given by

$$\sigma_M = \left\{ \frac{\alpha \cos(\theta/2)}{2\epsilon \sin^2(\theta/2)} \right\}^2. \tag{4.2}$$

For an electromagnetic current operator $\hat{J}_\mu = (\hat{\rho}, \hat{\mathbf{J}})$. Accordingly the longitudinal and transverse responses can then be expressed as (Alberico, De Pace *et al.*, 1988)

$$R_L(q,\omega) = \left(\frac{q^2}{Q^2}\right)^2 \left\{ R(QQ; q\omega) \right.$$
$$\left. - \frac{2\omega}{q} \sum_l \frac{q_l}{q} R_l(QJ; q\omega) + \frac{\omega^2}{q^2} \sum_{ll'} \frac{q_l q_{l'}}{q^2} R_{ll'}(JJ; q\omega) \right\} \tag{4.3}$$

and

$$R_T(q,\omega) = \sum_{ll'} \left(\delta_{ll'} - \frac{q_l q_{l'}}{q^2} \right) R_{ll'}(JJ; q\omega) \tag{4.4}$$

where "Q" and "J" are used to label how the responses contain the bilinear combinations of $\mu = 0$ and $\mu = 1, 2, 3$ projections of the 4–vector current, respectively.

The charge–charge (R), charge–current (R_l) and current–current $(R_{ll'})$ responses are so defined:

$$R(QQ; q\omega) = \sum_n \delta(\hbar\omega - E_n + E_0)\delta_{\mathbf{q},\mathbf{P}_n} < \Psi_0|\hat{\rho}^\dagger|\Psi_n >< \Psi_n|\hat{\rho}|\Psi_0 > \tag{4.5a}$$

$$R_l(QJ; q\omega) = \sum_n \delta(\hbar\omega - E_n + E_0)\delta_{\mathbf{q},\mathbf{P}_n}$$
$$\times \frac{1}{2}\left\{ < \Psi_0|\hat{J}_l^\dagger|\Psi_n >< \Psi_n|\hat{\rho}|\Psi_0 > + < \Psi_0|\hat{\rho}^\dagger|\Psi_n >< \Psi_n|\hat{J}_l|\Psi_0 > \right\} \tag{4.5b}$$

and

$$R_{ll'}(JJ; q\omega) = \sum_n \delta(\hbar\omega - E_n + E_0)\delta_{\mathbf{q},\mathbf{P}_n}$$
$$\times \frac{1}{2}\left\{ < \Psi_0|\hat{J}_l^\dagger|\Psi_n >< \Psi_n|\hat{J}_{l'}|\Psi_0 > + < \Psi_0|\hat{J}_{l'}^\dagger|\Psi_n >< \Psi_n|\hat{J}_l|\Psi_0 > \right\}. \tag{4.5c}$$

In the above $|\Psi_0>$ is the ground state of the system and $|\Psi_n>$ a complete set of excited states, with energy E_n and (in an homogeneous system) momentum $\mathbf{p}_n$.

If we restrict ourselves to consider the pure (non–relativistic) nucleonic current in the non–interacting, symmetric nuclear matter framework then, for example, the charge longitudinal response becomes:

$$
\begin{aligned}
R_L(q,\omega) &= R(Q_N Q_N; q\omega) \\
&= f^2(Q^2)\frac{3\pi^2 A}{k_F{}^3}\int \frac{d\mathbf{k}}{(2\pi)^3}\theta(k_F - k)\theta(|\mathbf{q}+\mathbf{k}| - k_F)\delta\left(\hbar\omega - \frac{\hbar^2 q^2}{2M} - \frac{\hbar^2 \mathbf{q}\cdot\mathbf{k}}{M}\right) \\
&= f^2(Q^2)\frac{3\pi^2 A}{k_F{}^3}\left(-\frac{1}{\pi}\right)\mathrm{Im}\Pi^0(q,\omega)
\end{aligned}
\tag{4.6}
$$

where we have exploited current conservation (gauge invariance) to reduce (4.3) to the pure charge–charge response. The form factor $f(Q^2)$ takes into account the finite size of the nucleon: for practical purposes it can be assumed to be the usual dipole electric form factor $G_E(Q^2)$.

The transverse response (4.4), instead, (neglecting the small contribution from the nucleonic convection current) reads:

$$
R_T(q,\omega) = \frac{\hbar^2 q^2}{2M^2}(\mu_p^2 + \mu_n^2)G_E^2(Q^2)\frac{3\pi^2 A}{k_F{}^3}\left(-\frac{1}{\pi}\right)\mathrm{Im}\Pi^0(q,\omega)
\tag{4.7}
$$

where $\mu_{p(n)}$ are the proton (neutron) total magnetic moments (in units of the Bohr magneton).

Obviously (4.6) and (4.7) can be generalized, not only to include correlated intermediate states, but also other components of the electromagnetic current, which are present in a nucleus beyond the pure nucleonic one. In particular, the charged mesons exchanged between the nucleons can couple directly to the external photon, giving rise to the so–called meson exchange currents (MEC). The latter are, by intrinsic nature, two–body currents and naturally induce 2p–2h excited states, whose relevance will be later explored.

4.1 The Charge Longitudinal Response Function

The Rosenbluth separation of the experimental longitudinal and transverse response functions in the energy domain of the quasi-elastic peak (QEP) gave rise to a challenging problem for the nuclear physicists. Indeed the total response function in the QEP was previously believed to be accounted for fairly well by the Fermi Gas Model with a few additional ingredients to explain the experimentally found shift of

the response peak with respect to the Fermi Gas prediction. Thus, utilizing a Fermi Gas-inspired model with three parameters (effective mass, nucleon average binding energy and the Fermi momentum k_F) Moniz (1969) succeeded in getting in touch with the experimental data for a variety of nuclei.

The achievement of the transverse/longitudinal separation drastically changed this situation, asking for a subtler interpretation of the underlying physics. To analyze it we first focuss on the charge channel. Here experimental data are presently available for a large set of nuclei, ranging from ^{3}He to ^{238}U (Altemus, 1980; Quinn et al., 1988; Marchand et al., 1985; Dow, 1987; Barreau et al., 1983; Meziani et al., 1984; Meziani et al., 1985; Blatchey et al., 1986). The main features of the experimental results are:

1. the charge response considerably varies over the nuclear chart,
2. differences are present even at the level of the isotopes of a given nucleus like, e.g., ^{40}Ca and ^{48}Ca,
3. for moderate momenta the frequency behaviour of the charge response tends to be rather flat, but for the lightest nuclei.

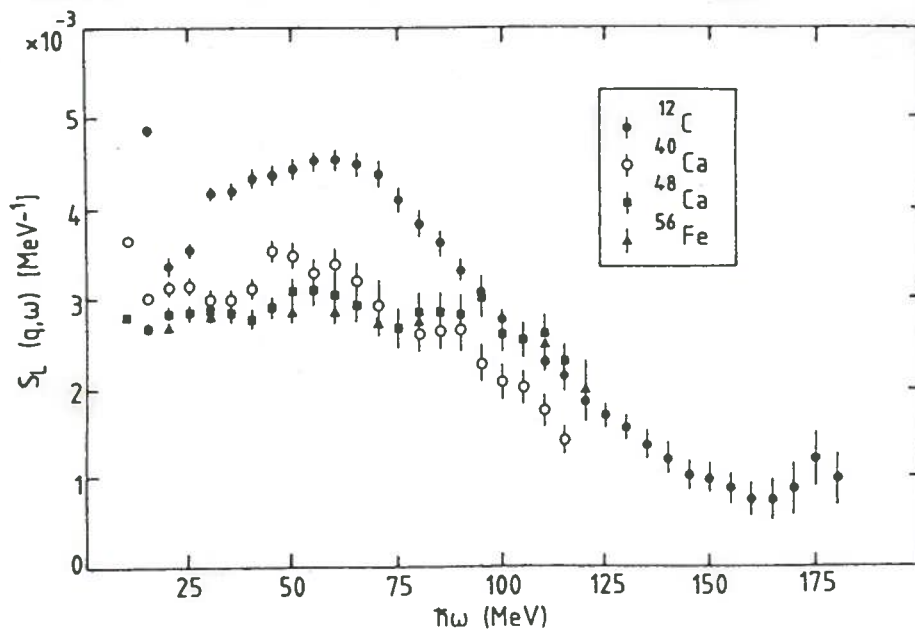Fig. 4.1 – The experimental longitudinal response function (divided by Z) from (e, e') scattering in C^{12}, Ca^{40}, Ca^{48} and Fe^{56}, at $q = 300$ MeV/c. Data are taken from Barreau et al., (1983); Meziani et al.,(1984,1985).

The Fermi Gas model is clearly unable to encompass these features, (see, e.g., the experimental data at $q = 300\,\text{MeV/c}$ displayed in Fig. 4.1) and accordingly we resort to the RPA based on the Landau-Migdal effective ph interaction (see for instance Migdal, 1967)

$$V^{ph} = C_0 \left[\mathcal{F}_0 + \mathcal{F}'_0\, \tau_1 \cdot \tau_2 + \mathcal{G}_0\, \sigma_1 \cdot \sigma_2 + \mathcal{G}'_0\, \tau_1 \cdot \tau_2\, \sigma_1 \cdot \sigma_2 \right] \qquad (4.8)$$

where clearly the two first pieces only are relevant for the channel we are interested in. As we have seen in Sect. 3, for infinite nuclear matter the following expression

$$\Pi(q,\omega) = \frac{1}{2} \left\{ \frac{\Pi^0(q,\omega)}{1 - 4C_0\mathcal{F}\Pi^0(q,\omega)} + \frac{\Pi^0(q,\omega)}{1 - 4C_0\mathcal{F}'\Pi^0(q,\omega)} \right\}, \qquad (4.9)$$

yields the ph propagator in RPA. In the above

$$C_0 = \frac{\pi^2 \hbar^2}{2k_F M^*(k)|_{k=k_F}} \qquad (4.10)$$

(M^* being the nucleon effective mass) as prescribed by the Landau theory.

Using (4.9) we can examine the influence of the RPA correlations on the nuclear responses setting, for simplicity, $\mathcal{F} = \mathcal{F}'$; then it is immediate to get

$$\text{Im}\Pi(q,\omega) = \frac{\Pi^0(q,\omega)}{\left\{1 - 4C_0\mathcal{F}\text{Re}\Pi^0(q,\omega)\right\}^2 + \left\{4C_0\mathcal{F}\text{Im}\Pi^0(q,\omega)\right\}^2} . \qquad (4.11)$$

Now, at the top of the peak, i.e. at $\omega = q^2/2M$, the real part of $\Pi^0(q,\omega)$, which coincides with its advanced part, is negative, being approximately given (for $q > 2k_F$) by

$$\Pi^0_{\text{adv}}(q,\omega) \approx -\frac{\rho}{\omega + q^2/2M} \qquad (4.12)$$

As a consequence, for a repulsive interaction $\mathcal{F}$, the denominator in (4.11) is surely larger than one and accordingly the response is quenched. Moreover the retarded part of $\Pi^0(q,\omega)$ is negative for $\omega < q^2/2M$ and positive on the other side of the peak. Therefore $\text{Re}\Pi^0_{\text{ret}}(q,\omega)$ tends to deplete the response for $\omega < q^2/2M$ and to enhance it for $\omega > q^2/2M$. Thus the RPA correlations induced by a repulsive interaction not only reduce (quench), but also deform (harden) the QEP and, in addition, they do not conserve the total strenght. Actually, as we shall see, the physical situation is more involved of what above outlined, since two different Landau parameters enter into the longitudinal response.

The problem of their determination however cannot yet be considered fully solved. Indeed while the repulsive nature of the force in the isovector channel is a well established fact, a considerable uncertainty remains in the isoscalar one. For instance

the phenomenological analysis of Speth *et al.*, (1976) yields $\mathcal{F}_0 \simeq 0$ and $\mathcal{F'}_0 \simeq 0.65$ respectively. On the other hand the Landau-Migdal parameters obtained from the Skyrme forces [a translation from the particle–particle to the particle–hole channels for these interactions may be found, for instance, in (Alberico, Cenni *et al.*, 1982)] turn out to vary quite extensively: for example the values for $\mathcal{F}_0$ range between -0.45 and 0.74 whereas $\mathcal{F'}_0$ is at least always repulsive. In particular Skyrme III yields $\mathcal{F}_0 \simeq 0.3$ and $\mathcal{F'}_0 \simeq 0.87$.
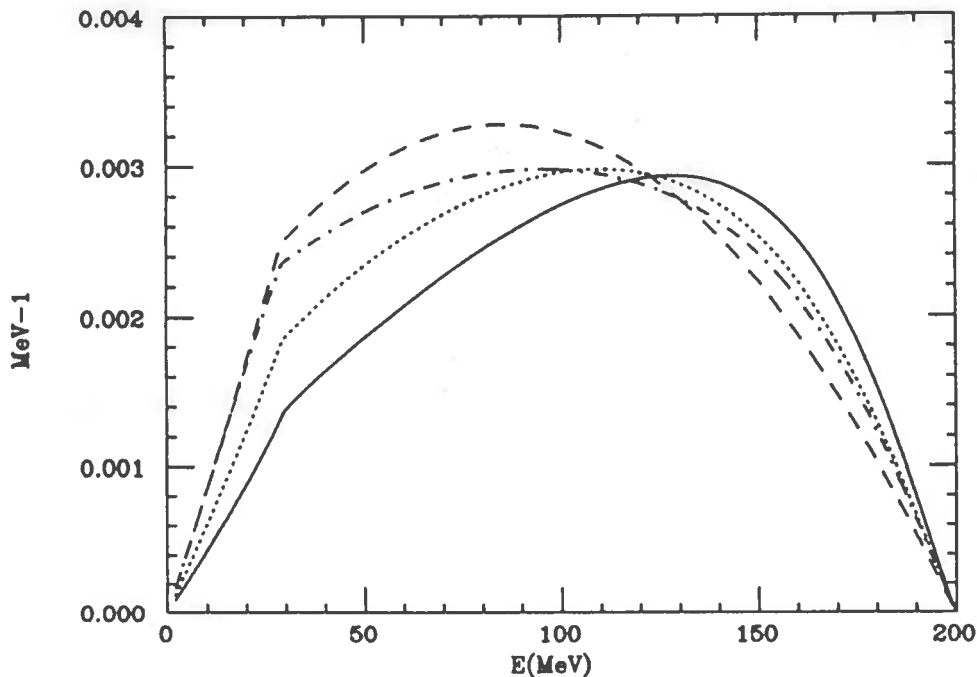

Fig. 4.2 – Charge RPA responses evaluated in nuclear matter with the force of Speth *et al.*, (1976) (continuous line), and with the Skyrme III (dotted line) and Ska (dot–dashed line) interactions. The free Fermi gas response is also displayed (dashed line). The momentum transfer is $q = 300$ MeV/c.

For the purpose of illustration we display in Fig. 4.2 the charge RPA responses corresponding to the force of Speth *et al.*, (1976) and to two Skyrme forces (III and Ska). One can there appreciate how the effective interaction works in reshaping the independent particle charge response; it is especially remarkable that if $\mathcal{F}_0$ corresponds to an attraction (as in the case of Ska) then a rather flat response might indeed result (an outcome on which we shall later comment).

Obviously a realistic approach should not treat the Landau parameters as such, since they are related to relevant macroscopical properties of the nuclear matter and

moreover should properly deal with the surface of the system, whose important role is transparently illustrated, e.g., by the comparison of the experimental responses of ^{12}C and ^{40}Ca shown in Fig. 4.1. It is indeed apparent that the response is strongly enhanced at low energy for the nucleus with a larger (with respect to the volume) surface.

We have seen in Sect. 3 that two methods are available to include surface effects in the formalism. One corresponds to directly evaluate the response for a finite nucleus in the framework of the continuum RPA using effective interactions like the Skyrme ones (Cavinato et $al.$, 1984); the other is the semiclassical approach, which introduces a radial dependence (see Sect. 3.2) for M^*, k_F and the Landau parameters. The latter method, although obviously less accurate, has the advantage of linking more clearly the calculations with the underlying physics.

We thus utilize the polarization propagator Π of eq.(3.25) letting k_F and the effective mass to carry an R-dependence dictated, e.g., by a Wood–Saxon potential well. In addition the effective interaction in the σ, τ channel will also be R–dependent according to the expression

$$\mathcal{V}^{\sigma,\tau}_{ph}(q) = \Lambda^\tau(q) \frac{2\pi^2 \hbar^2}{k_F(R) M^*(R)} F^{\sigma,\tau}_0(R) \qquad (4.13)$$

(a q–dependence has also been ascribed to the effective force; unfortunately, at present, not much is known on the momentum evolution of the parameters $\mathcal{F}_l, \mathcal{F}'_l$).

Now, the Landau parameters we are interested in are related to the compression modulus and to the symmetry energy coefficients (Migdal, 1967) through the relations

$$\mathcal{F}_0 \equiv F^{0,0}_0 = \frac{3M^*(R)}{k_F{}^2} \mathcal{K} - 1 \qquad (4.14)$$

$$\mathcal{F}'_0 \equiv F^{0,1}_0 = \frac{3M^*(R)}{k_F{}^2} b_{\mathrm{symm}} - 1, \qquad (4.15)$$

$\mathcal{K}$ and b_{symm} being R–dependent in a nucleus. In particular, for what concerns the compression modulus $\mathcal{K}$, one may identify a volume and a surface contribution and, for ^{40}Ca, a microscopic calculation based on Skyrme III yields (Blaizot et $al.$, 1976)

$$\mathcal{K}_V \approx 40 \text{ MeV} , \qquad \mathcal{K}_S \approx -16 \text{ MeV}. \qquad (4.16)$$

The relevant point here is that the compressibility is expected to be negative in the surface region, where the density is very low and consequently nuclear matter far from stability: nuclear matter prefers indeed much higher densities in order to gain in binding energy.
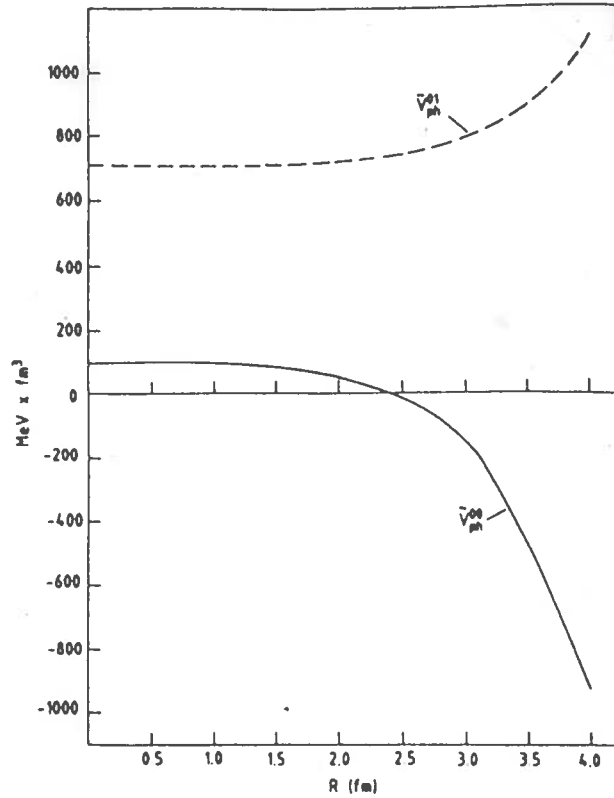
Fig. 4.3 – Radial behaviour of the isoscalar $\mathcal{V}_{ph}^{0,0}(R)$ and isovector $\mathcal{V}_{ph}^{0,1}(R)$ p–h interactions in ^{40}Ca, as given in eq.(4.13), at $q = 300$ MeV.

We may accordingly assume for $\mathcal{K}$ the smooth density dependence

$$\mathcal{K}(\rho) = a\rho + b\rho^2 \tag{4.17}$$

with a and b set by requiring $\mathcal{K}(\rho_0) = \mathcal{K}_V$ and $\mathcal{K}(\rho_0/2) = \mathcal{K}_S$, ρ_0 being the usual nuclear density well inside the nucleus ($R = 0$).

For b_{symm} microscopic calculations suggest (Siemens, 1970)

$$b_{\text{symm}}(\rho) = b_{\text{symm}}^0 \left(\frac{\rho}{\rho_0}\right)^{2/3} \tag{4.18}$$

with

$$b_{\text{symm}}^0 \approx 70 \pm 10 \text{ MeV} . \tag{4.19}$$

The behaviour of the effective interaction thus obtained (including the factor $\Lambda^\tau(q)$ on which we shall later return) is plotted as a function of R, at q fixed, in Fig. 4.3. It is seen that the negative compressibility leads to an effective interaction $\mathcal{V}_{ph}^{0,0}$ negative too on the nuclear surface and much stronger than in the interior of the nucleus [remarkably a self–consistent continuum RPA calculation for ^{12}C provides essentially the same trend (Cavinato et al., 1988)]. As a consequence the contribution to the nuclear response associated with the surface region will be quite different from the one arising from the bulk of the nucleus and, at low energy, will be controlled by the isoscalar force only.

Indeed, just as we have previously argued [cfr. eq.(4.11)] that a repulsive interaction implies a quenching of the norm and a shift of the peak of the charge response to higher energies, in the same way the opposite features can be shown to hold (although to a lesser extent) for an attractive force. Accordingly the surface component of the scalar–isoscalar effective interaction tends to enhance the low energy side of the QEP. It is in fact remarkable how such an interaction, whose strength is set by the negative $\mathcal{K}_S$, is not only able to organize a surface collective mode (the breathing mode), but also strongly influences at finite q's the charge response. As a consequence the latter turns out to be much sensitive to the actual values of the nuclear symmetry energy and, even more, of the compression modulus, on the surface, thus reflecting a subtle balance between volume and surface effetcs.

It remains to be seen whether this picture is sufficient to explain the experimentally observed flattening of the longitudinal QEP. To illustrate this point in Fig. 4.4 some typical longitudinal responses are reported, together with the separated contributions in the $T = 0$ and $T = 1$ channel. One sees that while the shape of the charge response is indeed fairly well reproduced by the RPA theory with the above discussed values for the parameters, the norm is far from being so.

In connection with the norm two different (and in some sense complementary) interpretations have thus far been offered: the first one simply amounts to introduce more complicated Feynman diagrams (of course in a many body problem a well defined criterion for selecting classes of diagrams is always searched for), the other postulates a modification of the nucleon electromagnetic form factor inside the nuclear medium.

This last possibility stems from the consideration that in the MIT bag model the quarks are confined inside the nucleon by an external pressure, which may be weakened if other nucleons are nearby, as it happens inside a nucleus. Note that this swelling of the nucleon can be invoked not only to account for the depletion of the longitudinal response (Noble, 1981; Celenza et al., 1985), but to interpret the EMC effect as well (Close et al., 1985; Cleymans and Thews, 1985). To give an example
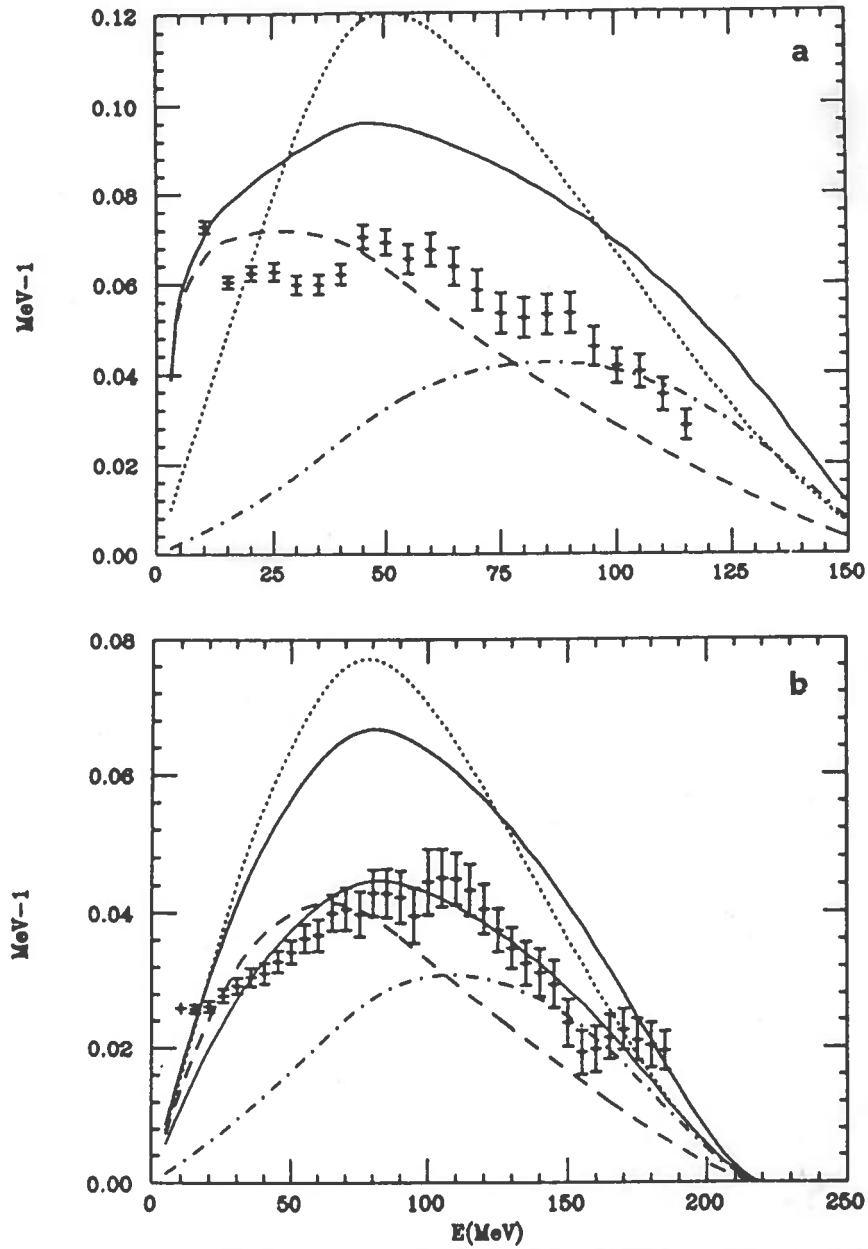
Fig. 4.4 – Comparison of the theoretical and experimental charge responses in Ca^{40} at $q = 300$ MeV/c (a) and $q = 370$ MeV/c (b). The theoretical curves are in semiclassical approximation: the dotted line is the independent particle response, the thick continuous line the RPA one [evaluated with the interaction (4.13) and with the usual e.m. dipole form factor]; also shown are the isoscalar (dashed line) and isovector (dot–dashed line) contributions. In (b) the effect of a modified e.m. form factor ($\Lambda^2 = 10.8 \text{fm}^{-2}$) on the RPA response is illustrated by the thin continuous line.

of how it affects the nuclear response, we display in Fig. 4.4(b) the RPA charge response evaluated utilizing a modified electromagnetic form factor (the usual cut–off of the e.m. form factor, $\Lambda = 18.1$ fm^{-2}, being replaced by $\Lambda = 10.8$ fm^{-2}). As previously mentioned, a phenomenological q–dependence of the Landau parameters has been introduced as well; for details see (Alberico, Czerski *et al.*, 1987).

One sees that, when tested against the experimental data, the swollen nucleon conjecture seems indeed to work quite well. Its interpretation however requires a great deal of caution, because it is not clear which microscopic phenomena are responsible for the swelling of the nucleon and, moreover, whether the latter should be thought of in QCD or within the meson theory.

In the mesonic framework it has been suggested (Ericson and Rosa-Clot, 1986) that an increase of the e.m. radius of the proton may be obtained by including vertex corrections with particle–hole intermediate states. In the language of the polarization propagator this amount to include the second order perturbative contributions to Π discussed in Sect. 3.1 and displayed in Figg. 3.3. These diagrams indeed span both the 2p–2h sector of the excited states and the p–h one. An advantage of this scheme, when compared with the MIT bag model, is that the vertex corrections should be channel dependent: accordingly the photon would see different radii of the proton in the longitudinal and transverse channel, a prediction that can be experimentally tested.

Furthermore, since the 2p–2h excitations have an enlarged response region, as compared with the p–h ones, a significant imaginary part of Π^{2p-2h} should be present on the right side of the QEP. Thus, as already remarked, the second order polarization propagator partly brings in additional strength on the tail of the QEP by spanning the 2p–2h sector of the excited states, partly it depletes the QEP when it involves instead intermediate states of the p–h sector. A recent calculation (Co' *et al.*, 1988) indicates in fact that the second order propagator induces a further depletion of the QEP, more pronounced at small energies. The contribution of 2p–2h states has been also examined in the context of the y–scaling in ref. (Butler and Koonin, 1988) for large negative y, i.e. well outside the QEP, and it has been found quite relevant.

In this connection it is also worth mentioning the nuclear matter variational approach of Fantoni and Pandharipande (1986), which appears to be remarkably successfull in quenching the longitudinal response. This is shown in Fig. 4.5, where the curve labelled by $\bar{R}_{L,C}$ clearly displays the reduction associated with 2p–2h ONC states. These results, however, deserve a few comments: i) the above mentioned 2p–2h are included via a complex optical potential, which accounts only approximately for the full complexity of this type of contributions; ii) the important surface effects, which have been previously discussed at length, are obviously ignored by a nuclear matter treatment; iii) at higher momentum transfers (say 500 MeV/c) the approach
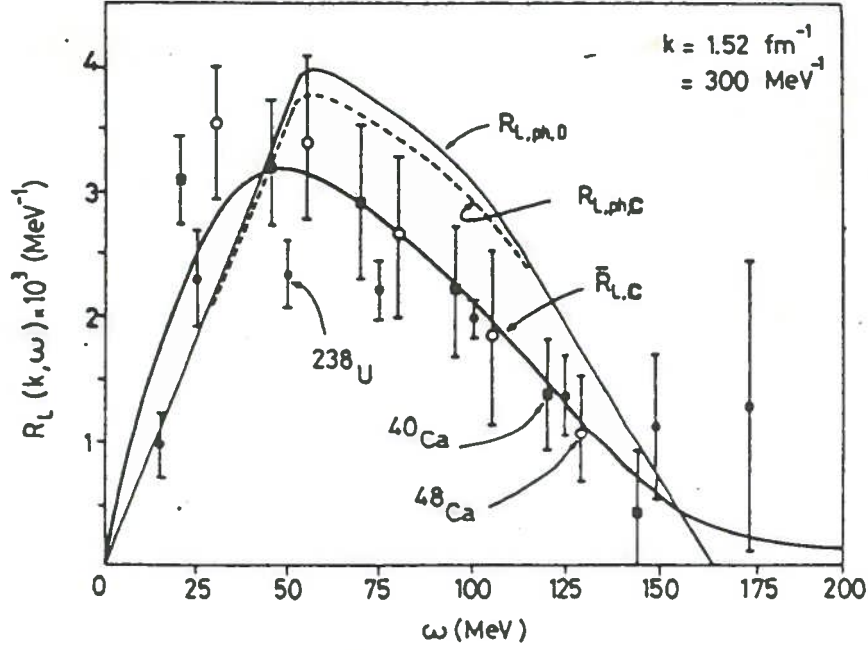
Fig. 4.5 – Longitudinal response function of nuclear matter at $q = 300$ MeV/c, evaluated with variational techniques and compared with the experimental data on Ca^{40} and Ca^{48} (at $q = 290$ MeV/c) and U^{238} (at $q = 300$ MeV/c). The error bars are large enough to contain both the *Saclay* and the *Bates* results. [Taken from (Fantoni and Pandharipande, 1986)].

is clearly insufficient to account for the data.

In spite of all these investigations, therefore, we have not yet reached a convincing solution of the problem of the norm and of the tail of the charge longitudinal QEP. In the quest for the latter it is of great help to explore these questions also in the context of the so–called Coulomb sum rule: here they are generally referred to as the missing strength problem. In this connection it is of importance to shortly revisit the derivation of the Coulomb sum rule, focussing the attention on the assumptions lying at its basis.

Let us then consider the longitudinal response to the charge fluctuation operator. To start with we assume the following form for the operator:

$$\tilde{\rho}(x) = \hat{\rho}(x) - \frac{< \Psi_0 | \hat{\rho}(x) | \Psi_0 >}{< \Psi_0 | \Psi_0 >} \qquad (4.20)$$

$$\hat{\rho}(x) = \hat{\psi}^\dagger(x) \frac{1 + \tau_3}{2} \psi(x) \qquad (4.21)$$

which amounts to conceive *the nucleon as a pointlike particle, i.e. without an electromagnetic charge form factor.* With this definition for the charge operator we proceed to evaluate the quantity

$$S(q) = \int\limits_0^\infty R_L(q,\omega)d\omega \ . \tag{4.22}$$

which, recalling the connection between R_L and Π, also reads

$$S(q) = -\frac{1}{\pi} \int\limits_0^\infty \mathrm{Im}\Pi^{\mathrm{ret}}(q,\omega)d\omega \ = \ -\frac{1}{\pi} \int\limits_0^\infty \mathrm{Im}\Pi(q,\omega)d\omega \ ; \tag{4.23}$$

since the advanced part of the polarization propagator has no imaginary part for positive energies. The Lehmann representation for Π immediately provides

$$S(q) = \sum_{n\neq0} |< \Psi_n|\tilde{\rho}(q)|\Psi_0 >|^2 \tag{4.24}$$

where the charge fluctuation operators $\tilde{\rho}(q)$ has to be thought of in Fourier transform and in Schrödinger picture. To proceed further we only need to apply closure and to explicitly introduce the nuclear ground state, thus arriving at the final, well known result

$$S(q) = Z + Z(Z-1) \int d^3x\, d^3y \, \exp\left\{i\mathbf{q}\cdot(\mathbf{x}-\mathbf{y})\right\} g(\mathbf{x},\mathbf{y}) - Z^2|F(q)|^2 \tag{4.25}$$

$g(\mathbf{x},\mathbf{y})$ being the pair correlation function of the protons inside the nucleus and $F(q)$ the elastic form factor, both normalized to unity at zero momentum transfer. Since it is conceivable that the pair correlation function in Fourier transform vanishes for $\mathbf{q} \to \infty$, we conclude that

$$\lim_{q\to\infty} S(q) = Z. \tag{4.26}$$

This is the Coulomb sum rule. In passing we note that the explicit evaluation of the pair correlation function is possible for simple models; for example the free Fermi gas yields

$$S(q) = \begin{cases} \dfrac{3}{4}\dfrac{q}{k_F}\left(1 - \dfrac{q^2}{12k_F{}^2}\right) & \text{for } q \leq 2k_F, \\[2mm] 1 & \text{for } q > 2k_F, \end{cases} \tag{4.27}$$

which clearly shows the influence of the Pauli correlations for $q \leq 2k_F$.

Now the data presently available for the nuclear charge response refer to momentum transfers presumably still far from the limiting situation (4.26): to assess how much,
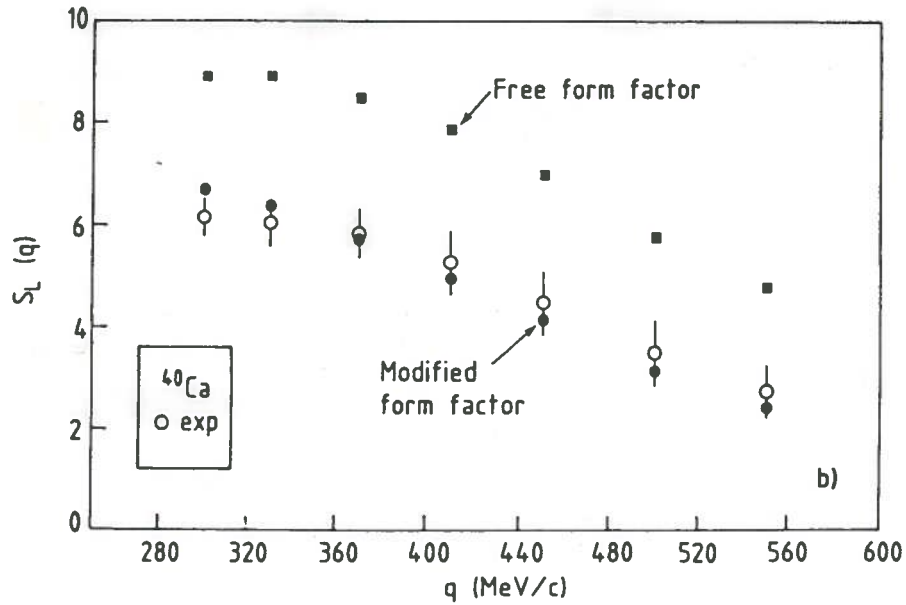
Fig. 4.6 – Coulomb sum rule in Ca^{40}: open circles are the experimental data, the squares represent the RPA sum rule with the free nucleon e.m. form factor, whereas the black points correspond to the modified form factor.

however, it is a very challenging question, also related to the difficulty of disentangling the nucleonic degrees of freedom from the nuclear ones. Indeed the situation illustrated in Fig. 4.6 clearly shows the fall off of the experimental data due to the presence of the nucleon e.m. form factor, which we have not included till now in our considerations.

Assuming, as a working hypothesis, a simple factorization to hold, then the Coulomb sum rule would read

$$\lim_{q \to \infty} \frac{S(q)}{G_E(q^2)} = Z. \tag{4.28}$$

$G_E(q^2)$ being the Sach's electric form factor. If we stick to this minimal (but numerically most relevant) assumption, then the experimental sum rule at the largest measured momentum transfers appears indeed far from the saturation point.

Two possibilities should then be considered: either the frequency integration has been performed over a too narrow range, so that some strength in the sum rule is being missed at higher energies, or correlations of some kind strongly influence the pair distribution function well beyond $2k_F$.

Concerning the first possibility, we have already mentioned that 2p–2h excitations give rise to some strength located in the energy region beyond the QEP (of course

in the space–like region) and the data appear to show that some hard to detect response is indeed there, but it seems doubtful that this can account for the whole missing strength.

The second option instead lead us to question whether the strenght is missing at all. In this connection a correct interpretation of the Coulomb sum rule requires as a preliminary a discussion of the following important points:

1. Can the original assumption (4.20) on the charge operator be trusted? The diagrammatic analysis requires that each diagram entering the perturbative expansion of Π must be multiplied by $G_E^2(q^2)$, hence the factorization of the latter. However this procedure clearly neglects off–shell effects. In fact G_E is just the on–shell representation of the true form factor which, on the other hand, also depends upon the initial and/or final momenta of the nucleon. When inserted into a many body system the nucleon may be off–shell as well and the factorization (4.28) is likely to break down. One recognizes here the interplay between the properties of theory in the vacuum (true QFT effects) and the effects of the medium (many–body effects) and unfortunately a theory handling at the same level the QFT aspects of a process and its many–body corrections is not yet available.

2. The NN correlations also asks for a deeper investigation. We have seen in Sect. 3 the reach variety of Feynman diagrams contributing to the nuclear response. We shall return on this issue in the section dedicated to the functional methods. At present essentially phenomenological calculations have been carried out, for example using the quasi–deuteron model (Ericson *et al.*, 1988), but we don't know yet which Feynman diagrams are being parametrized in it. Also the role of the short range correlations in channels different from the quasi deuteron one is poorly know. Furthermore we are aware of the importance, for the charge response, of the dynamical correlations carried by the pion. These have been explored in the first order of perturbation theory. What about the contribution in second and higher order?

3. Finally the RPA correlations themselves are in need of further studies given their pronounced sensitivity to the density dependence and to the poorly known momentum evolution of the effective p–h interaction. Clearly the RPA correlations vanish at large q thus allowing the recovering of the limiting value of the Coulomb sum rule. However, in this kinematical domain a non–relativistic treatment of the many–body problem is doubtfull. In addition relativity entails that as q becomes large the nucleon form factor acquires a substantial magnetic component: accordingly it might be unwarranted to divide the data by the electric form factor $G_E^2(q^2)$ alone as done in (4.28). We shall return on this most important point in Sect. 6.

4.2 The Spin Response Functions

Unlike their charges, the spins of the nucleons in an atomic nucleus appear to respond to an external electromagnetic field just as a piece of nuclear matter. Indeed the main features of the nuclear spin responses appear to be

1. a certain degree of universality (they change very little all over the nuclear chart),
2. a certain quenching with respect to the independent particle model, as far as the transverse coupling is concerned,
3. a substantial modification of the properties of the Δ resonance, with respect to the ones in the free space, when the latter is involved in the nuclear response.

When discussing the spin responses in nuclei one should realize from the outset that these fall into two categories, namely the spin–transverse and the spin–longitudinal ones, driven by the operators

$$\hat{O}_T = (\boldsymbol{\sigma} \times \mathbf{q})\tau_a \, \exp\{i\mathbf{q}\cdot\mathbf{r}\} \qquad (4.29)$$

and

$$\hat{O}_L = (\boldsymbol{\sigma} \cdot \mathbf{q})\tau_a \, \exp\{i\mathbf{q}\cdot\mathbf{r}\} \qquad (4.30)$$

respectively. Only the transverse response can be induced by an electromagnetic probe, whereas the spin–longitudinal one, which has proved to be quite elusive, requires the use of hadronic projectiles.

The formal treatment of the spin excitations should again include, as for the charge longitudinal channel and at the very least, the Hartree-Fock mean field and the RPA correlations. However, in addition to the short range component of the p–h interaction (4.8), now embodied in the Landau–Migdal parameter g', long range components of the force here come into play as well, at variance with the charge channel.

In the mesonic model these are carried by the pion and by the ρ meson. Accordingly, in the momentum space, the p–h force reads

$$V_L(q,\omega) = \Gamma_\pi^2(q_\mu^2)\frac{f_\pi^2}{\mu_\pi^2}\left\{g'\boldsymbol{\sigma}_1\cdot\boldsymbol{\sigma}_2 - \frac{(\boldsymbol{\sigma}_1\cdot\mathbf{q})(\boldsymbol{\sigma}_2\cdot\mathbf{q})}{q^2+\mu_\pi^2-\omega^2}\right\}(\boldsymbol{\tau}_1\cdot\boldsymbol{\tau}_2) \qquad (4.31)$$

in the spin longitudinal channel and

$$V_T(q,\omega) = \left\{\Gamma_\pi^2(q_\mu^2)\frac{f_\pi^2}{\mu_\pi^2}g'\boldsymbol{\sigma}_1\cdot\boldsymbol{\sigma}_2 - \Gamma_\rho^2(q_\mu^2)\frac{f_\rho^2}{\mu_\rho^2}\frac{(\boldsymbol{\sigma}_1\times\mathbf{q})(\boldsymbol{\sigma}_2\times\mathbf{q})}{q^2+\mu_\rho^2-\omega^2}\right\}(\boldsymbol{\tau}_1\cdot\boldsymbol{\tau}_2) \qquad (4.32)$$

in the spin transverse one. In the above we have arbitrarily ascribed to the parameter g' the momentum evolution of the πNN form factor $\Gamma_\pi(q_\mu^2)$. As already mentioned

in the context of the charge longitudinal response this is a topic which needs further investigations. One should, however, keep in mind that the G-matrix calculations of Dickhoff *et al.* (1981) does not foresee a violent momentum dependence of g' up to 2–2.5 fm^{-1}. The momentum evolution of the p–h direct matrix elements $[\mathcal{V}_L(q,\omega)$ and $\mathcal{V}_T(q,\omega)$, respectively] of the interactions (4.31) and (4.32), at zero frequency, are displayed in Fig. 4.7.
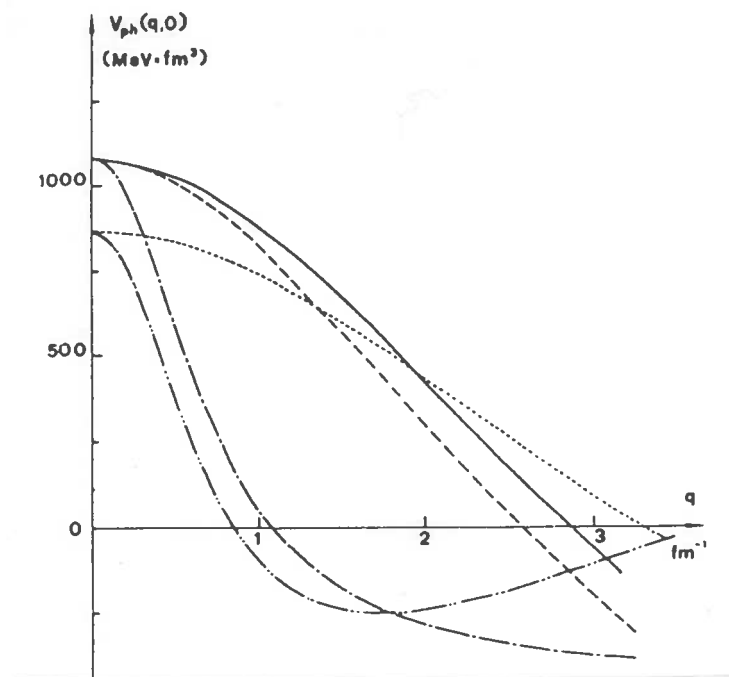

Fig. 4.7 – The spin–transverse and spin–longitudinal particle–hole interactions as a function of q, at zero frequency.

We shall consider later (see Section 5) the expected features of the spin–longitudinal response, as induced by (4.31). Here we focus the attention on the spin–transverse one, as measured by inelastic electron scattering. Arguing along the same lines as we did for the charge response, it is immediately apparent that the transverse p–h force, which is essentially repulsive up to large momenta, will produce quenching and hardening in the $(\boldsymbol{\sigma} \times \mathbf{q})$ RPA response:

$$R_T(q,\omega) = -\frac{\hbar^2 q^2}{2M^2}(\mu_p^2 + \mu_n^2)G_E^2(Q^2)\frac{3\pi A}{k_F^3}\mathrm{Im}\Pi_T^{RPA}(q,\omega)$$

$$= -\frac{\hbar^2 q^2}{2M^2}(\mu_p^2 + \mu_n^2)G_E^2(Q^2)\frac{3\pi A}{k_F^3}$$

$$\times \mathrm{Im} \left\{ \frac{\Pi_N^0(q,\omega) + \Pi_\Delta^0(q,\omega)}{1 - \mathcal{V}_T(q,\omega)[\Pi_N^0(q,\omega) + \Pi_\Delta^0(q,\omega)]} \right\}. \qquad (4.33)$$

In the above the free Δ–hole propagator, Π_Δ^0, has been added to the $N - N^{-1}$ one, since the operator (4.29) can excite the Δ_{33} resonance as well. A more detailed discusssion of this topic will be presented in the next subsection. Here we only remind that the imaginary part of Π_Δ^0, is vanishing in the quasi–elastic peak region, but the real part is quite sizable, thus emphasizing the RPA quenching of the transverse response. Also we notice that, for simplicity, a universal NN, $N\Delta$ and $\Delta\Delta$ interaction is assumed, although a truly realistic calculation should account for the distinction among the various forces. In particular the $N\Delta$ interaction is known to be substantially weaker than the NN one.

Fig. 4.8 shows the comparison of the theoretical curve (4.33) with the experimental, transverse response function of Fe^{56} (Alberico *et al.*, 1982). In the low–energy region the RPA cross section fits the data fairly well, while at higher energies the theoretical curve is lower than the experiment, although it correctly reproduces the hardening of the peak (whereas the free Fermi gas response would fail on both items).
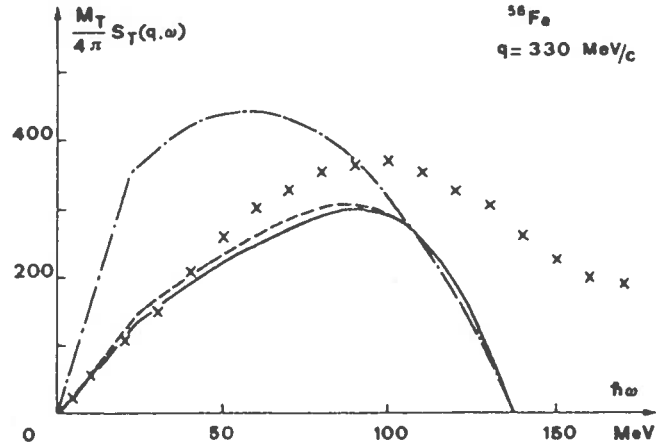
Fig. 4.8 – The separated transverse, magnetic response in Fe^{56} at $q = 330$ MeV/c as a function of $\hbar\omega$. The experimental crosses are taken from Altemus (1980). The continuous line is the RPA response (4.33) with $g' = 0.7$; the dot–dashed line is the free Fermi gas response.

This shortcoming points to the relevance of more complicated excited states: the data in the region of deep inelasticity and in particular in the so–called dip–region

(between the quasi–elastic and the Δ–peak), cannot be accounted for without including 2p–2h states. The latter come naturally into play when two–body currents, beside the nucleonic one, are coupled to the external photon. Among these currents we shall first consider here the longest range components of the MEC, namely the ones mediated by a pion.
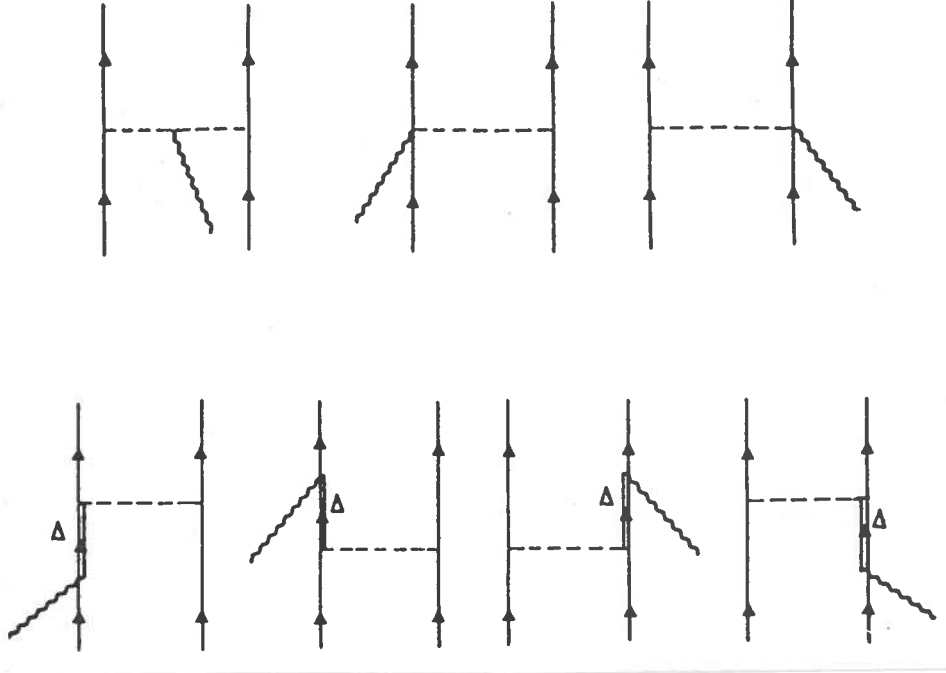

Fig. 4.9 – The meson exchange current diagrams. In the upper graphs the pion–in–flight and contact terms are shown; in the lower graphs the pionic current is coupled to a Δ intermediate state.

In connection with the nuclear quasi–elastic response, the MEC have been first considered by Van Orden and Donnelly (1981). The non–relativistic expression of the mesonic currents associated with the pion read:

$$\mathbf{J}_\pi(\mathbf{p}_1' - \mathbf{p}_1, \mathbf{p}_2' - \mathbf{p}_2)$$
$$= -\frac{4M^2}{V^2} \frac{f_\pi^2}{m_\pi^2} \chi_{s_1'}^\dagger \frac{\sigma \cdot \mathbf{k}_1}{k_1^2 + m_\pi^2} \chi_{s_1} \chi_{s_2'}^\dagger \frac{\sigma \cdot \mathbf{k}_2}{k_2^2 + m_\pi^2} \chi_{s_2}(\mathbf{k}_2 - \mathbf{k}_1) 4t_1 \mathcal{F}_E, \quad (4.34)$$

$$\mathbf{J}_{cont}(\mathbf{p}_1' - \mathbf{p}_1, \mathbf{p}_2' - \mathbf{p}_2) = -\frac{4M^2}{V^2} \frac{f_\pi^2}{m_\pi^2} \left[\chi_{s_1'}^\dagger \sigma \chi_{s_1} \chi_{s_2'}^\dagger \frac{\sigma \cdot \mathbf{k}_2}{k_2^2 + m_\pi^2} \chi_{s_2} \right.$$
$$\left. - \chi_{s_1'}^\dagger \frac{\sigma \cdot \mathbf{k}_1}{k_1^2 + m_\pi^2} \chi_{s_1} \chi_{s_2'}^\dagger \sigma \chi_{s_2} \right] 4t_1 \mathcal{F}_E \qquad (4.35)$$

and

$$\mathbf{J}_\Delta(\mathbf{p}_1' - \mathbf{p}_1, \mathbf{p}_2' - \mathbf{p}_2) =$$
$$\frac{8Mik^*hf_\pi(2M_\Delta + 3M)}{3V^2 m_\pi^2(M_\Delta^2 - M^2)}\left[(\mathbf{q}\times\mathbf{k}_2)\delta_{s_1's_1}\chi_{s_2'}^\dagger\frac{\boldsymbol{\sigma}\cdot\mathbf{k}_2}{k_2^2 + m_\pi^2}\chi_{s_2}2t_2\right.$$
$$\left. + (\mathbf{q}\times\mathbf{k}_1)\chi_{s_1'}^\dagger\frac{\boldsymbol{\sigma}\cdot\mathbf{k}_1}{k_1^2 + m_\pi^2}\chi_{s_1}\delta_{s_2 s_2'}2t_1\right]\mathcal{F}_D \qquad (4.36)$$
$$- \frac{4Mk^*hf_\pi(2M_\Delta + M)}{3V^2 m_\pi^2(M_\Delta^2 - M^2)}\left[\chi_{s1'}^\dagger\frac{\boldsymbol{\sigma}\cdot\mathbf{k}_1}{k_1^2 + m_\pi^2}\chi_{s_1}\chi_{s_2'}^\dagger\mathbf{q}\times(\mathbf{k}_1\times\boldsymbol{\sigma})\chi_{s_2}\right.$$
$$\left. - \chi_{s_1'}^\dagger\mathbf{q}\times(\mathbf{k}_2\times\boldsymbol{\sigma})\chi_{s_1}\chi_{s_2'}^\dagger\frac{\boldsymbol{\sigma}\cdot\mathbf{k}_2}{k_2^2 + m_\pi^2}\chi_{s_2}\right]4t_1\mathcal{F}_E,$$

where

$$\mathcal{F}_E = (1 - \delta_{t_1 t_2})(1 - \delta_{t_1' t_1})(1 - \delta_{(t_2' t_2)}), \qquad (4.37a)$$

$$\mathcal{F}_D = \delta_{t_1' t_1}\delta_{t_2' t_2}. \qquad (4.37b)$$

and $\mathbf{k}_1 = \mathbf{p}_1' - \mathbf{p}_1$, $\mathbf{k}_2 = \mathbf{p}_2' - \mathbf{p}_2$, $\mathbf{q} = \mathbf{k}_1 + \mathbf{k}_2$. The χ's are the standard Pauli spinors, $s_i(s_{i'})$ and $t_i(t_{i'})$ being the third components of the initial (final) nucleonic spin and isospin. The quantities $\mathbf{J}_\pi$, $\mathbf{J}_{cont}$ and $\mathbf{J}_\Delta$ are commonly referred to as the pion–in–flight, contact and delta current, respectively. They are illustrated in Fig. 4.9. In the above expressions $h^2 = 0.29$ and $k^* = 5.0$ are the $\pi N\Delta$ and $\gamma N\Delta$ coupling constants of the Peccei Lagrangian (Peccei, 1968 and 1969), m_π is the pion mass and M_Δ is the mass of the delta resonance.

In addition to these currents one has to consider processes where the photon couples to a pair of correlated nucleons; for consistency (and gauge invariance) requirements one must include at least the pion–correlated two–body current, which is illustrated in Fig. 4.10 and reads (in the non–relativistic limit):

$$\mathbf{J}_{corr}(\mathbf{p}_1'\mathbf{p}_1;\mathbf{p}_2'\mathbf{p}_2) = \frac{4M^2}{V^2}\frac{f_\pi^2}{m_\pi^2}\frac{\chi_{s_2'}^\dagger(\mathbf{k}_2\cdot\boldsymbol{\sigma})\chi_{s_2}}{k_2^2 + m_\pi^2}\left\{\frac{1}{2M\omega - \mathbf{q}\cdot(\mathbf{p}_1' + \mathbf{p}_1 - \mathbf{k}_2)}\right.$$
$$\times\left[\chi_{s_1'}^\dagger i(\boldsymbol{\sigma}\times\mathbf{q})(\mathbf{k}_2\cdot\boldsymbol{\sigma})\chi_{s_1}[(\mu_s + 2t_2\mu_v)\mathcal{F}_E + t_2(\mu_v + 2t_1\mu_s)\mathcal{F}_D]\right.$$
$$\left. + (\mathbf{p}_1' + \mathbf{p}_1 - \mathbf{k}_2)\chi_{s_1'}^\dagger(\mathbf{k}_2\cdot\boldsymbol{\sigma})\chi_{s_1}[(1 + 2t_2)\mathcal{F}_E + t_2(1 + 2t_1)\mathcal{F}_D]\right]$$
$$- \frac{1}{2M\omega - \mathbf{q}\cdot(\mathbf{p}_1' + \mathbf{p}_1 + \mathbf{k}_2)}\left[\chi_{s_1'}^\dagger i(\mathbf{k}_2\cdot\boldsymbol{\sigma})(\boldsymbol{\sigma}\times\mathbf{q})\chi_{s_1}\right.$$
$$\times[(\mu_s - 2t_2\mu_v)\mathcal{F}_E + t_2(\mu_v + 2t_1\mu_s)\mathcal{F}_D]$$
$$\left.\left. + (\mathbf{p}_1' + \mathbf{p}_1 + \mathbf{k}_2)\chi_{s_1'}^\dagger(\mathbf{k}_2\cdot\boldsymbol{\sigma})\chi_{s_1}[(1 - 2t_2)\mathcal{F}_E + t_2(1 + 2t_1)\mathcal{F}_D]\right]\right\}$$
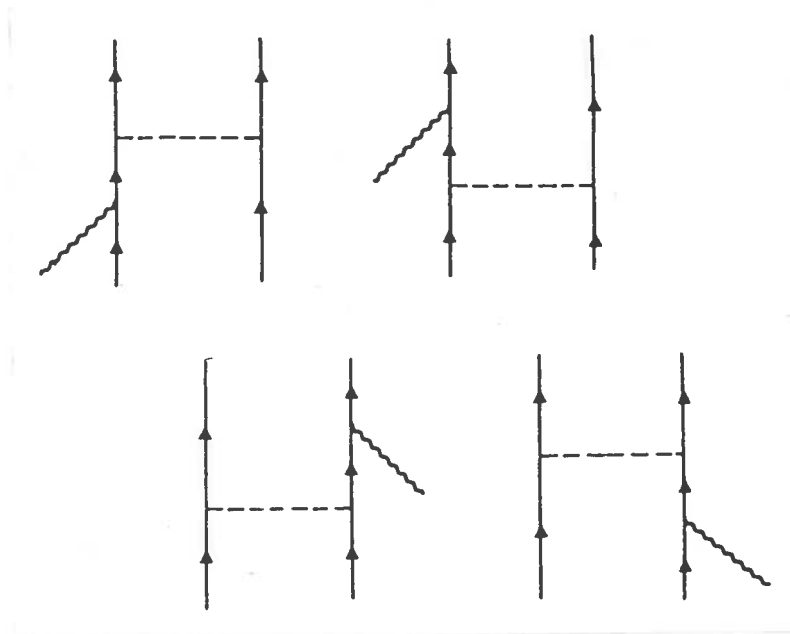$$+ \{1 \longleftrightarrow 2\}, \qquad (4.38)$$

Fig. 4.10 – Diagrams for the coupling of a photon to a pair of correlated nucleons (π–correlation "current").

Once inserted into (4.4) (with $|2p2h>$ intermediate states) the above currents provide three different classes of contributions to the transverse response:

1. pure MEC response,
2. pure two–body π–correlations,
3. interference MEC–correlations.

It is important to note that the contributions of class 2 coincide with the ones derived in second–order perturbation theory for the polarization propagator (see Subsection 3.1), as far as the NN interaction is mediated by the pion only.

The explicit evaluation of the spin–transverse response associated with some of the above 2p-2h contributions can be found in (Alberico et al., 1984). Fig. 4.11 illustrates their relevance: indeed the 2p-2h response (which is added incoherently to the RPA one) remarkably improve the agreement with the data in the quasi–elastic peak region. At the same time they yield a significant contribution in the energy range between the quasi–elastic and the Δ–peak.

Before concluding this section let us briefly consider the spin–response within a finite nucleus RPA framework. Here of course the loss of translational invariance does not allow to write simple expressions like (4.33) for Π^{RPA}. In fact, the calculation of
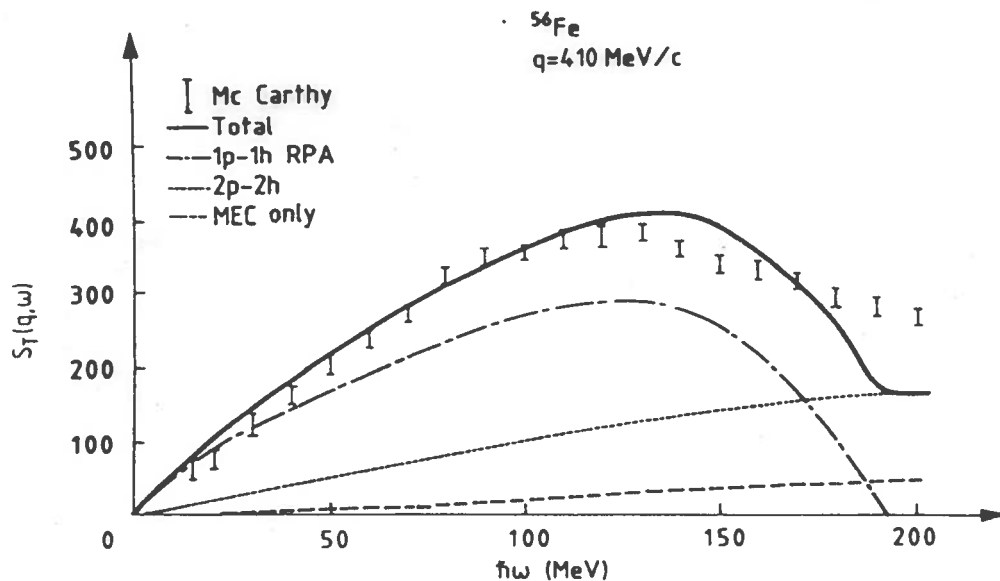
Fig. 4.11 – The separated transverse magnetic response in Fe^{56} at $q = 410$ MeV/c as a function of $\hbar\omega$. The experimental points are taken from (McCarthy, 1980). The dot–dashed line is the pure RPA response, while the continuous line contains, in addition, the whole 2p–2h contribution.

the spin-isospin (σ, τ) responses in the nuclei requires, in principle, the solution of three coupled integral equations, a situation contrasting the nuclear matter problem which reduces to two uncoupled, algebraic equations only. The detailed treatment of the spin–isospin RPA responses in nuclei will be presented in Section 5. It is worth pointing out here that the resulting transverse electromagnetic response does not differ dramatically from the nuclear matter one [see (Alberico *et al.*, 1986)]; indeed the electron can penetrate well inside the nucleus, thus probing the bulk of the nuclear density, which is fairly well described already in nuclear matter. An example of this finite nucleus RPA calculation is shown in Fig. 4.12.

4.3 The Δ–Excitation

Above the quasi–elastic peak, the spin–transverse response displays an impressive, broad peak, which is associated with the excitation of the Δ_{33}–resonance. For energies above the π–threshold, the Δ can be directly excited by a transverse photon, through the vertex $\gamma N\Delta$. The complicated structure of this vertex (Jones and Scadron, 1973) is known to be dominated by the M1 term. The corresponding
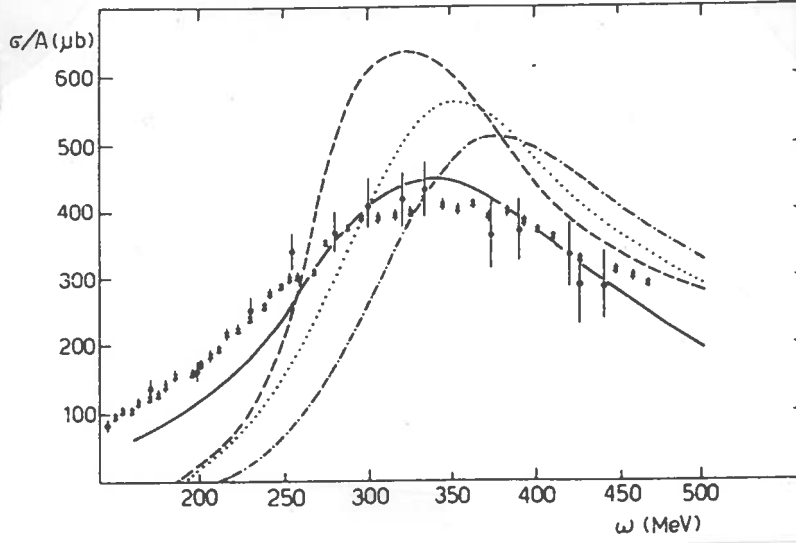
Fig. 4.12 – The separated transverse magnetic response in Ca^{40} at $q = 410$ MeV/c as a function of $\hbar\omega$. The experimental points are taken from (Meziani *et al.*, 1984,1985). The dashed line is the finite nucleus RPA response, the continuous line is obtained by adding the 2p–2h contribution evaluated in nuclear matter.

(transverse) current, in momentum space, reads

$$\hat{\mathbf{J}}_\Delta(\mathbf{q}) = \mathbf{q} \times \hat{\mathbf{j}}(\mathbf{q}) \qquad (4.39)$$

with

$$\hat{\mathbf{j}}(\mathbf{q}) = \frac{f_{\gamma N\Delta}}{m_\pi} \int d^3p\, \hat{\psi}_\Delta^\dagger(\mathbf{p} + \mathbf{q}) S T_3 \hat{\psi}(\mathbf{p}) + \text{h.c.}, \qquad (4.40)$$

$\psi_\Delta(x)$ being a 4–component non–relativistic isospinor and S and T the spin and isospin transition operators converting a nucleon into a Δ. A relativistic treatment of the Rarita–Schwinger field would be also possible (Peccei, 1969; Weber and Arenövel, 1978) but only at the tree level. However, since in the following self–energy insertions for the Δ–propagator, which require renormalization, will be considered a non–relativistic fully renormalizable scheme is preferable (Cenni and Dillon, 1980).

The main experimental features of the cross section associated with (4.39) are:
  a) the total cross section in the Δ-region is essentially linear with A,
  b) the Δ-peak appears remarkably larger in a nucleus than in the vacuum.

The first property, experimentally established by Chollet *et al.* (1983) for the Δ–photoexcitation and by O'Connell *et al.* (1984) for the electro–excitation, is simply

interpreted in terms of a sum rule, which closely reminds the Coulomb sum rule described in Subsection 4.1. Indeed, in the hypothesis of the "Δ-dominance", which simulates with an effective $\gamma N \Delta$ coupling the excitation of the Δ, the associated response function reads:

$$R_T(q,\omega) = \frac{1}{4\pi} \sum_{\lambda = \pm 1} \sum_n \delta(E_n - E_0 - \hbar\omega)$$

$$\times \left| \epsilon_\lambda \cdot <\Psi_n| \int d^3r \, \hat{\mathbf{J}}_\Delta(\mathbf{r}) \exp\{-i\mathbf{q}\cdot\mathbf{r}\}|\Psi_0> \right|^2 \qquad (4.41)$$

and the corresponding sum rule is:

$$S_\Delta(q) \equiv \int d\omega \, R_T(q,\omega) \qquad (4.42)$$

$$= \frac{1}{4\pi} \sum_{\lambda = \pm 1} <\Psi_0| \int d^3r \, d^3r' \, \hat{\mathbf{J}}_\Delta^\dagger(\mathbf{r}') \cdot \hat{\mathbf{J}}_\Delta(\mathbf{r}) \exp\{i\mathbf{q}\cdot(\mathbf{r}' - \mathbf{r})\}|\Psi_0> .$$

In (4.42) the evaluation of the remaining integrals is straightforward *if no Δ are present in the ground state*. In such a case $<\Psi_0|\hat{\psi}_\Delta^\dagger(\mathbf{r}')\hat{\psi}_\Delta(\mathbf{r})|\Psi_0> = \delta(\mathbf{r}' - \mathbf{r})$ and the remaining operators, at variance with the Coulomb sum rule, do not introduce correlations, but simply count the number of nucleons, yielding (Cenni *et al.*, 1985)

$$S_\Delta(q) = \frac{q^2}{4\pi} \frac{8}{9} A . \qquad (4.43)$$

The above sum rule is supported by theoretical estimates of the Δ-component in the nuclear ground state, which turns out to be about 5% (Anastasio *et al.*, 1979; Cenni *et al.*, 1989).

An analogous result, for the photon absorption in the Δ region, may be obtained from the corresponding cross section

$$\sigma(\omega) = \frac{1}{2} \sum_{\lambda = \pm 1} \sum_n \delta(E_n - E_0 - \hbar\omega)$$

$$\times \frac{\pi}{\omega} \left| \epsilon_\lambda \cdot <\Psi_n| \int d^3r \, \hat{\mathbf{J}}_\Delta(\mathbf{r}) \exp\{-i\omega\hat{\mathbf{q}}\cdot\mathbf{r}\}|\Psi_0> \right|^2 . \qquad (4.44)$$

With the approximation $E_n - E_0 \approx \hbar\omega_R$ (the resonance energy), some simple algebra leads then to the energy-weighted sum rule (Cenni *et al.*, 1984; Arenhövel and Giannini, 1985)

$$\int d\omega \, \sigma(\omega) = \frac{\pi}{2} \frac{f_{\gamma N\Delta}}{m_\pi^2} \sum_{\lambda = \pm 1} \int d^3r \, d^3r' \, \exp\{i\omega_R\hat{\mathbf{q}}\cdot(\mathbf{r} - \mathbf{r}')\}$$

$$\times <\Psi_0|[\hat{j}_\lambda(\mathbf{r}),[\hat{H},\hat{j}_\lambda(\mathbf{r}')]]|\Psi_0> , \qquad (4.45)$$
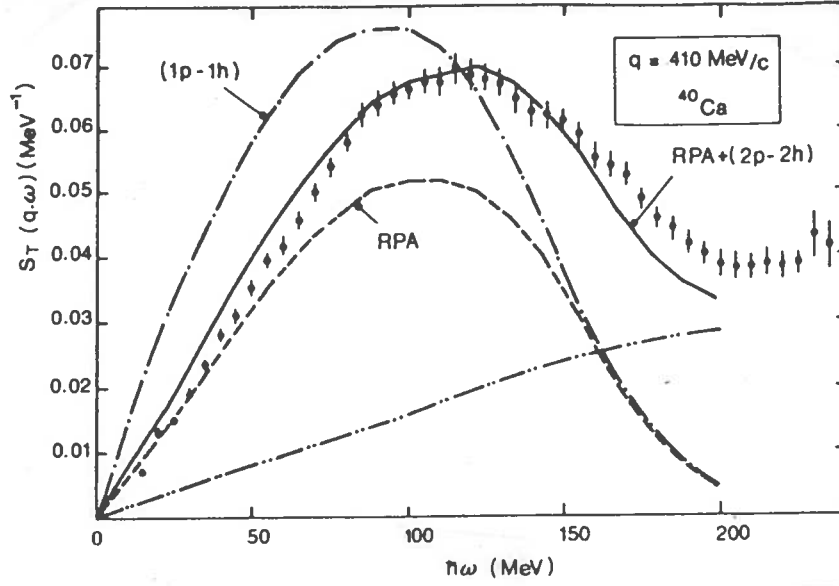
Fig. 4.13 – Photoabsorption cross section per nucleon: data are taken from Chollet *et al.*, (1983). The dashed line represents the predictions of the free Fermi gas model ($k_F = 1.3\mathrm{fm}^{-1}$), the dotted and dot–dashed lines correspond to an RPA model with ρ–exchange and short range correlations ($g' = 0.3$ and $g' = 0.5$, respectively). The solid line is the result of the self–consistent calculation ($g' = 0.3$) of Cenni *et al.*, (1984). The effective value of $f_{\gamma N\Delta}$ is 0.116, according to Koch and Moniz (1979).

where

$$\hat{H} = \hat{T}_N + \hat{T}_\Delta + \hat{U}_\Delta + \hat{V}_{NN}. \tag{4.46}$$

is the total hamiltonian of the system, $\hat{T}_N$ and $\hat{T}_\Delta$ the non–relativistic kinetic energies of nucleons and Δ's, $\hat{V}_{NN}$ the NN potential and

$$\hat{U}_\Delta = \delta M \int d^3 r \, \hat{\psi}_\Delta^\dagger(\mathbf{r})\hat{\psi}_\Delta(\mathbf{r}). \tag{4.47}$$

accounts for the mass difference between N and Δ. The sum rule (4.45) becomes then:

$$\int d\omega \, \sigma(\omega) = \frac{4\pi}{9} \frac{f_{\gamma N\Delta}}{m_\pi^2} \left[\delta M \, A + \frac{\hbar \omega_R^2}{2M_\Delta} A - \frac{\delta M}{M_\Delta} < T_N > -2 < V_{NN} > \right], \tag{4.48}$$

where only the last two terms in the r.h.s. may get a contribution from the surface of the nucleus. However they are quite small, being of the same order of magnitude of the nuclear binding energy, while the first term, proportional to the mass difference between N and Δ, is ten times larger. Thus the latter, clearly a volume effect, dominates the sum rule (4.48).

For what concerns the shape of the Δ–peak, the experimental data show that its width is remarkably increased with respect to the free resonance. The interpretation of this finding requires a more detailed knowledge of the Δ dynamics in the medium. The simplest approach to describe the Δ–peak utilizes a Δ-hole propagator similar to the free p–h propagator of the Fermi gas:

$$\Pi^0_\Delta(k,\omega) = \frac{16}{9} \int \frac{d^3 p}{(2\pi)^3} \frac{\theta(k_F - p)}{\hbar\omega + \frac{\hbar^2 p^2}{2M} - \delta M - \frac{\hbar^2(\mathbf{p} + \mathbf{k})^2}{2M_\Delta} + \frac{i}{2}\Gamma_\Delta(\omega)} \tag{4.49}$$

which accounts for the natural width of the Δ in the vacuum, Γ_Δ, (somewhat simplifying the kinematics, however, in order to facilitate the analytical evaluation of (4.49) (Brown and Weise, 1975; Cenni and Dillon, 1983). Within this scheme, which embodies the spreading of the peak due to the Fermi motion, the nuclear response both to real and virtual photons is easily evaluated (see, for example the dashed line of Fig. 4.13 and the dash–dotted lines of Fig. 4.14). Clearly the shape is badly reproduced, since the height of the peak is overestimated and the Fermi motion spreading is insufficient to explain the width of the resonance inside the medium.

One is thus lead to consider the effect of the medium on the Δ propagation. Since the dominant dynamics of the Δ–resonance is the one of a strongly interacting $\pi - N$ pair, the most relevant self–energy diagram for the Δ is, likely, the one illustrated in Fig. 4.15. The nuclear medium affects this diagram in two different ways:

i) inside the medium the Pauli principle substantially blocks the intermediate states available for the nucleon (Cenni and Dillon, 1980; Moniz and Sevgen, 1981) yielding (contrary to the experimental evidence) a narrowing of the resonance;

ii) self-energy corrections, induced by the nuclear medium, affect the pion propagator. In other words the internal pion line in Fig. 4.15 are dressed by p–h and Δ–h insertions. Actually this effect is the dominant one.

Formally the pion self–energy may be expressed as

$$\Sigma_\pi(q,\omega) = \Sigma^{(N)}_\pi(q,\omega) + \Sigma^{(\Delta)}_\pi(q,\omega) \tag{4.50}$$

where

$$\Sigma^{(N)}_\pi(q,\omega) = -4\frac{f^2_{\pi NN}}{m^2_\pi}q^2 v^2_N(q^2) \int \frac{d^3 p}{(2\pi)^3}\frac{dE}{2\pi i}G(|\mathbf{p} - \mathbf{q}|, E - \omega)G(p, E) \tag{4.51}$$

and

$$\Sigma^{(\Delta)}_\pi(q,\omega) = -\frac{16}{9}\frac{f^2_{\pi N\Delta}}{m^2_\pi} \int \frac{d^3 p}{(2\pi)^3}\frac{dE}{2\pi i}k^2 v^2_\Delta(k^2)G(|\mathbf{p} - \mathbf{q}|, E - \omega)G_\Delta(E, p) \tag{4.52}$$
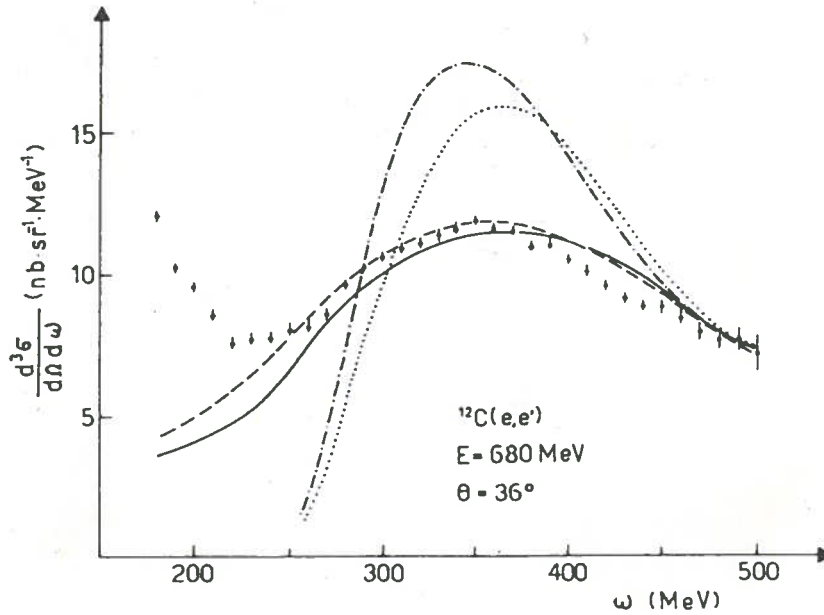
Fig. 4.14 – The (e, e') cross section on C^{12} at fixed scattering angle, in the Δ region: data are taken from Barreau *et al.*, (1983). The dot–dashed line represents the free Fermi gas predictions ($k_F = 1.3\text{fm}^{-1}$), the dotted line corresponds to an RPA model with ρ–exchange and short range correlations ($g' = 0.3$), the solid and dashed lines are the result of the self–consistent calculation of Cenni and Dillon, (1984), with two different choices of the model parameters.

correspond to the p–h and Δ–h insertions, respectively. In the above G denotes the nucleon propagator, for example in the HF approximation, and G_Δ is the Δ propagator

$$G_\Delta(p, e) = \frac{1}{E - \dfrac{p^2}{2M_\Delta} - \delta M + \dfrac{i}{2}\Gamma(E - \dfrac{p^2}{2M_\Delta}) - \Sigma_\Delta(p, E)}. \qquad (4.53)$$

Strictly speaking the Δ–self-energy should account for both the renormalization in the vacuum and the corrections induced by the medium. Actually the free width Γ corresponds to the renormalized self-energy in the vacuum and all the many–body contributions are accounted for by Σ_Δ. Two phenomenological form factors, v_N and v_Δ, have also been introduced. It is worth pointing out that in the Δ–h polarization propagator the relative momentum k of the πN pair intervenes, instead of the pion momentum q. [2]

---

[2] Vertex corrections, parametrized as usual with the Landau parameter g', should

The Δ–self–energy in the propagator (4.53) reads instead

$$\Sigma_\Delta(p,E) = -\frac{f_{\pi N\Delta}^2}{m_\pi^2} \int \frac{d^3q}{(2\pi)^3} \frac{d\omega}{2\pi i} (\mathbf{S} \cdot \mathbf{k})(\mathbf{S}^\dagger \cdot \mathbf{k})\{G(|\mathbf{p} - \mathbf{q}|, E - \omega)\Delta(q,\omega)$$
$$- G_{k_F=0}(|\mathbf{p} - \mathbf{q}|, E - \omega)\Delta_{k_F=0}(q,\omega)\} \qquad (4.54)$$

where the contribution of the vacuum has been subtracted out to ensure renormalization and $\Delta(q,\omega)$ is the pion propagator in the medium:

$$\Delta(q,\omega) = \frac{1}{\omega^2 - q^2 - m_\pi^2 - \Sigma_\pi(q,\omega)}. \qquad (4.55)$$

The set of equations (4.50)–(4.55) forms a system of coupled non–linear integral equations for the unknown complex functions $\Sigma_\pi^{(\Delta)}$ and Σ_Δ.
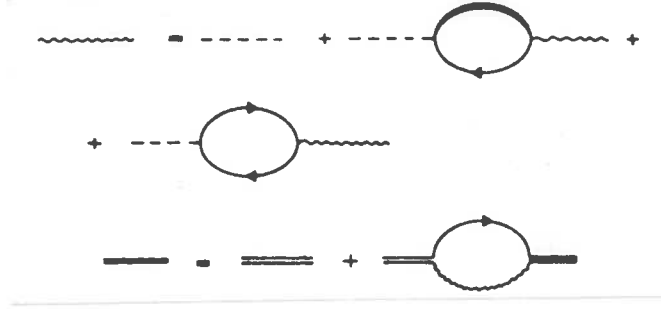
Fig. 4.15 – The coupled Dyson equations, which define the π– and Δ– propagators in a self–consistent way.

To solve this problem is clearly very difficult. However, a numerical solution has been found (Cenni *et al.*, 1981; Cenni and Dillon, 1983), utilizing the so–called "quasi–particle approximation" (QPA) for both the pion and the Δ propagators. Within QPA the two propagators display a single–pole structure, reading

$$G_\Delta(p,E) = \frac{Z(p)}{E - E^*(p) + \frac{i}{2}\Gamma(p,E)} \qquad (4.56)$$

and

$$2\omega_q\Delta(q,\omega) = \frac{z(q)}{\omega - \omega(q) + \frac{i}{2}\gamma(q,\omega)}, \qquad (4.57)$$

also be accounted for. Here they are neglected for sake of simplicity. See (Cenni and Dillon, 1983) for details.
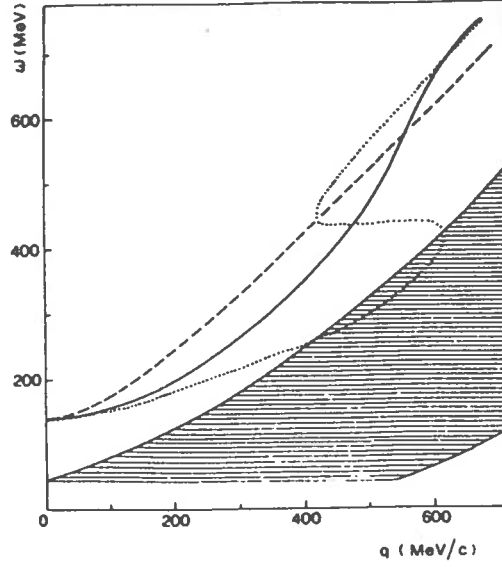
Fig. 4.16 – The self-consistent π–dispersion relation in the medium at $k_F = 1.36$ fm^{-1} (solid line) compared to the first–order result (dotted line). The dashed line is the free π–dispersion relation. The hatched area corresponds to the p–h excitation region.

the widths being approximated by

$$\Gamma(p, E) \simeq \Gamma(p, E(p)) + (E - E(p))\frac{\partial \Gamma}{\partial E}\Big|_{E=E(p)}, \qquad (4.58a)$$

$$\gamma(q, \omega) \simeq \gamma(q, \omega(q)) + (\omega - \omega(q))\frac{\partial \gamma}{\partial \omega}\Big|_{\omega=\omega(q)}. \qquad (4.58b)$$

Then the problem reduces to solve a set of coupled equations for the dispersion relations $E(p)$, $\omega(q)$, the residua and the widths. The obtained solutions display a non–trivial structure: for example, already by approximating the pion self–energy with its lowest order value [i.e. neglecting Σ_Δ in eq. (4.53)], the so–called multiple eigenmodes of propagation appear (Lenz, 1975; Moniz, 1975; Lenz and Moniz, 1975). In fact for a fixed momentum q the pion propagator may display three different poles (see, e.g., the dotted line of Fig. 4.16), which implies that the iterative procedure starting from $\Sigma_\Delta = 0$ breaks down. Choosing a more convenient starting point convergence is instead achieved after a rather small number of iterations. In Fig. 4.16 the pion dispersion relation coming from the solution of the above set of integral equations is also displayed.

A few comments are in order on this approach to the Δ propagator:

1) the procedure, by summming up a complicated series of diagrams with any number of p–h excitations, should yield a substantial increase of the Δ–width (as well as of the one of the pion). The relevance of many particles–many holes excitations in the Δ self–energy has also been emphasized recently by Oset and Salcedo (1987).

2) The QPA is still valid even if it breaks down at the lowest order. Nevertheless QPA badly accounts for off-shell effects. Moreover other diagrams, which are expected to be weakly momentum– and energy–dependent (at least around the Δ mass shell) have been neglected (for instance the direct Δ interaction with the surrounding medium). To account phenomenologically for these effects one could add a potential V_0 (eventually complex) to the Δ self–energy. Obviously how to determine V_0 and how to go beyond the QPA remain open questions.

Once the solution of the self–consistent equations has been obtained, the polarization propagator and the response function follow. This has been done by Cenni *et al.* (1985) for the case of the photon absorption (Fig. 4.13) and by Cenni and Dillon (1984) for the case of the electron scattering (Fig. 4.14) with a satisfactory agreement between theory and experimental data. One would thus conclude that the present approach appropriately describes the Δ dynamics in the medium *at least in the region of the resonance*. However off–shell behaviour, short–range correlations and other possible effects (providing they are slowly varying with energy and momentum) are instead parametrized. Consequently the present approach should be improved upon before being extended, e.g., to the dip–region, in particular in order to avoid double–counting with the contributions discussed in the Subsection 4.2.

5. THE NUCLEAR RESPONSES TO HADRONIC PROBES IN THE SPIN–ISOSPIN CHANNEL

Many efforts have been made in the recent years to understand the spin–isospin nuclear responses, both experimentally and theoretically. In the low energy region the strong NN interaction induces collective effects giving rise to the well established giant Gamow–Teller (GT) resonance (Gaarde *et al.*,1982) and, as we have seen in Section 4, to a pronounced quenching and hardening of the transverse e.m. structure function. The collective nature of the $\sigma\tau$ responses at finite momentum transfers, however, seems still to be somewhat elusive, particularly in the pionic channel.

Indeed, only hadronic [e.g. (p,p')] or semihadronic [e.g. $(e,e'\pi)$] probes are suitable to measure both the spin–transverse and the spin–longitudinal nuclear responses, but they cannot penetrate the nuclear interior owing to the strongly absorptive hadron–nucleus interaction. As a consequence, what is actually probed in a hadronic process is the *surface* response of the nucleus rather than the *volume* one. A relevant

question is then to ascertain how much of the collective features of a volume response are left out in a surface one.

Experimentally two attempts have been made, until now, to unravel collective effects in the $\sigma\tau$ nuclear responses at finite momentum transfers. The first one, carried out in Los Alamos (Carey *et al.*, 1984; Rees *et al.*, 1986), measured the polarization transfer coefficients in the deep inelastic, inclusive, polarized (p,p') scattering. The ratio $\mathcal{R}$ between the spin–longitudinal $(R_L^{\sigma\tau})$ and spin–transverse $(R_T^{\sigma\tau})$ responses, a critical test of their contrast, can then be extracted. A second experiment, which however cannot *explicitly* separate the transverse and longitudinal channels, measured the charge–exchange (He^3, t) reaction cross section in a wide range of momentum and energy transfers (Bergqvist *et al.*, 1987).

Before commenting on these data, let us briefly remind the naive nuclear matter theoretical expectations (obviously referring to volume responses). In this framework the RPA responses driven by the operators (3.29) and (3.30) read:

$$R_{L(T)}^{\sigma\tau}(q,\omega) = -\frac{2A}{\pi\rho}\,\mathrm{Im}\Pi_{L(T)}^{RPA}(q,\omega) = -\frac{2A}{\pi\rho}\,\mathrm{Im}\left\{\frac{\Pi^0(q,\omega)}{1-\mathcal{V}_{L(T)}^{ph}(q,\omega)\Pi^0(q,\omega)}\right\}, \quad (5.1)$$

where $\mathcal{V}_{L(T)}$ is the direct $\sigma,\tau = 1$ p–h matrix element of the interaction (4.31) [(4.32), respectively] and $\Pi^0 = \Pi_N^0 + \Pi_\Delta^0$.

The effects on the transverse response of the (essentially repulsive) p–h force $\mathcal{V}_T$ have been already discussed at length in the Subsection 4.2 [actually (4.33) and the above $R_T^{\sigma\tau}$ differ by trivial factors]. Instead, for momenta larger than, say, 1 fm^{-1} the attractive nature of $\mathcal{V}_L$ (see for example Fig. 4.7) should induce a softening and an enhancement in the spin–longitudinal response. It is worth stressing that these features would reflect the strengthening of the pion field inside the nucleus, clearly a precursor effect of the pion condensation in nuclei. Indeed, in a schematic notation, the longitudinal polarization propagator can be rewritten as follows:

$$\Pi_L^{RPA}(q,\omega) = \frac{\Pi^0(q,\omega)}{1-(g'+V_\pi)\Pi^0(q,\omega)} \quad (5.2)$$

$$= \frac{\Pi^0(q,\omega)}{1-g'\Pi^0(q,\omega)}\frac{1}{1-V_\pi\frac{\Pi^0(q,\omega)}{1-g'\Pi^0(q,\omega)}} = \frac{\Pi^0(q,\omega)}{1-g'\Pi^0(q,\omega)}\frac{\Delta^{RPA}(q,\omega)}{\Delta^0(q,\omega)}$$

which clearly shows how the RPA dressed π–propagator (Δ^{RPA}) becomes larger than the bare one (Δ^0), since the repulsive g' obviously lowers $\Pi^0(q,\omega)$.

According to the previous considerations, there exists an intermediate range of momentum transfers for which, being $\mathcal{V}_T$ repulsive and $\mathcal{V}_L$ attractive, the collective

RPA effects on the corresponding responses should be quite different: in particular, one would expect large values for the ratio $\mathcal{R} = R_L^{q\tau}/R_T^{q\tau}$ at low frequencies and for momenta of the order of $1.8 \div 2 \text{ fm}^{-1}$.

The measurement of this ratio, obtained with polarized proton scattering on ^{40}Ca and ^{208}Pb, has shown no evidence for such an enhancement of $\mathcal{R}$ (Carey et al., 1984; Rees et al., 1986). This finding points to the inadequacy of a nuclear matter treatment for comparing with hadronic processes.[3] In particular no mixing between the spin–transverse and spin–longitudinal couplings affects the RPA treatment of the translationally invariant nuclear matter. Now the above mentioned, different collective behaviours of the two channels arise from the opposite nature of the longitudinal and transverse p–h forces; therefore a mixing between the two spin–couplings, which occurs in finite systems, could partly smear out the sharp effects predicted in nuclear matter.

5.1 Volume Spin–Isospin Responses

Before dealing specifically with hadronic responses, we shall develop here (with some more details than in Sects. 3 and 4) the RPA theory for the spin–isospin responses in finite nuclei. In this context it is both appropriate and advisable to distinguish between *volume* and *surface* responses, according to the leptonic or hadronic nature of the external probe. Indeed if the projectile is, e.g., an electron, it can penetrate deeply inside the target nucleus, thus involving any nucleon in the nuclear volume. On the contrary, the incoming wavefunction of an hadronic projectile can be distorted by the strong interaction and eventually get absorbed within a short distance from the surface of the target nucleus. In this case the peripheral nucleons only will directly respond to the external probe (Esbensen et al., 1985).

Let us then consider the $\sigma\tau$ polarization propagators in nuclei. Since in the finite system translational invariance no longer holds, one can now define three different p–h polarization propagators, according to the nature of the operators ($\hat{O}_L$ or $\hat{O}_T$) in the two (external) vertices: transverse–transverse ($\Pi_{ma,nb}$), longitudinal–longitudinal ($\Pi_{a,b}$) and transverse–longitudinal ($\Pi_{a,mb}$ or $\Pi_{ma,b}$), the latter being identically zero in nuclear matter.

The RPA equations for these propagators read (a,b,c,d are isospin indices):

$$\Pi_{ma,nb}^{RPA}(\mathbf{q},\mathbf{q}';\omega) = \Pi_{ma,nb}^0(\mathbf{q},\mathbf{q}';\omega) + \int \frac{d\mathbf{k}}{(2\pi)^3} \Pi_{ma,c}^0(\mathbf{q},\mathbf{k};\omega) V_{cd}^L(k) \Pi_{d,nb}^{RPA}(\mathbf{k},\mathbf{q}';\omega)$$

---

[3] It should also be kept in mind, however, that a consistent isoscalar contamination in the experimental ratio, as compared with the purely isovector theoretical one, can be responsible for a sizable reduction of the collective effects on $\mathcal{R}$.

$$+ 4 \sum_{l=0,\pm 1} \int \frac{d\mathbf{k}}{(2\pi)^3} \Pi^0_{ma,lc}(\mathbf{q},\mathbf{k};\omega) V^T_{cd}(k) \Pi^{RPA}_{ld,nb}(\mathbf{k},\mathbf{q}';\omega), \quad (5.3a)$$

$$\Pi^{RPA}_{a,b}(\mathbf{q},\mathbf{q}';\omega) = \Pi^0_{a,b}(\mathbf{q},\mathbf{q}';\omega) + \int \frac{d\mathbf{k}}{(2\pi)^3} \Pi^0_{a,c}(\mathbf{q},\mathbf{k};\omega) V^L_{cd}(k) \Pi^{RPA}_{d,b}(\mathbf{k},\mathbf{q}';\omega)$$

$$+ 4 \sum_{l=0,\pm 1} \int \frac{d\mathbf{k}}{(2\pi)^3} \Pi^0_{a,lc}(\mathbf{q},\mathbf{k};\omega) V^T_{cd}(k) \Pi^{RPA}_{ld,b}(\mathbf{k},\mathbf{q}';\omega), \quad (5.3b)$$

$$\Pi^{RPA}_{a,nb}(\mathbf{q},\mathbf{q}';\omega) = \Pi^0_{a,nb}(\mathbf{q},\mathbf{q}';\omega) + \int \frac{d\mathbf{k}}{(2\pi)^3} \Pi^0_{a,c}(\mathbf{q},\mathbf{k};\omega) V^L_{cd}(k) \Pi^{RPA}_{d,nb}(\mathbf{k},\mathbf{q}';\omega)$$

$$+ 4 \sum_{l=0,\pm 1} \int \frac{d\mathbf{k}}{(2\pi)^3} \Pi^0_{a,lc}(\mathbf{q},\mathbf{k};\omega) V^T_{cd}(k) \Pi^{RPA}_{ld,nb}(\mathbf{k},\mathbf{q}';\omega), \quad (5.3c)$$

It is worth pointing out that in using the operators (3.29) and (3.30), we are necessarily dealing with volume responses. In fact the plane wave $\exp\{i\mathbf{q}\cdot\mathbf{r}\}$ is nothing but the product of the undistorted incoming and outgoing waves of the projectile.

As in the example illustrated in Section 3, we shall describe the nucleus within the usual HO shell model, with the residual p–h interactions (4.31) and (4.32): in this framework the independent particle propagators, can be analytically evaluated [see, e.g., eq. (3.37) for $\Pi^0_{a,b}$]. The eqs. (5.3) are integral equations, coupled among each other through the *mixed* propagator $\Pi_{a,nb}$. Notably, in (5.3a) and (5.3b) both interactions V_L and V_T are present, at variance with the corresponding RPA equations for nuclear matter. This mixing between the $(\boldsymbol{\sigma}\times\mathbf{q})$ and $(\boldsymbol{\sigma}\cdot\mathbf{q})$ couplings, although differently weighted in the two channels, tends to smear out the contrast between the collective features of the longitudinal and transverse responses.

By performing the usual multipole expansion in the angular momentum basis, the three above equations reduce to the *unique* set of RPA integral equations (3.44) for the different multipolarities (which embody the dynamical part of the propagators). It is clear from eqs. (5.3) (as remarked in Section 3) that the p–h force entering into (3.44) is the full spin–isospin interaction, including both the longitudinal and transverse components:

$$[U_J(k,\omega)]_{l_1 l_2} = a_{Jl_1} \mathcal{V}_L(k,\omega) a_{Jl_2} + \mathcal{V}_T(k,\omega)(\delta_{l_1 l_2} - a_{Jl_1} a_{Jl_2}), \quad (5.4)$$

with the a_{Jl} given by (3.41).

The equations (3.44) have been solved (Alberico *et al.*, 1986) with an approximate method, originally proposed by Toki and Weise (Toki and Weise, 1979), which exploits the quasi–diagonality of the propagators in momentum space, a property well satisfied for medium–heavy nuclei and in the quasi–elastic peak region. This approximate, algebraic solution of eqs. (3.44) requires the introduction of an average

momentum $\bar{q}$, whose value for fixed q, ω and J is set by certain mathematical relations. This represents a convenient shortcut to the heavy numerics entailed by the continuum RPA equations with finite range forces.

The transverse and longitudinal $\sigma\tau$ responses:

$$R_T^{\sigma\tau}(q,\omega) = -\frac{1}{\pi} \sum_{m,n} \delta_{m,n} \mathrm{Im}\, \Pi_{m3,n3}(\mathbf{q},\mathbf{q};\omega), \qquad (5.5)$$

$$R_L^{\sigma\tau}(q,\omega) = -\frac{1}{2\pi} \mathrm{Im}\, \Pi_{3,3}(\mathbf{q},\mathbf{q};\omega), \qquad (5.6)$$

can then be analytically expressed. For the sake of illustration we report here the transverse one:

$$
\begin{aligned}
R_T^{\sigma\tau}(q,\omega) = -\frac{1}{16\pi^2} \mathrm{Im} \sum_{J=1}^{\infty} \Bigg\{ & \frac{(2J+1)\hat{\Pi}_J^0(q,\omega)}{1 - \frac{\gamma\bar{q}^2}{(2\pi)^3}\mathcal{V}_T(\bar{q},\omega)\hat{\Pi}_J^0(\bar{q},\omega)} \\
& + \frac{(J+1)\hat{\Pi}_{J-1}^0(q,\omega)}{1 - \frac{\gamma\bar{q}^2}{(2\pi)^3}\mathcal{V}_T(\bar{q},\omega)\hat{\Pi}_{J-1}^0(\bar{q},\omega) + \frac{J}{2J+1}\mathcal{F}_{J+1}(\bar{q},\omega)} \\
& + \frac{J\hat{\Pi}_{J+1}^0(q,\omega)}{1 - \frac{\gamma\bar{q}^2}{(2\pi)^3}\mathcal{V}_T(\bar{q},\omega)\hat{\Pi}_{J+1}^0(\bar{q},\omega) + \frac{J+1}{2J+1}\mathcal{F}_{J-1}(\bar{q},\omega)} \Bigg\},
\end{aligned}
\qquad (5.7)
$$

where

$$\mathcal{F}_{J-1}(\bar{q},\omega) = \frac{\gamma\bar{q}^2}{(2\pi)^3} \left[\mathcal{V}_T(\bar{q},\omega) - \mathcal{V}_L(\bar{q},\omega)\right] \frac{\hat{\Pi}_{J+1}^0(\bar{q},\omega) - \hat{\Pi}_{J-1}^0(\bar{q},\omega)}{1 - \frac{\gamma\bar{q}^2}{(2\pi)^3}\mathcal{V}_T(\bar{q},\omega)\hat{\Pi}_{J-1}^0(\bar{q},\omega)} \qquad (5.8a)$$

$$\mathcal{F}_{J+1}(\bar{q},\omega) = \frac{\gamma\bar{q}^2}{(2\pi)^3} \left[\mathcal{V}_T(\bar{q},\omega) - \mathcal{V}_L(\bar{q},\omega)\right] \frac{\hat{\Pi}_{J-1}^0(\bar{q},\omega) - \hat{\Pi}_{J+1}^0(\bar{q},\omega)}{1 - \frac{\gamma\bar{q}^2}{(2\pi)^3}\mathcal{V}_T(\bar{q},\omega)\hat{\Pi}_{J+1}^0(\bar{q},\omega)}. \qquad (5.8b)$$

In these nuclear matter–like responses $\gamma \approx \pi/R$ (R being the nuclear r.m.s. radius) and the functions $\mathcal{F}$ embody the effects associated with the non–uniformity of the nuclear density. They are, however, also partly embedded into $\bar{q}$. The volume response (5.7) has been successfully compared with the electron scattering data: the degree of quenching and hardening provided by this finite nucleus RPA is quite similar to the one achieved in nuclear matter. In addition the effect of the mixing between the two spin–couplings remains small, at most of the order of 10%. This last outcome stems from two reasons: the first one lies in the weakness of $\mathcal{V}_L$ in the momentum range of interest for the (e, e') data. The second one is linked to the selecting character of the mixing with respect to the various multipolarities: indeed it affects more the high J's than the low ones. Now the volume responses are

only little concerned with the highest multipolarities, since they involve peripheral nucleonic orbitals. As we shall see in the next subsection, this behaviour is far more relevant for hadronic interactions.

5.2 Surface Spin–Isospin Responses

As mentioned before, the most recent measurements of the spin–longitudinal and transverse responses have been obtained with hadronic probes. For them the nucleus is a strongly absorptive medium and the scattering is confined to the surface region. A proper treatment of these processes should employ, for example, the DWIA (Distorted Wave Impulse Approximation) framework (Ichimura *et al.*, 1989): the associated formalism, however is quite cumbersome and the numerical results are in qualitative agreement with the ones illustrated in the following, which are based on Glauber's theory. Accordingly, we shall obtain the $\sigma\tau$ *surface* responses by modifying the external vertices of the polarization propagators as follows (Alberico *et al.*, 1988):

$$\hat{O}_{L,T} \rightarrow \hat{O}_{L,T}^{surf} = F(r)\hat{O}_{L,T}. \tag{5.9}$$

Before sticking to the determination of $F(r)$, we notice that the vertex (5.9) entails the introduction of two new propagators, one with a volume and a surface vertex (Π^s) and the other with two surface vertices (Π^{ss}). Then, instead of eq. (3.44), we get the following two "chain" integral equations:

$$[\hat{\Pi}_J^{RPA,ss}(q,q';\omega)]_{ll'} = [\hat{\Pi}_J^{0,ss}(q,q';\omega)]_{ll'} +$$
$$+ \frac{1}{(2\pi)^3}\sum_{l_1 l_2}\int_0^\infty dk\, k^2 [\hat{\Pi}_J^{0,s}(q,k;\omega)]_{ll_1}[U_J(k)]_{l_1 l_2}[\hat{\Pi}_J^{RPA,s}(k,q';\omega)]_{l_2 l'}, \tag{5.10}$$

$$[\hat{\Pi}_J^{RPA,s}(q,q';\omega)]_{ll'} = [\hat{\Pi}_J^{0,s}(q,q';\omega)]_{ll'} +$$
$$+ \frac{1}{(2\pi)^3}\sum_{l_1 l_2}\int_0^\infty dk\, k^2 [\hat{\Pi}_J^{0}(q,k;\omega)]_{ll_1}[U_J(k)]_{l_1 l_2}[\hat{\Pi}_J^{RPA,s}(k,q';\omega)]_{l_2 l'}. \tag{5.11}$$

They are diagrammatically illustrated in Fig. 5.1, where a black vertex represents the vertex (5.9). It is clear from this figure that the excitation is bound to be produced in the outer region of the nucleus, but it can then propagate to the interior through the residual interaction.

The equations (5.11) can be solved with the same approximate method utilized for the RPA volume propagators; one obtains the following expressions for the transverse

$$R_T^{surf}(q,\omega) = R_T^{0,surf}(q,\omega) - \frac{1}{16\pi^2}\text{Im}\sum_{J=1}^\infty \left\{ \frac{(2J+1)[\hat{\Pi}_J^{(1),ss}(q,\omega)]_{J,J}}{1 - \frac{\gamma\bar{q}^2}{(2\pi)^3}\mathcal{V}_T(\bar{q},\omega)\hat{\Pi}_J^0(\bar{q},\omega)} + \right.$$
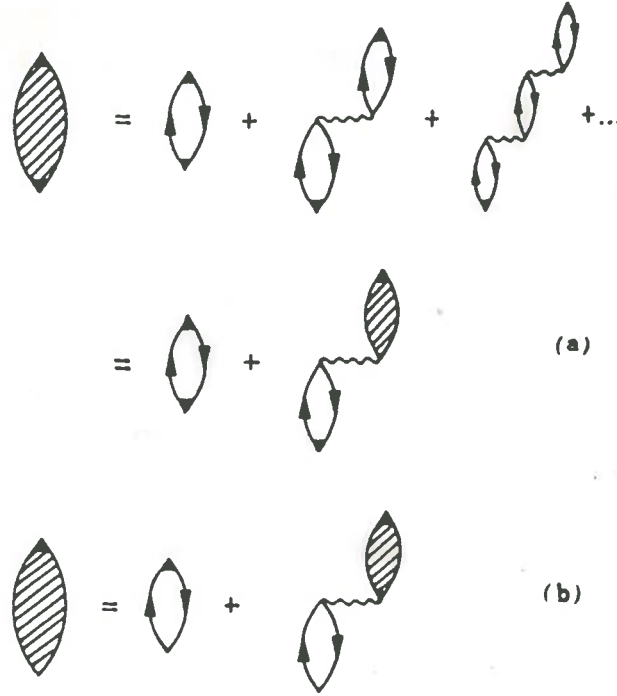
Fig. 5.1 – Diagrams representing the surface RPA equations (5.10) and (5.11) for the dynamical propagator; the p–h propagator includes both N–h and Δ–h excitations.

$$
+ \frac{(J+1)[\hat{\Pi}_J^{(1),ss}(q,\omega)]_{J-1,J-1} + \sqrt{J(J+1)}[\hat{\Pi}_J^{(1),ss}(q,\omega)]_{J+1,J-1}}{1 - \frac{\gamma\bar{q}^2}{(2\pi)^3}\mathcal{V}_T(\bar{q},\omega)\hat{\Pi}_{J-1}^0(\bar{q},\omega) + \frac{J}{2J+1}\mathcal{F}_{J+1}(\bar{q},\omega)} +
$$

$$
\left. + \frac{J[\hat{\Pi}_J^{(1),ss}(q,\omega)]_{J+1,J+1} + \sqrt{J(J+1)}[\hat{\Pi}_J^{(1),ss}(q,\omega)]_{J-1,J+1}}{1 - \frac{\gamma\bar{q}^2}{(2\pi)^3}\mathcal{V}_T(\bar{q},\omega)\hat{\Pi}_{J+1}^0(\bar{q},\omega) + \frac{J+1}{2J+1}\mathcal{F}_{J-1}(\bar{q},\omega)} \right\} \qquad (5.12)
$$

and for the longitudinal

$$
R_L^{surf}(q,\omega) = R_L^{0,surf}(q,\omega) -
$$

$$
- \frac{1}{8\pi^2}\text{Im}\sum_{J=0}^{\infty}\left\{ \frac{J[\hat{\Pi}_J^{(1),ss}(q,\omega)]_{J-1,J-1} - \sqrt{J(J+1)}[\hat{\Pi}_J^{(1),ss}(q,\omega)]_{J+1,J-1}}{1 - \frac{\gamma\bar{q}^2}{(2\pi)^3}\mathcal{V}_L(\bar{q},\omega)\hat{\Pi}_{J-1}^0(\bar{q},\omega) + \frac{J+1}{2J+1}\mathcal{G}_{J+1}(\bar{q},\omega)} + \right.
$$

$$
\left. + \frac{(J+1)[\hat{\Pi}_J^{(1),ss}(q,\omega)]_{J+1,J+1} - \sqrt{J(J+1)}[\hat{\Pi}_J^{(1),ss}(q,\omega)]_{J-1,J+1}}{1 - \frac{\gamma\bar{q}^2}{(2\pi)^3}\mathcal{V}_L(\bar{q},\omega)\hat{\Pi}_{J+1}^0(\bar{q},\omega) + \frac{J}{2J+1}\mathcal{G}_{J-1}(\bar{q},\omega)} \right\} \qquad (5.13)
$$

surface response functions. In the above formulas the $[\hat{\Pi}_J^{(1),ss}]_{J,J'}$ are the first–order surface propagators.

In order to determine $F(r)$ we resort to Glauber's theory (Glauber, 1959). Within this framework, the effective number of nucleons taking part in the (one–step) reaction is given by the expression

$$N_{eff} = \frac{\sigma^{(1)}}{\sigma_{tot}} = \frac{1}{\sigma_{tot}} \int_0^\infty db \, 2\pi b \, \chi(b) e^{-\chi(b)}, \qquad (5.14)$$

where $\chi(b)$ is the phase–shift function

$$\chi(b) = \sigma_{tot} \int_{-\infty}^\infty dz \, \rho\left(r = \sqrt{z^2 + b^2}\right), \qquad (5.15)$$

ρ being the nuclear density and σ_{tot} the total *probe–nucleon* cross section.

On the other hand, for a spherical nucleus and at momenta large enough to neglect the Pauli correlations, N_{eff} can also be expressed in terms of the sum rule:

$$N_{eff} = \int_0^\infty d\omega \, R^{surf}(q,\omega) = 4\pi \int_0^\infty dr \, r^2 |F(r)|^2 \rho(r). \qquad (5.16)$$

By comparing (5.16) and (5.14) one can thus fix the form of $F(r)$. The integrand of the rhs of eq. (5.16), e.g. for $\sigma_{tot} = 40\,(55)$ mb, turns out to be peaked in the surface region, at $\rho = \bar{\rho} = 0.28\rho_0$ ($\rho = \bar{\rho} = 0.20\rho_0$), ρ_0 being the central nuclear density.

There remains to be seen whether in such dilute media the p–h interaction is still able to set up collective effects, either locally or by spreading inside the system, and how the corresponding surface responses compare with the experiment. We remind that this surface RPA formalism for finite nuclei accounts, notwithstanding the above outlined approximations, for the mixing between the $\boldsymbol{\sigma} \cdot \mathbf{q}$–$\boldsymbol{\sigma} \times \mathbf{q}$ couplings, for the non–uniformity of the nuclear density (which involves the coupling of different angular momenta in the multipole expansion of $R_{L,T}^{\sigma\tau}$) and finally for the surface absorption of the external probe. As a matter of fact, *all these factors work against collectivity*, but not necessarily wash it completely out.

Let us compare now these surface responses with the experimental data, starting from the above mentioned ratio $\mathcal{R}$. As already remarked, the (p,p') experiment cannot separate the isovector contribution ($\tau = 1$) from the isoscalar one ($\tau = 0$); thus it actually measures the combination

$$\tilde{\mathcal{R}} = \left(\frac{2.15}{4.62}\right) \frac{3.62 R_L^{\tau=1}(q,\omega) + R_L^{\tau=0}(q,\omega)}{1.15 R_T^{\tau=1}(q,\omega) + R_T^{\tau=0}(q,\omega)}. \qquad (5.17)$$
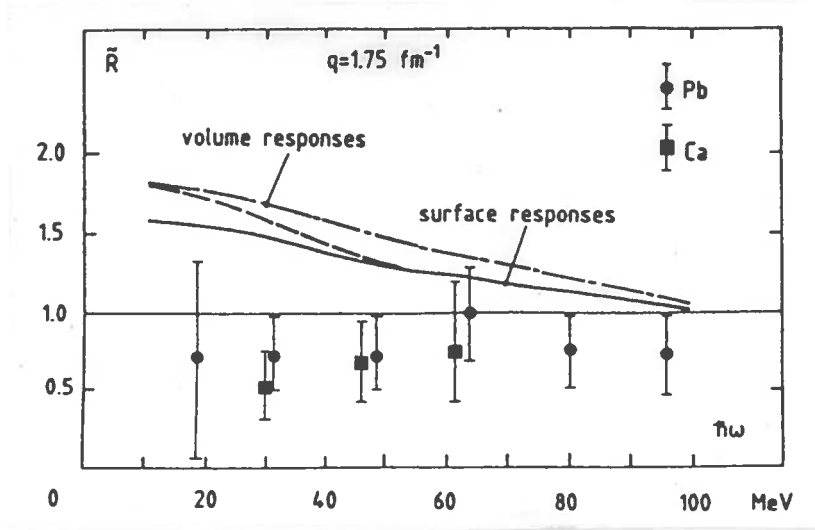
Fig. 5.2 – The ratio $\tilde{\mathcal{R}}$ at $q = 1.75\,\mathrm{fm}^{-1}$ as a function of $\hbar\omega$. The dot–dashed line is the prediction of the RPA theory of the volume responses; the surface RPA prediction is given by the solid and dashed lines, with and without the $(\boldsymbol{\sigma} \cdot \mathbf{q})$–$(\boldsymbol{\sigma} \times \mathbf{q})$ mixing, respectively; $g' = 0.7$.

Both the numerator and the denominator are obtained as ratios of the corresponding quantities in Ca^{40} (or Pb^{208}) and H^2.

To compare with the experiment the ratio (5.17) has been evaluated utilizing the surface RPA responses (with $\sigma_{tot} = 40$ mb) in the isovector channel and the independent particle surface responses in the isoscalar one; the results are displayed in Fig. 5.2, at $q = 1.75\,\mathrm{fm}^{-1}$. With respect to the old predictions of nuclear matter the ratio $\mathcal{R}$ appears to be considerably reduced: in particular the surface character of the process helps in bringing it down towards unity, as it can be inferred from the comparison with the corresponding ratio between the *volume* responses, which is also shown in the figure. The effect of the mixing between the two spin–modes is quite sizable, since at this momentum transfer the rather large transverse p–h interaction strongly affects R_L.

With respect to the experimental points there remain discrepancies on the low energy side. However it is worth pointing out that the measured $\tilde{\mathcal{R}}$ lies even below unity: this could be an indication of the presence of some collective effects in the isoscalar channel. Indeed, treating the $R^{\tau=0}$ as independent particle responses seems to be a suitable approximation, since the central $\tau = 0$ p–h force is known to be rather weak. But from sum rule considerations there is some evidence (Orlandini *et al.*, 1986) for a collective (and of opposite nature than the isovector ones) character of the isoscalar responses.

Turning now to the analysis of the charge–exchange (He^3,t) reaction cross sections measured at Saturne (Bergqvist *et al.*, 1987), a few points should be kept in mind:

i) the He^3 projectiles undergo an even more peripheral scattering than the protons; indeed the *effective* σ_{tot} to be used in the determination of $F(r)$ is $\sigma_{tot} = 55\,\mathrm{mb}$

ii) The charge exchange reactions are pure isovector processes, but no observation of polarization transfers were made in the Saturne experiment; thus Bergqvist and collaborators essentially measured a *mixture* of the $\boldsymbol{\sigma} \cdot \mathbf{q}$ and $\boldsymbol{\sigma} \times \mathbf{q}$ nuclear responses (with the He^3 bombarding energy of 2 GeV the non–spin–flip NN amplitudes are practically negligible).

In the single step approximation, the cross section for this reaction may be written as follows:

$$\frac{d^2\sigma}{d\Omega\,d\omega} = N_{eff}\left\{(|\beta|^2 + |\epsilon|^2)R_T(q,\omega) + |\delta|^2 R_L(q,\omega)\right\}FF^2, \qquad (5.18)$$

FF being the (He^3,t) form factor, β and ϵ the charge exchange spin–transverse NN amplitudes and δ the spin–longitudinal one.

Before considering the cross sections in detail, it is interesting to look at the position of their peaks (ω_M),which is displayed in Fig. 5.3 for different momentum transfers, together with the curves representing the peak positions in a free Fermi gas (both non–relativistic and relativistic). While at small momenta the experimental points exhibit a hardening with respect to the Fermi gas, at larger q they display an increasing softening.

This outcome could be nicely interpreted in terms of collective effects providing that at small q the transverse response (which is quenched and hardened by the RPA correlations) be the dominant one, whereas at large q the longitudinal response (enhanced and softened) should be the major component in the rhs of (5.18). Indeed, this seems to be the case at the incident energy of about 700 MeV/nucleon of the Saturne experiment: the ratio $|\delta|^2/(|\beta|^2 + |\epsilon|^2)$ is almost linearly increasing from 0.4 at $q = 1.4\,\mathrm{fm}^{-1}$ to 1.5 at $q = 2.4\,\mathrm{fm}^{-1}$. Thus, although R_L and R_T cannot be separated, one can envisage a natural explanation of the above mentioned behaviour of ω_M, by ascribing the low momentum hardening to the dominant transverse component and the high momentum softening to the longitudinal one.

The cross section (5.18) have been evaluated utilizing the surface RPA responses with the vertex function $F(r)$ corresponding to $\sigma_{tot} = 55$ mb; in spite of the low density at which the excitation takes place, still some collective effects are found in both channels. In particular, at $q = 2.4\,\mathrm{fm}^{-1}$ and with $g' = 0.7$ the softening of the peak, with respect to the Fermi gas, is of about 8 MeV, to be compared with the experimental value of ~ 18 MeV. However, a smaller value of g' might be more
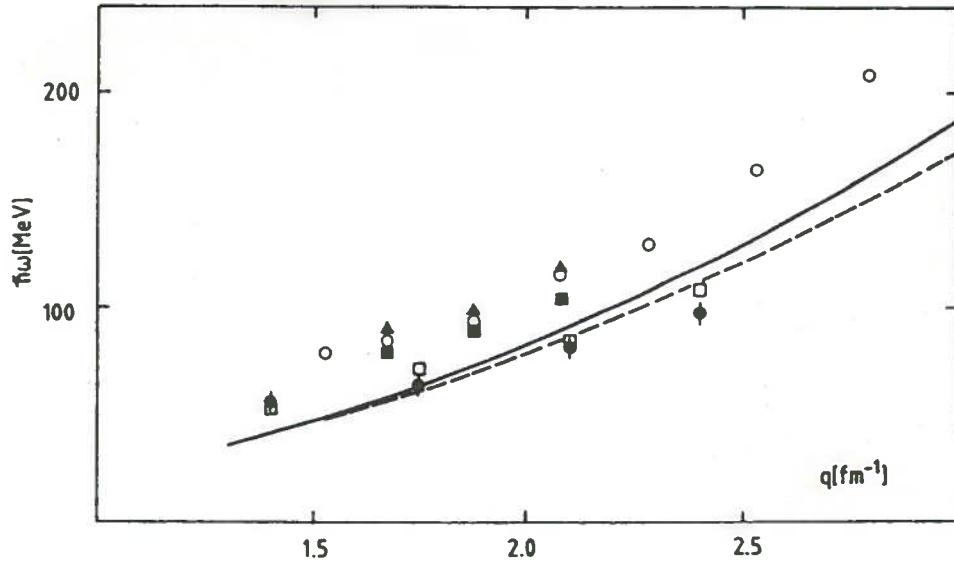
Fig. 5.3 – Peak position of the QEP in the reaction $C^{12}(He^3,t)$ at 2 GeV (black dots) and $Ca^{40}(e,e')$ (circles); theoretical predictions for the volume RPA (black squares) and the RPA + 2p–2h (triangles) isovector transverse responses are also displayed; the empty squares are the surface RPA predictions for the (He^3,t) reaction; solid and dashed lines represent the peak position of the non–relativistic and relativistic Fermi gas responses, respectively.

suitable here, since at such a low density the assumption of universality is no longer valid and the Δ is likely to experience a weaker short range repulsion (Hosaka and Toki, 1986). An effective value, e.g., $g' = 0.6$ yields a downward shift in the cross section of ~ 11 MeV.

In Fig. 5.4a→d we compare the surface RPA cross sections with the available experimental data, for q ranging from 1.4 to 2.4 fm^{-1}. The agreement between theory and experiment is fairly good, but for the highest momentum, where the calculated softening does not fully account for the observed one. In order to cure this failure one should probably utilize a better treatment of the distortion, rather than the Glauber's approach employed here. Also, one should not forget the influence of relativistic effects: indeed, as it appears in Fig. 5.3, already at the level of the free Fermi gas, the use of relativistic kinematics provides a substantial softening of the peak (with respect to the non–relativistic one) at the higher momenta.

One can conclude that the observed features of the spin–isospin nuclear responses are not incompatible with a collective interpretation of the processes. In particular
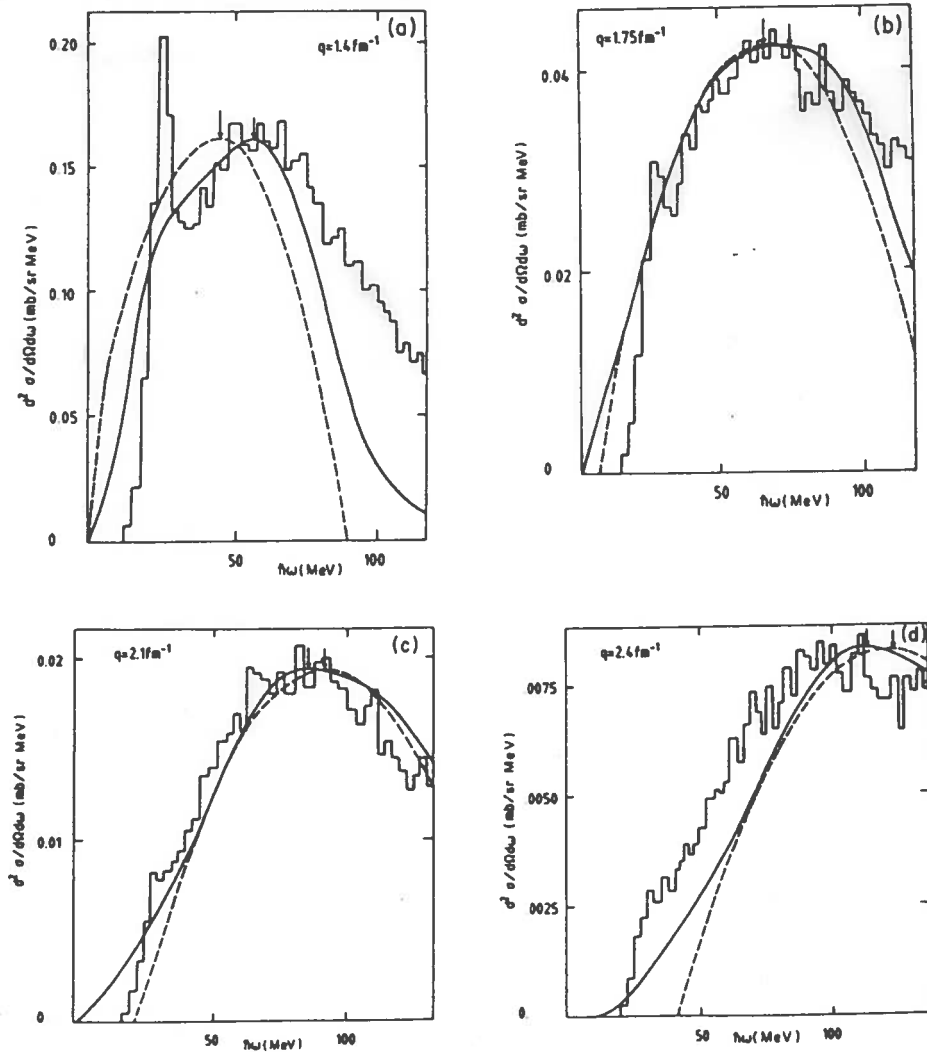
Fig. 5.4 – Experimental and surface RPA (solid line) cross sections for the
(He^3,t) reaction as a function of ω; $g' = 0.6$. The cross section for a
non–relativistic Fermi gas (with $k_F = 0.79$) is also shown for compari-
son. Arrows indicate the peak position.

it seems natural and appealing to ascribe the rather spectacular effects measured in
the charge exchange (He^3,t) reactions, at such low densities and short wavelengths,
to the long range nature of the pion, whose role in nuclear structure deserves further
investigations. [4]

---

[4] In this respect one should also remind that the experimental data show an even
more pronounced (and appealing) softening in the region of the Δ peak.

6. RELATIVISTIC ASPECTS OF THE NUCLEAR RESPONSES

Since in the near future the investigation of the atomic nuclei is expected to be carried out with increasingly energetic probes, the nuclear many–body problem will be more and more confronted with in the relativistic domain: a challenging issue indeed, exactly solvable only for a non–interacting system.

Therefore in this section we shall treat, to start with, the relativistic Fermi gas (RFG), a topic naturally bringing us to deal with the scaling properties of the response functions. The next step beyond the RFG, which entails the introduction of the forces, will be limited to the first order of perturbation theory, by switching on the pion–carried interaction. We shall also explore how RPA scales, however in the non–relativistic regime.

Finally we shall shortly outline a possible scheme for a fully relativistic description of the nuclear dynamics, focussing in particular on the connection between the nuclear response functions and the nucleon's structure functions.

6.1 The RFG

For this system the inclusive responses to an e.m. field are (Alberico, Molinari *et al.*, 1988)

$$R_{L,T} = \frac{3\mathcal{N}}{4M\kappa\eta_F{}^3}(\varepsilon_F - \Gamma)\theta(\varepsilon_F - \Gamma)\times$$

$$\times \begin{cases} \dfrac{\kappa^2}{\tau}\Big[\{(1+\tau)W_2(\tau) - W_1(\tau)\} + W_2(\tau)\Delta\Big], & \text{for } L, \\[2ex] 2W_1(\tau) + W_2(\tau)\Delta, & \text{for } T, \end{cases} \qquad (6.1)$$

where

$$\Delta \equiv \frac{\tau}{\kappa^2}\left\{\frac{1}{3}(\varepsilon_F{}^2 + \varepsilon_F\Gamma + \Gamma^2) + \lambda(\varepsilon_F + \Gamma) + \lambda^2\right\} - (1+\tau). \qquad (6.2)$$

In the above we have introduced the dimensionless variables

$$\left.\begin{array}{l} \kappa \equiv q/2M \\[1ex] \lambda \equiv \omega/2M \end{array}\right\} \implies \quad \tau = \kappa^2 - \lambda^2 \qquad (6.3)$$

$$\eta_F \equiv k_F/M, \qquad \varepsilon_F \equiv \sqrt{1 + \eta_F{}^2}$$

and the combinations

$$W_1(\tau) = \tau G_M^2(\tau) \qquad (6.4a)$$

$$W_2(\tau) = \frac{1}{1+\tau}\left(G_E^2(\tau) + \tau G_M^2(\tau)\right) \qquad (6.4b)$$

of the Sachs electric G_E and magnetic G_M form factors. Note that to get the full inclusive cross section, the sum of two contributions with $\mathcal{N} = Z$ (and G_E^p, G_M^p) and $\mathcal{N} = N$ (and G_E^n, G_M^n) should be taken. Furthermore in (6.1)

$$\Gamma \equiv \max\left\{(\varepsilon_F - 2\lambda), \gamma_- \equiv \kappa\sqrt{1+1/\tau} - \lambda\right\}, \qquad (6.5)$$

the first option holding in the Pauli blocked region.

Now, in the non–relativistic case, the inclusive cross section for $q \geq 2k_F$

$$\frac{d^2\sigma}{d\Omega d\epsilon'} = \sigma_M G_E^2(Q^2)\left\{\left(\frac{Q^2}{q^2}\right)^2 + \left(\frac{1}{2}\left|\frac{Q^2}{q^2}\right| + \tan^2\frac{\theta}{2}\right)\frac{\hbar^2 q^2}{2M^2}(\mu_p^2 + \mu_n^2)\right\} A\frac{M}{q}F_L^0(y)$$
$$(6.6)$$

is clearly factorized into the product of a purely nucleonic term and a many–body one. In the above we have introduced the scaling function

$$F_L^0(y) = -\frac{2q}{\pi\rho M}\operatorname{Im}\Pi^0(\mathbf{q}, \omega), \qquad (6.7)$$

ρ being the nuclear density. Thus, as already remarked in Section 3.1, the many–body content of (6.6), namely the function F_L^0, becomes function of the single scaling variable y when $\kappa \geq \eta_F$ (or $q \geq 2k_F$). In contrast the same does not occur for the RFG, the reason being that in calculating the responses the single nucleon current should be Lorentz transformed from the rest frame to frames moving with velocities dictated by the nucleon momentum distribution in the nucleus.

Yet one would like to recover in the relativistic domain some factorization as well by choosing
  a) a scaling variable ψ vanishing at the peak of the QEP and being ± 1 at the borders of it;
  b) a scaling function $S(\psi, \eta_F)$ parabolic in the scaling variable and *satisfying a sum rule*.

These are logical conditions, if one wishes to naturally recover the non–relativistic regime and are met with the definitions (Alberico, Molinari *et al.*, 1988)

$$\psi \equiv \sqrt{\frac{1}{\xi_F}(\gamma_- - 1)} \times \begin{cases} +1 & \lambda \geq \lambda_0 \\ -1 & \lambda \leq \lambda_0, \end{cases} \qquad (6.8)$$

where γ_-, defined in (6.5), has the physical significance of the minimum "energy", compatible with the overall energy conservation, a nucleon can have inside the nucleus, and

$$S(\psi; \eta_F) \equiv (1 - \psi^2)\theta(1 - \psi^2)\frac{3\xi_F}{\eta_F^3} \quad (\xi_F = \epsilon_F - 1). \qquad (6.9)$$

They lend the following factorization of the cross section

$$\frac{d^2\sigma}{d\Omega d\epsilon'} == \frac{\mathcal{N}}{4M\kappa}\sigma_M X(\theta,\tau,\psi;\eta_F)S(\psi;\eta_F), \qquad (6.10)$$

with

$$X(\theta,\tau,\psi;\eta_F) = \left[W_2(\tau) + 2W_1(\tau)\tan^2\frac{\theta}{2}\right] \qquad (6.11)$$

$$+ W_2(\tau)\left[\left\{\frac{\tau(1+\tau)}{\kappa^2} - 1\right\} + \left\{\frac{3}{2}\left(\frac{\tau}{\kappa^2}\right) + \tan^2\frac{\theta}{2}\right\}\Delta\right],$$

which unambiguously prescribes for what the cross section should be divided for, namely the function X, in order to "extract" the scaling function. Remarkably the function X, besides mildly depending upon η_F, also allows to recover the free-nucleon cross section for $\eta_F \to 0$, as it can be proved with an explicit calculation. Moreover the scaling function obeys the sum rule

$$\sum \equiv \int_0^\infty d\lambda S(\psi;\eta_F) \qquad (6.12a)$$

$$= \frac{3\xi_F}{\eta_F{}^3}(\lambda_2 - \lambda_1)\left[1 + \frac{1}{\xi_F} + \frac{1}{2\xi_F}(\lambda_2 + \lambda_1)\right]$$

$$- \frac{3\xi_F}{\eta_F{}^3}\frac{\kappa\sqrt{\kappa^2+1}}{\xi_F}\left[\mathrm{E}\left(\arcsin\frac{\lambda_2}{-\kappa},\sqrt{\frac{\kappa^2}{\kappa^2+1}}\right) - \mathrm{E}\left(\arcsin\frac{\lambda_1}{\kappa},\sqrt{\frac{\kappa^2}{\kappa^2+1}}\right)\right]$$

$$\qquad (6.12b)$$

$$\xrightarrow[\kappa\to 0]{} 2\kappa\{1 + \mathcal{O}(\eta_F{}^2)\} \qquad (6.12c)$$

$$\xrightarrow[\kappa\to\infty]{} 1 + \mathcal{O}(\eta_F{}^2), \qquad (6.12d)$$

where E is the Legendre integral of second kind. Note that Σ at first grows with κ and then stabilizes to unity for asymptotic values of κ, thus reflecting the constancy of the width of the relativistic QEP (namely $2k_F$). This is at variance with the non–relativistic situation where the R_L for a Fermi gas fullfils the sum rule (4.26) because the $1/q$ factor in R_L [see (3.3) and (4.6)] is compensated by the width of the QEP, linearly growing with the momentum: clearly then R_L only scales if multiplied by q.

In general the concept of scaling has any hope of being realized in nature only for large negative ψ, namely for large momentum transfers and on the low energy side of the QEP, where the nucleonic internal degrees of freedom and multiparticle–multihole excitations can be safely neglected. In this connection it should be noticed

that all the various scaling variables introduced in the past, notable among them the one introduced by Ciofi degli Atti, (1987) , while coming very close to the RFG motivated expression (6.9), differ substantially from the latter precisely for large negative ψ, as shown by Alberico, Molinari *et al.*, (1988). However in all the approaches to scaling the asymptotic scaling function turns out to be simply expressed in term of the nucleon momentum distribution, providing that separation energy and/or final state interaction effects can be ignored, which seems plausible for large κ. For example a generalization of the RFG model to allow momentum distributions different from the θ–function utilized in deriving (6.1) leads to the asymptotic scaling function

$$S(\psi) \xrightarrow[\kappa \to \infty]{} \int_{\gamma_- = \xi_F \psi^2 + 1}^{\infty} d\epsilon\, n(\sqrt{\epsilon^2 - 1}). \tag{6.13}$$

an expression indeed simply related to the nucleon momentum distribution $n(p)$.

In fact, in the context of the generalized RFG model, this outcome holds valid only as far as the transverse response is concerned, which anyway dominates the cross section in the asymptotic regime, but fails to be true for the longitudinal response which turns out to be characterized by a quite involved relationship between the asymptotic scaling function and the nucleons momentum distribution.

Concentrating on the global cross section, a central issue to be faced is how scaling is approached. For the purpose of investigating this point one can utilize momentum distributions generated, in the Brückner–Hartree–Fock (BHF) scheme, via a Reid soft core potential (Van Orden *et al.*, 1980) and insert them in the RFG framework. To show then the importance important of properly selecting the quantity one divide the cross section for in order to obtain the scaling function, we explore two prescriptions: the first (a) corresponds to divide by the single nucleon cross section (i.e., by X in the limit $\eta_F \to 0$), the second one (b) by the full function X. The results obtained within this generalized RFG model, displayed in Fig. 6.1, show that:

  a) for moderate excursions from the QEP the scaling is quite good;
  b) for both prescriptions, as κ increases, the scaling functions "increase" until they reach a maximum for some $\kappa = \bar{\kappa}$. Then, for $\kappa > \bar{\kappa}$ the scaling functions decrease approaching the asymptotic value (6.13). We refer to this effect as "false scaling" and its "onset" is clearly prescription dependent. Indeed, for $\theta = 10°$, $\bar{q} \simeq 8$ GeV/c for prescription (a), but only 1.6 Gev/c for prescription (b);
  c) the violation of scaling is also prescription dependent. For example, at $\theta = 10°$ and $\psi = -2$, for $\bar{q} = 2$ Gev/c the scaling function is twice as large as the asymptotic limit for the prescription (a), but only 30% larger for the prescription (b).The latter practically scales at $q = 10$ GeV/c, whereas the former even at 100 GeV/c is still 50% too large (!);
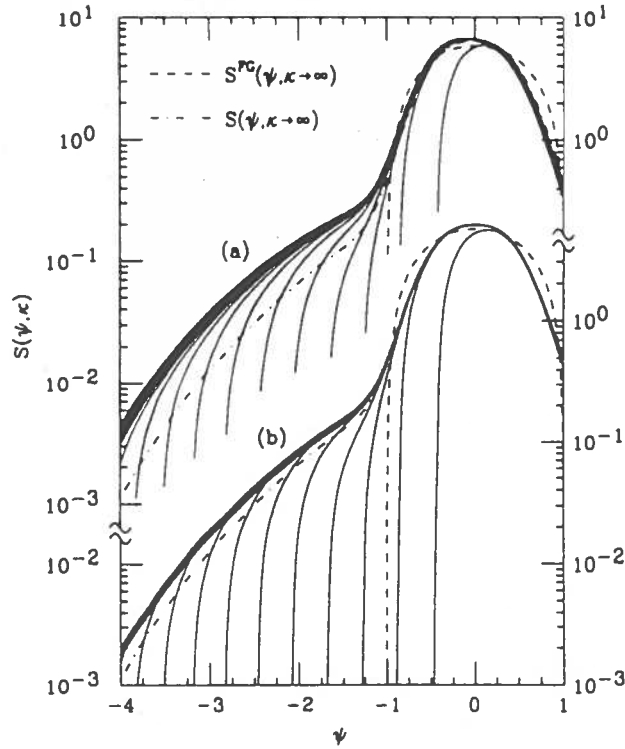
Fig. 6.1 – The scaling function derived from the total (L+T) cross section for
O^{16} at $\theta = 10°$ for three–momentum transfers ranging from 0.2 to 4.0
GeV/c by steps of 0.2 GeV/c and progressing from right to left in the
plots. The cross sections were calculated using the momentum density
of Van Orden *et al.*, (1980). The dot–dashed line is the asymptotic
answer in this model; the dashed line is the same quantity, but for the
RFG.

d) finally, and importantly, the approach to scaling is θ–dependent. Thus, at
$\theta = 180°$ (cross section purely transverse) the scaling regime is rapidly reached;
at $\theta = 90°$ prescription (b) is comparable with prescription a at $\theta = 10°$. This
indicates that R_L is the major responsible for scaling violations, the reason
being the substantial magnetic cotribution to the charge response induced by
relativity at large momenta [see (Alberico, Molinari *al.*, 1988)].

Obviously, as we have seen in Section 4, other important correlations are at work
inside nuclei, notably the RPA ones. Since they cannot be presently treated within
a fully relativistic scheme, let us explore how they affect scaling limiting our consid-
erations to a non– relativistic framework: this will be sufficient for exploring more
deeply the connection between scaling and Coulomb sum rule. In fact, also for fulfill-
ing the latter, it is clearly of crucial importance to control the momentum evolution

of the correlations and, more specifically, how fast they die with increasing q. This is best appreciated by changing the integration over ω into an integration over y (which introduces a factor q/M). The latter just accounts for the replacement of R_L with F_L:

$$F_L(y, q) = \frac{q}{M} R_L(q, \omega). \tag{6.14}$$

It thus follows that the scaling hypothesis, if fulfilled, authomatically implies the saturation of the Coulomb sum rule as well, hence the importance of examining how the nuclear dynamics breaks the y-scaling.

Now, we have seen that the function (6.14) scales for the free Fermi gas [see Section 3.1 and eq. (6.7)]. The same is no longer true within the Hartree–Fock approximation, although, at least within a schematic model for the nucleon self–energy, the scaling hypothesis still holds valid, up to quite small deviations, providing one performs a suitable change of the scaling variable ref[Ce-Ci-Sa-88].

Concerning the RPA correlations engrained, e.g., in (4.9), we first notice that the retarded part of the free polarization propagator, "scales": i.e.

$$\frac{q}{M} \Pi^0_{\text{ret}}(q, \omega) = f^0(y) \tag{6.15}$$

while its advanced part (always real in the positive–energy region) violates scaling [it depends, in fact, on the variable $(\omega + q^2/2M)M/q$] already at the level of the free Fermi gas (recall however that the previously discussed BHF correlations prevent anyway an early occurrence of scaling since they affect both the retarded and the advanced parts of the polarization propagator). Be as it may we ignore in the following BHF, writing in the pure RPA scheme ($q \geq 2k_F$)

$$F_L^{RPA}(y, q) = \frac{F_L^0(y)}{\{1 - V^{ph} \operatorname{Re}\Pi^0(q, \omega)\}^2 + \{(\pi\rho M/2q)V^{ph}F_L^0(y)\}^2} \tag{6.16}$$

This equation shows that the onset of the scaling regime is opposed by the presence, in $\operatorname{Re}\Pi^0$, of its advanced part, by the occurrence of a factor q^{-2} in the second term of the denominator and obviously by the q-dependence of the p–h interaction. Of course this *by no means implies a violation of the Coulomb sum rule* since the q-dependences referred to above are washed out in the limit $q \to \infty$ thus allowing the recovering of scaling. As a consequence, the frequency integral of the longitudinal response function exactly counts the charges of the nucleus in the asymptotic regime. In other words the RPA correlations are entirely compatible with the Coulomb sum rule, although possibly inducing a strong depletion of the QEP at finite q.

The crucial question for an experimental test of the Coulomb sum rule is, however, whether a large, but finite, momentum exists, such as to allow a simple disentangling

of the nucleonic dynamics from the nuclear one, which is the underlying hypothesis of (4.26). Equivalently at that momentum the internal degrees of freedom of the nucleon should still be somewhat frozen. The next question, from the theoretical viewpoint, is then whether a non–relativistic approach is still adequate for large q and we are inclined to think that this should not be the case.

Nevertheless sticking to the non–relativistic scheme, we like to remark that the reverse of our arguing is also true: indeed if the Coulomb sum rule is satisfied, then the scaling hypothesis is certainly verified. Notice also that the latter should obviously not be identified with the absence of correlations, as it is well illustrated by the BHF scaling function we have previously considered.

6.2 The Pion in the RFG Response

To provide an orientation on how the RFG response is acted upon by the interaction, we consider in this subsection the polarization propagator dressed, in the first order of perturbation theory, by the interaction carried by the pion. The corresponding contributions are those displayed in Fig. 3.1 [(a) and (b) of course identically vanish for a spin–isospin force and (e) is neglected for the present purposes]. They are naturally obtained, utilizing formulas (4.3)–(4.7), by adding to the purely nucleonic current (2.4) the two–body MEC and pion correlated currents, whose fully covariant expression is well–known. Indeed the previously reported currents (4.34)–(4.38) represent nothing but their leading order in the non–relativistic expansion.

In going beyond the extreme non–relativistic limit, we shall keep, closely following Alberico et al., (1989), all the contributions up to the second order in the expansion in powers of $1/M$ as far as the pionic currents are concerned. The purely nucleonic current instead will be treated in an approximate relativistic form, which gives results within, say, a 10% accuracy with respect to the fully covariant one. The rationale for this procedure stems from the recognition that, in the problem of identifying the expansion parameter for the non–relativistic reduction of the response of a collection of pions and nucleons to an external e.m. field, two scales are in fact present. The first one is associated with the dynamics of the system (namely the nucleonic motion and the exchange of pions) and is naturally identified with the expansion parameter q/M, the second instead is introduced by the e.m. interaction and it emerges already at the level of the single nucleon, being essentially related to the large anomalous magnetic moment of the latter. It is precisely this second scale which forces one to keep as far as possible the fully covariant nucleonic current, otherwise meaningless results could be obtained in pushing the investigation of the nuclear responses up to momenta of the order of, say, 1 GeV/c.

Although with obvious limitations the model we are discussing has the merit of

consistently dealing with the dual role played inside the nuclear structure by the pion, which is simultaneously glue of nuclear matter (OPEP) and current carrier (MEC). Furthermore it allows to test fundamental properties as the gauge invariance of the theory, which can only be fulfilled providing there are MEC in the current and pionic correlations in the dynamics, i.e. in the Hamiltonian.

Current	$O(1)$	$O(\kappa)$	$O(\kappa^2)$	$O(\kappa^3)$
Q_N	$\otimes$	—	$\otimes$	—
Q_{MEC}	—	—	$\otimes$	—
Q_{corr}	$\otimes$	—	$\otimes$	—
$\mathbf{J}_N$	—	$\otimes$	—	$\otimes$
$\mathbf{J}_{MEC}$	—	$\otimes$	—	$\otimes$
$\mathbf{J}_{corr}$	—	$\otimes$	—	$\otimes$

Table 1. Orders in $\kappa = q/2M$ of the non–relativistic expansion of the nucleonic, MEC and pionic two–body currents.

We also like to argue that, as far as the nuclear responses are concerned, in the region of deep inelasticity the pion might be the most relevant component of the NN interaction, this not being the case in the dynamical situation characterizing the ground state of nuclear matter. In this connection it would be of much interest to test this conjecture by comparing the responses of the present pionic model with the ones obtained from other relativistic nuclear models, notably the one of Walecka, which resorts to the use of the σ and ω mesons (Serot and Walecka, 1986).

We restrict ourselves here to consider the responses within the p–h sector of the nuclear excitations [although the two–body currents we are considering also play an important role in the 2p–2h sector, as we have seen in considering the transverse response (Section 4.2)], because in the QEP the interplay between the MEC and the correlation current is more transparent. In order to keep track of the various contributions to the nuclear responses, we indicate in table 1 (with self–explanatory

notations) all the terms in the non–relativistic expansion up to the order $1/M^3$ of both the nucleonic and pionic currents entering in the present analysis.

We have already given the explicit expressions for the space–components of the pion–in–flight, contact and π–correlation currents in Section 4.2. Here we report the corresponding charges. They read:

$$Q_\pi(\mathbf{k}_1, \mathbf{k}_2) = -\frac{2M}{\Omega^2} \frac{f_\pi^2}{m_\pi^2} \chi_{s_1'}^\dagger \frac{\boldsymbol{\sigma} \cdot \mathbf{k}_1}{k_1^2 + m_\pi^2} \chi_{s_1} \chi_{s_2'}^\dagger \frac{\boldsymbol{\sigma} \cdot \mathbf{k}_2}{k_2^2 + m_\pi^2} \chi_{s_2}$$
$$\times [(\mathbf{p'}_2^2 - \mathbf{p}_2^2) - (\mathbf{p'}_1^2 - \mathbf{p}_1^2)] 4 t_1 \mathcal{F}_E, \tag{6.17}$$

$$Q_{cont}(\mathbf{k}_1, \mathbf{k}_2) = -\frac{2M}{\Omega^2} \frac{f_\pi^2}{m_\pi^2} \left[\chi_{s_1'}^\dagger \boldsymbol{\sigma} \cdot (\mathbf{p}_1' + \mathbf{p}_1) \chi_{s_1} \chi_{s_2'}^\dagger \frac{\boldsymbol{\sigma} \cdot \mathbf{k}_2}{k_2^2 + m_\pi^2} \chi_{s_2} \right.$$
$$\left. - \chi_{s_1'}^\dagger \frac{\boldsymbol{\sigma} \cdot \mathbf{k}_1}{k_1^2 + m_\pi^2} \chi_{s_1} \chi_{s_2'}^\dagger \boldsymbol{\sigma} \cdot (\mathbf{p}_2' + \mathbf{p}_2) \chi_{s_2} \right] 4 t_1 \mathcal{F}_E \tag{6.18}$$

and

$$Q_{corr}(\mathbf{p}_1' \mathbf{p}_1; \mathbf{p}_2' \mathbf{p}_2) =$$
$$\frac{16 M^3}{\Omega^2} \frac{f_\pi^2}{m_\pi^2} \frac{\chi_{s_1'}^\dagger (\mathbf{k}_2 \cdot \boldsymbol{\sigma}) \chi_{s_1} \chi_{s_2'}^\dagger (\mathbf{k}_2 \cdot \boldsymbol{\sigma}) \chi_{s_2}}{\{[2M\omega - \mathbf{q} \cdot (\mathbf{p}_1' + \mathbf{p}_1)]^2 - (\mathbf{q} \cdot \mathbf{k}_2)^2\}(k_2^2 + m_\pi^2)}$$
$$\times \{[2M\omega - \mathbf{q} \cdot (\mathbf{p}_1' + \mathbf{p}_1)] 2 t_2 \mathcal{F}_E - (\mathbf{q} \cdot \mathbf{k}_2)[\mathcal{F}_E + t_2(1 + 2t_1)\mathcal{F}_D]\}$$

$$+ \{1 \longleftrightarrow 2\}, \tag{6.19}$$

respectively (Ω is the volume enclosing the system). Notice that the MEC charges are $\mathcal{O}(1/M^2)$, while the leading term of the non–relativistic reduction of the correlation current, [(eq. (6.19)] is of $\mathcal{O}(1)$ (see Table 1). The next term in the expansion of the latter (of order $1/M^2$) is given by a quite cumbersome expression, not reported here (see Alberico et $al.$, 1989).

With the above ingredients one can calculate, according to (4.3) and (4.4), the longitudinal and transverse response functions entering into the (e, e') inclusive cross sections. Just for the purpose of showing how the latter look like, we report here the contributions to R_L and R_T coming from the correlation current. They are separated into self–energy and exchange terms (corresponding to the diagrams (c,d) and (f) of Fig. 3.1) and read

$$\Delta R_{L(s.e.)}^{corr}(q, \omega) = f^2(Q^2) \frac{6 \xi_A}{k_F^3} \frac{f_\pi^2}{m_\pi^2}$$

$$\lim_{\alpha \to 0} \frac{\partial}{\partial \alpha} \int \frac{d\mathbf{k}}{(2\pi)^3} \theta(k_F - k) \theta(|\mathbf{q} + \mathbf{k}| - k_F) \delta\left(\omega + \alpha - \frac{\hbar^2 |Q^2|}{2M} - \frac{\hbar^2 \mathbf{q} \cdot \mathbf{k}}{M} \right)$$

$$\times \int \frac{d\mathbf{p}}{(2\pi)^3} \theta(k_F - p) \left\{ \frac{(\mathbf{p} - \mathbf{k})^2}{(\mathbf{p} - \mathbf{k})^2 + m_\pi^2} - \frac{(\mathbf{q} + \mathbf{k} - \mathbf{p})^2}{(\mathbf{q} + \mathbf{k} - \mathbf{p})^2 + m_\pi^2} \right\} \tag{6.20}$$

and

$$\Delta R_{L(exch)}^{corr}(q, \omega)$$

$$= f^2(Q^2) \frac{2M\xi_A}{k_F 3} \frac{f_\pi^2}{m_\pi^2} \int \frac{d\mathbf{k}}{(2\pi)^3} \theta(k_F - k) \theta(|\mathbf{q} + \mathbf{k}| - k_F) \delta\left(\hbar\omega - \frac{\hbar^2 |Q^2|}{2M} - \frac{\hbar^2 \mathbf{q} \cdot \mathbf{k}}{M} \right)$$

$$\times \int \frac{d\mathbf{p}}{(2\pi)^3} \theta(k_F - p) \left\{ \frac{1}{\mathbf{q} \cdot (\mathbf{k} - \mathbf{p})} \frac{(\mathbf{k} - \mathbf{p})^2}{[(\mathbf{k} - \mathbf{p})^2 + m_\pi^2]} \right.$$

$$- \frac{1}{\mathbf{q} \cdot (\mathbf{q} + \mathbf{k} - \mathbf{p})} \frac{(\mathbf{q} + \mathbf{k} - \mathbf{p})^2}{(\mathbf{q} + \mathbf{k} - \mathbf{p})^2 + m_\pi^2]}$$

$$\left. - \frac{(q^2 + 2\mathbf{q} \cdot \mathbf{k})}{2M^2 q^2} \left[\frac{(\mathbf{k} - \mathbf{p})^2}{(\mathbf{k} - \mathbf{p})^2 + m_\pi^2} - \frac{(\mathbf{q} + \mathbf{k} - \mathbf{p})^2}{(\mathbf{q} + \mathbf{k} - \mathbf{p})^2 + m_\pi^2} \right] \left(\frac{q^2}{Q^2} \right) \right\}, \tag{6.21}$$

for the longitudinal response, and

$$\Delta R_{T(s.e.)}^{corr}(q, \omega)$$

$$= -f^2(Q^2) \frac{3\xi_A}{2Mk_F 3} \frac{f_\pi^2}{m_\pi^2} \lim_{\alpha \to 0} \frac{\partial}{\partial \alpha} \int \frac{d\mathbf{k}}{(2\pi)^3} \theta(k_F - k) \theta(|\mathbf{q} + \mathbf{k}| - k_F)$$

$$\times \delta\left(\omega + \alpha - \frac{\hbar^2 |Q^2|}{2M} - \frac{\hbar^2 \mathbf{q} \cdot \mathbf{k}}{M} \right) \int \frac{d\mathbf{p}}{(2\pi)^3} \theta(k_F - p) \left[q^2(\mu_v^2 + \mu_s^2) \right.$$

$$\left. + 4k^2 - 4\frac{(\mathbf{q} \cdot \mathbf{k})^2}{q^2} \right] \left[\frac{(\mathbf{q} + \mathbf{k} - \mathbf{p})^2}{(\mathbf{q} + \mathbf{k} - \mathbf{p})^2 + m_\pi^2} - \frac{(\mathbf{p} - \mathbf{k})^2}{(\mathbf{p} - \mathbf{k})^2 + m_\pi^2} \right] \tag{6.22}$$

and

$$\Delta R_{T(exch)}^{corr}(q, \omega)$$

$$= -f^2(Q^2) \frac{\xi_A}{2Mk_F 3} \frac{f_\pi^2}{m_\pi^2} \int \frac{d\mathbf{k}}{(2\pi)^3} \theta(k_F - k) \theta(|\mathbf{q} + \mathbf{k}| - k_F) \delta\left(\hbar\omega - \frac{\hbar^2 |Q^2|}{2M} - \frac{\hbar^2 \mathbf{q} \cdot \mathbf{k}}{M} \right)$$

$$\times \int \frac{d\mathbf{p}}{(2\pi)^3} \theta(k_F - p) \left\{ \frac{1}{2M\omega + \mathbf{q} \cdot (\mathbf{q} - 2\mathbf{p})} \frac{1}{(\mathbf{q} + \mathbf{k} - \mathbf{p})^2 + m_\pi^2} \right.$$

$$\times \left[(3\mu_s^2 - \mu_v^2)\{\mathbf{q} \cdot (\mathbf{q} + \mathbf{k} - \mathbf{p})\}^2 - 4(\mathbf{q} + \mathbf{k} - \mathbf{p})^2 \left(\mathbf{k} \cdot \mathbf{p} - \frac{(\mathbf{q} \cdot \mathbf{k})(\mathbf{q} \cdot \mathbf{p})}{q^2} \right) \right]$$

$$- \frac{1}{2M\omega - \mathbf{q} \cdot (\mathbf{q} + 2\mathbf{p})} \frac{1}{(\mathbf{p} - \mathbf{k})^2 + m_\pi^2}$$

$$\left. \times \left[(3\mu_s^2 - \mu_v^2)\{\mathbf{q} \cdot (\mathbf{p} - \mathbf{k})\}^2 - 4(\mathbf{p} - \mathbf{k})^2 \left(\mathbf{k} \cdot \mathbf{p} - \frac{(\mathbf{q} \cdot \mathbf{k})(\mathbf{q} \cdot \mathbf{p})}{q^2} \right) \right] \right\}, \tag{6.23}$$

for the transverse one. In the above formulas $\xi_A = 3\pi^2 A$, $\mu_s = \mu_p + \mu_n$ and $\mu_v = \mu_p - \mu_n$).

One should notice that the energy conserving δ–function has an ω–dependence different from the corresponding non–relativistic expressions since in it $|Q^2| = |\omega^2 - q^2|$ (instead of q^2) appears. This affords an approximate (but accurate) treatment of the relativistic nucleonic current and makes a significant difference when considering large ω, especially on the high energy–loss side of the quasi–elastic response. Analogous arguments suggest the use of the Sach's form factor $G_E(Q^2)$ whenever the generic $f(Q^2)$ occurs.

Concerning the gauge invariance of the correlation current, the self–energy contribution (6.20) exactly fulfills it, being expressed through the charge–charge response $R(Q_N Q_{corr}; q\omega)$ alone [see also eq. (4.6)], whereas the exchange term (6.21) breaks gauge invariance, although mildly so, through the term proportional to (q^2/Q^2): indeed the above currents, while being gauge invariant both in the fully relativistic and in the extreme non–relativistic cases, do not necessarily satisfy this property at each order in the non–relativistic expansion in $1/M$. The numerical evaluation of these unwanted deviations shows, however, that, to the order $1/M^2$ included here, they are very small. Analogous considerations apply as well to the MEC contributions.

In Fig. 6.2 we display the longitudinal response including all diagrams with one pionic line and all contributions up to $1/M^2$ in the non–relativistic reduction; also shown is the free RFG response. At small q a substantial depletion of R_L on the low–energy side occurs, mostly induced by the correlation term and due to the coherent effect of the self–energy and exchange terms. Instead, on the high energy side, they tend to enhance the RFG response. These effects gradually fade away and are entirely washed out when the momentum transfer reaches, say, 1 GeV/c. Concerning the MEC contributions, they remains altogether small, although less so in the transverse channel, where the Δ–current increasingly reduces R_T (up to 30% for $q = 1$ GeV/c).

These results bear some consequences both on the Coulomb sum rule and on the scaling behaviour of the responses. The evaluation of the former can be performed according to the prescription of Donnelly *et al.* (1988): this allows an almost model independent parametrization of the dividing factor for the relativistic R_L (obviously providing the correct asymptotic value). The Coulomb sum rule is shown in Fig. 6.3, where it is clearly seen that the pionic correlations deplete S_L up to $q \simeq 900$ MeV/c. We remind the reader that, as previously discussed, RPA correlations deplete the sum rule as well: however in the longitudinal channel they are not carried by the pion and, moreover, they hardly lend themselves to a relativistic treatment.

The scaling properties of the cross sections evaluated within this "pionic" model
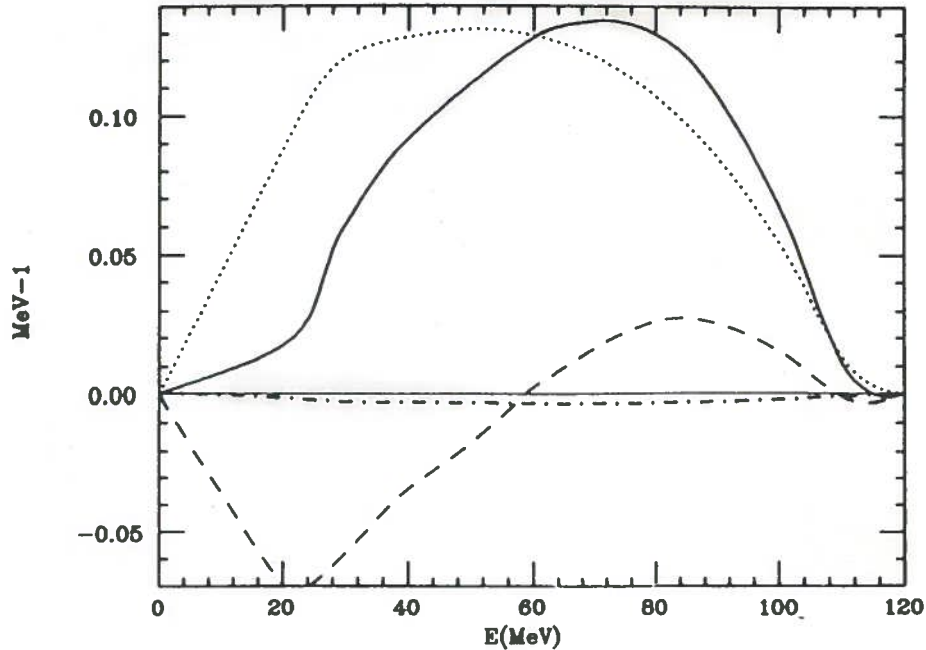
Fig. 6.2 – Longitudinal response function at $q = 300$ MeV/c. The dotted line
is the RFG response, the dashed line is the correction due to pionic
correlations [eqs. (6.20) and (6.21)] and the dot–dashed line the one
due to MEC. The continuous line is the total response.

and divided by the function X [eq. (6.11), as suggested by the RFG approach] turn
out to be somewhat affected in the negative ψ region and for not too large q-values.
Obviously once the pionic correlations are faded away, the same considerations apply
as for the RFG.

6.3 Beyond the Nucleon's Degrees of Freedom

The last decade has witnessed an impressive growth of the search for manifesta-
tions of subnuclear degrees of freedom inside nuclei, more at the level of theoretical
speculations than on the experimental side. Indeed, although the evidence till now
accumulated is admittedly limited, yet the subject has attracted such an intense
and widespread interest that it is an easy prediction to anticipate that the hunt for
quarks inside nuclei will be much strengthened in the future. Here we just want to
give a glance to this new field, which has added a truly new dimension to nuclear
physics.

As a first comment it is appropriate to remind that the advent of these new degrees
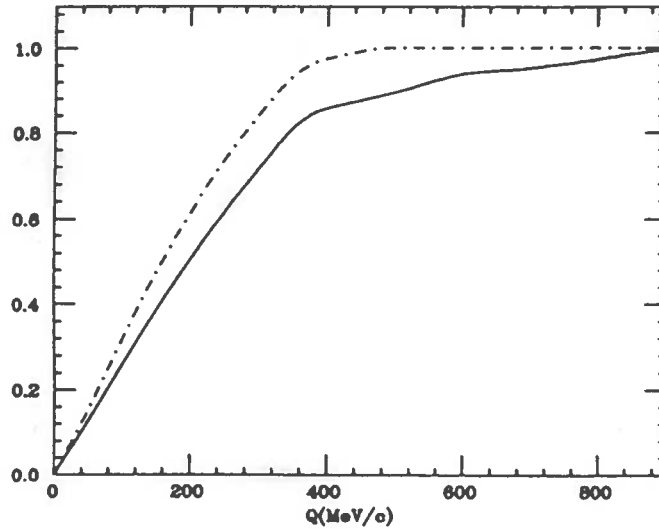
Fig. 6.3 – Coulomb sum rule with the correlations and MEC of the "pionic" model discussed in this subsection (continuous line). The longitudinal response has been divided by the "form factor" suggested by Donnelly *et al.*, (1988). The dashed line corresponds to the RFG sum rule.

of freedom has changed our conception of nuclear forces at short distances. Indeed, the repulsive core, which for years has been the most empirical component of the NN interaction, baffling any theoretical interpretation, begins now to be understood precisely in terms of quarks degrees of freedom. In fact it has been possible to show, relying on group theoretical methods, that the symmetry properties of the quarks states produce a node in the nucleon–nucleon wave function at short distances (Faessler *et al.*, 1982). Notable, in this connection, is the analogy with the forces governing molecular physics.

Concerning the response of the nucleus to both electromagnetic and hadronic probes, in extreme kinematical domains, the hope here is of unfolding the nucleonic structure inside the nucleus. Clearly the hard question is *how large* the energy employed in exploring the nucleus should be in order to unambiguously detect quarks degree of freedom. The difficulty in answering such a question lies in the present situation of intermediate and high energy nuclear physics where, in principle, a well–founded theory, QCD, is available, which is however extremely difficult to handle in practice. Accordingly, for use in the non perturbative regime, one is forced to reduce QCD to models like skyrmions, bags of various kinds, the confining quark model of Horowitz *et al.*, (1985) and the like [see, for example, (Skyrme, 1961, 1962), (Adkin *et al.*, 1983), (Thomas, 1983)]. As a consequence the interpretation of the available data

in terms of an underlying microscopy is never fully convincing. Yet the experiments points to the occurrence of some new dynamics inside nuclei and here we shortly summarize the related evidence.
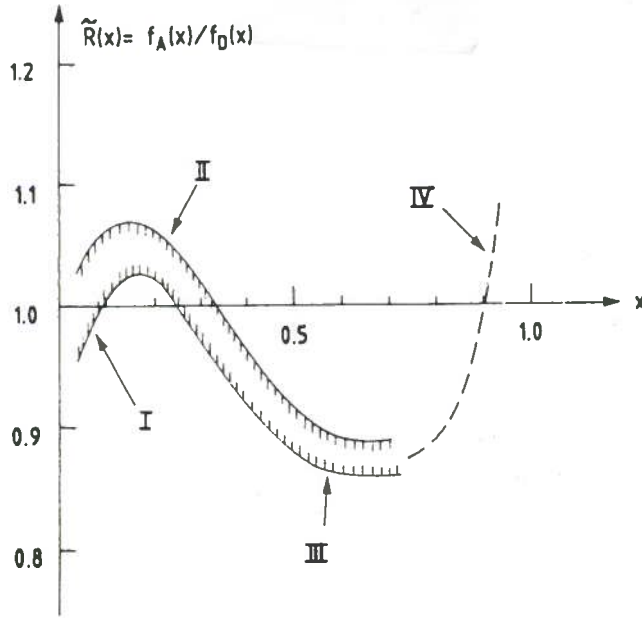

Fig. 6.4 – The EMC effect.

The first one is provided by the celebrated measurement, carried out in 1982 by the European Muon Collaboration (EMC) (and, since then, in different laboratories as well) via deep inelastic muon scattering, of the ratio

$$\tilde{\mathcal{R}} = \frac{\bar{F}_2^A(Q^2, X)}{\bar{F}_2^D(Q^2, X)} \tag{6.24}$$

between the structure functions of iron (A=56) and deuteron [normalized to a single nucleon, $\bar{F}_2^A = (1/A)F_2^A$] as a function of the Bjorken variable $X = Q^2/2M\nu$ ($\nu = K^\mu Q_\mu/M$). We remind that for small scattering angles the structure function F_2 is the dominant one, see (6.25). The results are displayed in Fig. 6.4, where the band embodies the Q^2-averaged experimental points, available up to the Summer 1987 (Van Hove, 1987), and it is indeed remarkable how reach is the physics conveyed by the data.

The growth in region IV stems simply by considering the momentum carried by a nucleon inside the nucleus (the Fermi motion). This quantity is in fact a fraction

$1/A$ of the total nuclear momentum, thus allowing the Bjorken variable X to exceed the maximum allowed value for a free nucleon, i.e. the unity, and such an effect is obviously more marked in a heavy nucleus than in deuterium.

The evident minimum of region III has been ascribed (Akulinichev *et al.*, 1985); Chanfray *et al.*, 1984; William and Thomas, 1986) to the binding effect which, by reducing the nucleon mass, correspondingly increases the value of the Bjorken variable. It is striking to see how a small effect can have such a conspicuous consequence on the ratio $\tilde{\mathcal{R}}$.

The decrease of $\tilde{\mathcal{R}}$ in the region I is thought to reflect the partial absorption of the virtual photon exchanged between the muon and the nucleus before the occurrence of the "hard" scattering. This process, referred to as "shadowing", has first been observed in the case of photon absorption in nuclei ($Q^2 = 0$) where it is associated with the well–known dominance of a vector boson in the hadronization of the photon wave function. Here, at large Q^2, it may possibly reflect instead a modification of the gluon and quark distribution in nuclei.

The same distortion of the quarks and gluons distribution inside nuclei has been especially invoked, as it is by now well–known, to account for the experimental increase of $\tilde{\mathcal{R}}$ in region II. This (see also Section 4.2) might lead to "swollen" nucleons inside the nucleus as a result of partial deconfinement, which in turn would entail colour conductivity. It should however be kept in mind that an enhancement of the nuclear sea (equivalently, of the pion field inside the nucleus), a conjecture which appears to be supported by the previously mentioned charge–exchange (He^3,t) experiment (see Section 5), would also lead to the observed increase of $\tilde{\mathcal{R}}$ in region II (Ericson and Thomas, 1983).

Further experiments are obviously needed to clarify this issue and so we are brought to examine new types of processes which could contribute for this purpose, namely the Drell–Yan ones. They correspond to purely hadronic collisions leading (quite rarely indeed) to the production of a dilepton. As a consequence the reaction is controlled by the structure function of the proton (in an p–p scattering) or of the proton and the pion (in a π–p one) thus complementing, in the time–like region, the deep inelastic lepton scattering above referred to. Remarkably an experiment carried out at CERN (Bordalo *et al.*, 1987) with a beam of negative pions impinging on deuterium and tungsten targets with laboratory energies of 140 and 286 Gev appear to confirm the modification of the nucleon structure function suggested by the EMC data.

Finally of much relevance are the experiments of inelastic proton scattering, with bombarding energy of 1 Gev, on a variety of nuclei. In fact here one observes the production of particles in the region kinematically forbidden in the scattering by a

free nucleon. This finding, referred to as " cumulative effect" (Andronenko *et al.*, 1983), also points in the direction of a possible new dynamics inside the nucleus.

To establish contact with the formalism of high energy physics, providing at the same time some hints for a better understanding of the physics discussed above, we just remind here that the double differential cross section for deep inelastic scattering of electrons out of the proton is expressed in terms of the invariants Q^2 and ν according to the formula

$$\frac{d^2\sigma}{d\Omega d\nu} = \frac{4\pi\alpha^2}{Q^4} \frac{\epsilon'}{\epsilon\nu} \cos^2\left(\frac{\theta}{2}\right) \left[F_2(Q^2,\nu) + \frac{2\nu}{M}F_1(Q^2,\nu)\tan^2\left(\frac{\theta}{2}\right)\right]. \qquad (6.25)$$

In the lab system (where, incidentally, $\nu = (Q^2/2M) = \epsilon - \epsilon' = \omega$) it is an easy matter to connect (6.25) with (4.1) by suitably defining formal relations between the nucleon structure functions $F_{1,2}$ and the nuclear response functions $R_{(L,T)}$.

As it is well known, the F_i's can also be looked upon as a function of X and Q^2 and, if the quarks are pointlike, in the limit of large Q and X finite they become functions of the scaling variable X only, thus leading to the celebrated Bjorken scaling.

For interpreting the physics addressed in this subsection a knowledge is clearly required of how the nucleon structure functions, expressed in terms of quarks degrees of freedom within the parton model, change in going from the free space to the nuclear medium and how the nuclear response (structure) functions are related to the corresponding nucleonic quantities. This is a chapter of physics which is currently undergoing a rapid development: accordingly we will touch upon it only very shortly without entering in details.

An important clue to the solution of the above problems is offered by the "rescaling" hypothesis of Close *et al.*, (1983) (CRR). It states that for two nuclei with mass number A and A', respectively, the following relation

$$\bar{F}_2^{A'}(X,Q^2) = \bar{F}_2^{A}\{X, \xi_{AA'}(Q^2)Q^2\}, \qquad (6.26)$$

holds, $\xi_{AA'}(Q^2)$ being a function, independent of A, A', whose Q^2 evolution is totally controlled by QCD. In other words the structure functions of nuclei, as a function of X, are connected by a change of scale in Q^2 which is universal.

A different approach to the same problem is the so-called convolution model which decomposes the nuclear wavefunction into basic components, the nucleons in the simplest case, and then add incoherently the structure functions of the constituents to provide the one of the nucleus. While there is no fundamental derivation of convolution model, various attempts have been made to build this bridge between nuclear, nucleonic and quark degrees of freedom. An example is offered in the

paper of Molinari and Vagradov (1989), who worked out the above connection in the framework of a fully covariant mesonic model of the nucleus.

7. THE PATH–INTEGRAL APPROACH TO THE NUCLEAR RESPONSE

In this section we aim at a more consistent theoretical foundation, as well as to a more advanced computational treatment, of the nuclear response functions, the motivation being that, in our view, a unified approach and a fully consistent approximation scheme are still lacking. In fact the Parquet equations, leaving aside the computational difficulties associated with their solution, in practice can only be tackled to a given order of approximation for their input, namely the set of irreducible diagrams Γ^{ij}, and the criteria for selecting these diagrams are euristic. On the other hand the variational scheme, although remarkably successfull in many instances, represents more an empirical approach to the nuclear responses than a truly theoretical framework.

With the same attitude, in all the cases previously discussed in this report, we have always chosen certain classes of diagrams, expected to describe the most relevant features of the experiment under consideration, without paying much attention to the mathematical coherence of the theory. In other words, the various approximation schemes were not conceived as a truncation of a well–defined power expansion of proved convergence properties in some parameter. Even when a set of diagrams was summed up to infinite order (as in the HF or RPA cases) no argument was given, beyond the relevance for the physics of concern, for their dominance.

At first sight this may not appear so important, since one aims, above all, to a sound description of the experimental data from the physical point of view. Yet to disregard too much the formal aspect of the theory may have serious drawbacks. The first one concerns, as above mentioned, the difficulties one encounters in dealing with the corrections to a given approximation scheme. The obvious example is the RPA itself. It is indeed hard to answer the question: under which conditions does RPA work and when, instead, it should be expected to give unreliable results? Another one concerns the violation of general theorems, which should hold valid for the exact many–body hamiltonian, induced by approximate frameworks. For example the Hugenholtz–Van Hove theorem (Hugenholtz and Van Hove, 1958), stating that at the Fermi wave number k_F the nucleon self–energy should be equal to the nucleon binding energy, holds good in HF, but breaks down in Brückner–HF. Analogous considerations apply to the compressibility sum rule [see e.g. (Pines and Nozières, 1966)], which links the second derivative with respect to the density of the binding energy with the static limit of the polarization propagator for vanishing momenta.

Of more direct concern for the nuclear responses are, as we have already seen, the constraints imposed by the gauge invariance and, if a relativistic description of the nuclear many–body response is attempted, by the covariance of the theory. In this connection the experience shows that the enforcing of these constraints is often realized through the cancellation of different diagrams, hence the failure in ensuring them might results in incorrect theoretical predictions.

Remarkably these drawbacks are not present in the approximation schemes of QFT, namely the perturbative approach and the loop expansion. Indeed in QFT it usually happens that a theorem, once proved in general, holds true as well order by order in the above mentioned expansions. Accordingly we shall pursue in this section the aim of dealing with the nuclear response functions in the modern QFT framework following, in so doing, the tradition, which goes back to the pioneering works of Migdal, Galitskii, Goldstone and others [see (Pines, 1962)], of closely linking QFT and many–body theory.

7.1 Response of a System of Nucleons and Pions to an External Pion–like Field

Consider as a first example a system of nucleons interacting via the exchange of pions. As usual we write the (unrenormalized) lagrangian of the system in the form

$$\mathcal{L} = \overline{\psi}\left(i\slashed{\partial} - M\right)\psi + \frac{1}{2}\left(\partial_\mu \Phi\right)^2 - \frac{m_\pi^2}{2}\Phi^2 - ig\overline{\psi}\gamma_5\tau\psi \cdot \Phi. \tag{7.1}$$

with obvious meaning of the symbols. The corresponding response function is immediately built up according to the prescription of Sect. 2, by adding to $\mathcal{L}$ a further term describing the interaction of the system with a *classical* external pion–like field [recall eq. (2.3)]:

$$\mathcal{L} \rightarrow \mathcal{L}' = \mathcal{L} - \mathbf{j}_A(x) \cdot \boldsymbol{\varphi}(x) \tag{7.2}$$

and then by applying eq. (2.15). Now the generating functional $Z[\varphi]$ is suitably represented in terms of Feynman path integrals as

$$Z[\varphi] = \frac{1}{\mathcal{N}} \int \mathcal{D}\left[\overline{\psi}, \psi, \Phi\right] \exp\left\{i \int dx \left[\mathcal{L} - \mathbf{j}_A(x) \cdot \boldsymbol{\varphi}(x)\right]\right\}. \tag{7.3}$$

This expression deserves the following comments
1. all the quantities appearing inside the functional integral have to be regarded as classical variables (eventually anticommuting when referring to fermion degrees of freedom);
2. from the generating functional all the physically relevant quantities are deduced by means of functional differentiations. In particular any theorem, when stated for Z, automatically holds (or it is immediately translated) for its derivatives;

3. in (7.3) the nuclear medium does not explicitly appear. However the presence of a nucleon back-ground (finite or infinite) is hidden in the boundary conditions to be imposed on the classical fermion fields $\overline{\psi}(x)$ and $\psi(x)$ for $t \to \pm\infty$ and must be kept into account when integrating over them.

4. In general for lagrangians as (7.1) one faces the renormalization problem. The procedure for solving it is well known in QFT (Bogoliubov and Parasyuk, 1957; Bogoliubov and Shirkov, 1959; Zimmermann, 1970), but in addition one can prove that each diagram in perturbation theory remains finite (*with the same set of counterterms*) in presence of the nuclear medium (Alberico, Cenni *et al.*, 1988).

Once the generating functional Z is known, it may be expanded in Feynman diagrams yielding the conventional perturbation theory, but one may also directly work on Z, thus eliminating some degrees of freedom by means of a functional integration.

The idea of dropping unwanted degrees of freedom is quite old in nuclear physics (Feshbach, 1962; Brandow, 1967): for example the pionic ones can be eliminated (Gari and Hyuga, 1976) by means of the Feshbach's projection technique or via the Foldy-Wouthuysen (FW) transformation. In the functional scheme a simple gaussian integration leads to the same result. Indeed one sees by inspection that the exponent in (7.3) is bilinear in the pionic field, thus allowing the explicit integration over Φ. One gets (up to irrelevant constants)

$$Z[\varphi] = \frac{1}{\mathcal{N}} \int \mathcal{D}\left[\overline{\psi}, \psi\right] \exp\left\{i \int dx \left[\overline{\psi}(x)\left(i\slashed{\partial} - M\right)\psi(x)\right.\right.$$
$$\left.\left. - \frac{g^2}{2}i \int dx\,dy\, \mathbf{j}_A(x)\Delta_0(x - y)\mathbf{j}_A(y) - i \int dx\, \mathbf{j}_A(x) \cdot \boldsymbol{\varphi}(x)\right]\right\}. \quad (7.4)$$

(Δ_0 being the free pion propagator).

Eq. (7.4) embodies *exactly* the same physics as (7.3), since in its derivation use has been made of an identity, but the remaining integration variable may now be interpreted as the physical fields to deal with and the exponent inside the integral as an effective action. In other words, without loosing any physical information, we have translated the original lagrangian in an effective one, reducing the degrees of freedom, since the pions have disappeared, being replaced by a quadrilinear non-local energy-dependent NN interaction. Of course the same result can be achieved in the frame of the FW transformation, but here we get the formal gain that the renormalization of the theory is ensured and needs not to be performed "by hands"[5]

---

[5] Actually this statement is not fully correct. In fact a furter term should be added to the lagrangian, namely a factor $\lambda/4!\,(\Phi^2)^2$, even if the renormalized value of λ is assumed to be 0, because in any case its counterterm must be present.

The alternative approach of eliminating the nucleonic degrees of freedom instead of the pionic ones is not trivial in the context of the FW transformation, but is simple in the frame of Feynman path integrals, because the fermion fields too appear bilinearly in the lagrangian and consequently may be again integrated out. In fact with the change of integration variable

$$\Phi(x) \rightarrow \Phi(x) - \frac{1}{g}\varphi(x) \tag{7.5}$$

the functional integral is recast in the form

$$Z[\varphi] = \frac{1}{\mathcal{N}} \exp\left\{\frac{i}{2g^2}\varphi \cdot \Delta_0^{-1}\varphi\right\} \int \mathcal{D}[\bar{\psi}\psi\Phi]$$
$$\times \exp\left\{i\left[\bar{\psi}S_0^{-1}\psi + \frac{1}{2}\Phi \cdot \Delta_0^{-1}\Phi - g\mathbf{j}_A \cdot \Phi + \frac{1}{g}\Phi \cdot \Delta_0^{-1}\varphi\right]\right\}, \tag{7.6}$$

S_0 being the free nucleon propagator and the space–time integrations being understood. Then the integrations over $\bar{\psi}$ and ψ are elementary yielding

$$Z[\mathbf{J}] = \frac{1}{\mathcal{N}} \exp\left\{\frac{i}{2g^2}\varphi \cdot \Delta_0^{-1}\varphi\right\} \int \mathcal{D}[\Phi]$$
$$\times \exp\left\{i\left[\frac{1}{2}\Phi \cdot \Delta_0^{-1}\Phi - V_\pi[\Phi] + \frac{1}{g}\Phi \cdot \Delta_0^{-1}\varphi\right]\right\}, \tag{7.7}$$

where the effective interaction V_π reads

$$V_\pi[\Phi] = -i\operatorname{tr}\sum_{n=1}^{\infty}\frac{1}{n}\left[ig\gamma_5\boldsymbol{\tau} \cdot \Phi S_0\right]^n$$
$$= \frac{1}{2!}\int dy\,dz\,\Pi^{kl}(z,y)\Phi_k(z)\Phi_l(y) + \mathcal{O}(\Phi^3), \tag{7.8}$$

where $\Pi^{ij} = \Pi^0\delta_{ij}$ notably coincides with the free polarization propagator, of course with suitably defined vertices.

The following comments are then in order

1. the physical system described in (7.7) appears to be different from the original one, since the functional integration is carried out on the pionic degrees of

---

This term prevent functional integration of the field Φ. Eq. (7.4) should then be regarded as the 0th order of the perturbative expansion in λ. Higher orders should cancel divergences connected with the $\pi - \pi$ amplitude which remain already present in (7.4). In other words the divergent diagrams with four–vertices closed fermion loops are still to be renormalized by hands.

freedom only. However the correspondence between the integration domain of the functional integral and the Hilbert space of the quantum system implies that we are dealing with a collection of pions interacting by means of an indeed complicated, highly non–local, self–interaction. Nevertheless eq. (7.7), together with the definition (7.8), embodies exactly the same physics as (7.3).

2. Once the nucleons have been integrated out, their dynamics is fully accounted for, together with the boundary conditions over the nucleon fields. In fact, while (7.3) shows no explicit dependence upon k_F, in (7.7) the k_F dependence is exhibited by S_0. For example, depending upon the boundary conditions, S_0 can be the usual Feynman propagator S_F of the nucleon in the case of fermions and pions in the vacuum, or we could take for it the expression corrected by the Fermi sea, namely

$$S_F^{(m)}(q) = S_F(q) + 2\pi i\delta(q_0 - E_q)\theta(k_F - q)\frac{\slashed{q} + M}{2E_q} \qquad (7.9)$$

and in this case we face the already mentioned problem of the renormalization of the theory in the medium and the complexity of the many–body problem (Alberico, Cenni *et al.*, 1988). Finally we can use the simple expression (3.2) when dealing with the non–relativistic many–body problem. It is remarkable that *in any case* the topological structure of the theory is exactly the same.

3. Finally the structure of the effective lagrangian is clear: its first term is simply the lagrangian of the free boson field, whereas the second one is a "potential" term which may be described in terms of Feynman diagrams of the original theory. In this frame $V_\pi[\Phi]$ is given by the sum of all the diagrams containing one closed fermion loop.

7.2 The Perturbative Expansion

In this paragraph we shortly outline the structure of the perturbative treatment of the effective lagrangian derived in the previous section. If we introduce for sake of simplicity the function

$$\gamma = \frac{1}{g}\Delta_0^{-1}\varphi \qquad (7.10)$$

and consider Z as a functional of γ, the second derivative of Z_c with respect to γ [recall eq. (2.10)] is just the pion Green's function with the two external legs cutted out, i.e. the total (reducible) pion self–energy.

The perturbative expansion is then immediately obtained in the closed form

$$Z[\gamma] = \frac{1}{\mathcal{N}}\exp\left\{\frac{i}{2}\gamma \cdot \Delta_0\gamma\right\}\exp\left\{-iV_\pi\left[\frac{1}{i}\frac{\delta}{\delta\gamma}\right]\right\}\exp\left\{-\frac{i}{2}\gamma \cdot \Delta_0\gamma\right\} \qquad (7.11)$$

as it can be seen, for instance, by multiplying by λ the effective potential, expanding in powers of λ and then setting $\lambda = 1$ at the end of the calculations.

It is worth noticing a topological analogy between (7.11) and the hole–line expansion for the Green's functions deducible from Z. We have already mentioned that, in terms of the original theory, the effective potential V_π includes all the diagrams with one fermion loop and as many vertices as desired. On the other hand the nth order contribution in perturbation theory will sum up all the diagrams (of the original theory) containing exactly n closed fermion loops. The analogy with the hole–line expansion is then clear since the momentum integration over each fermion loop is cut at k_F (because at least one of the internal lines of the loop is a hole line).

Of course the two expansions are not identical: indeed adiagrammatic analysis shows that (7.11) embodies both the p–p and the p–h ladders, being in addition well grounded and uniquely defined, while the hole–line expansion is not.

7.3 The Semiclassical Expansion

Another typical tool of QFT is the semiclassical ($\hbar$ or loop) expansion. At variance with QFT, in the present case perturbation theory and loop expansion do not coincide, because the potential V_π is not a monomial.

To understand how the semiclassical expansion works here let us consider first the lowest order, which simply amounts to evaluate the functional integral in the Stationary Phase Approximation (SPA). The saddle point [eq. (7.7)] satisfies the equation of motion

$$-(\Box + m_\pi^2)\Phi(x) = \frac{\delta}{\delta\Phi(x)}V_\pi(\Phi) - \gamma(x) \tag{7.12}$$

which describes the evolution of a *classical* pion field (we solve in fact the classical equation of the motion) under the effect of the potential V_π and of the external field γ. Once a solution of (7.12) has been found [let it be $\Phi_0(x)$] the SPA amounts to set

$$\int \mathcal{D}[\Phi]\exp\left\{i\left[\frac{1}{2}\Phi \cdot \Delta_0^{-1}\Phi - V_\pi[\Phi] + \Phi \cdot \gamma\right]\right\}$$

$$= \exp\left\{i\left[\frac{1}{2}\Phi_0 \cdot \Delta_0^{-1}\Phi_0 - V_\pi[\Phi_0] + \Phi_0 \cdot \gamma\right]\right\} \tag{7.13}$$

The exact solution $\Phi_0(x)$ cannot be written down explicitly, but in practice it is not needed, an expansion up to the 2nd order in γ being sufficient. The latter is easily obtained by noticing that the sum in V_π [see eq. (7.8)] starts from $n = 2$, which entails that $\delta V_\pi(\Phi)/\delta\Phi(x)$ is at least linear in Φ. Consequently if we let $\gamma \to 0$ into

(7.12) we find that one solution of the classical equation of motion is $\Phi = 0$. The latter is surely not the only one (Cenni and Saracco, 1988), but unfortunately other non–trivial solutions of (7.12) have not yet been sufficiently investigated.

Assuming nevertheless $\Phi = 0$ as a starting point for an expansion in powers of γ, we may set

$$\Phi_0(x) = \int dy\, C(x,y)\gamma(y) + \mathcal{O}(\gamma^2). \tag{7.14}$$

Then, from eq. (7.13), the action evaluated along the classical path is seen to be of second order in γ: precisely what is needed to evaluate the polarization propagator.

Equation (7.12) is now easily solved, since in $\delta V_\pi(\Phi)/\delta\Phi(x)$ only the term with $n = 2$ is of first order in γ. Thus, to this order and recalling (7.8), equation (7.12) will read

$$-\int dy\,(\Box + m_\pi^2)C(x,y)\gamma(y)$$
$$= \int dy\,dz\,\Pi^0(x-y)C(y,z)\gamma(z) - \gamma(x) \tag{7.15}$$

which is satisfied (with standard symbols) by

$$\int dy\, C(x,y)\gamma(y) = -\int dy\, \Delta_{RPA}(x-y)\gamma(y) \tag{7.16}$$

where

$$\Delta_{RPA} = \frac{1}{\Delta_0^{-1} - \Pi^0} \tag{7.17}$$

is nothing but the RPA–dressed pion propagator. Therefore the classical field solution is

$$\Phi_0(x) = -\int dy\, \Delta_{RPA}(x-y)\gamma(y) + \mathcal{O}(\gamma^2). \tag{7.18}$$

Then, from (7.6) and (7.13), one gets for the generating functional the expression

$$Z[\gamma] = \frac{1}{\mathcal{N}}\exp\left\{\frac{i}{2}\gamma\cdot(\Delta_0 - \Delta_{RPA})\gamma\right\}$$
$$\equiv \frac{1}{\mathcal{N}}\exp\left\{\frac{i}{2g^2}\varphi\cdot\Delta_0^{-1}(\Delta_0 - \Delta_{RPA})\Delta_0^{-1}\varphi\right\} \tag{7.19}$$

and, according to (2.15), two functional derivatives lead finally to the polarization propagator

$$\Pi = \frac{1}{g^2}\Delta_0^{-1}(\Delta_0 - \Delta_{RPA})\Delta_0^{-1} = \frac{1}{g^2}\frac{\Pi^0}{1 - \Delta_0\Pi^0} \tag{7.20}$$

We have thus recovered the familiar RPA expression for the polarization propagator, but we have also shown that in fact the RPA coincides with the semiclassical approximation of an effective theory. To go beyond, it is then sufficient to apply the rules of the loop expansion in QFT. Since the only degrees of freedom in our effective lagrangian are the pions, to construct the nth order correction these rules are the following:

1. Associate to any term of the interaction V_π a bubble with, say, k vertices,
2. draw all the topologically distinct diagrams with n loops which saturates all the vertices and with the desired number of external legs, *considering the bubbles as topologically equivalent to points*,
3. associate to any line a RPA–dressed pion line,
4. evaluate the diagram according to the usual Feynman rules.

7.4 The Response to an Electromagnetic Probe

We now let our system of pions and nucleons to interact with an external electromagnetic field (Alberico, Cenni *et al.*, 1987). The minimal coupling then prescribes of adding to the lagrangian (7.1) the free e.m. lagrangian and the interaction terms. Thus

$$\mathcal{L} \longrightarrow \mathcal{L} - \frac{1}{4} F_{\mu\nu} F^{\mu\nu} + j_\mu A^\mu + B_{\mu\nu} A^\mu A^\nu \qquad (7.21)$$

where

$$j_\mu = e\,\overline{\psi}\,\frac{1 + \tau_3}{2}\gamma_\mu\psi + e\,[\Phi \times \partial_\mu \Phi]_3 \qquad (7.22)$$

$$B_{\mu\nu} = e^2 g_{\mu\nu} \Phi^+ \Phi^- = \frac{e^2}{2} \left[\Phi_1^2 + \Phi_2^2\right] g_{\mu\nu}. \qquad (7.23)$$

The generating functional [for sake of simplicity we consider the coupling of the system to an external electromagnetic source, $j_\mu^{ex}(x)$, only] will then read

$$Z\left[j_\mu^{ex}\right] = \frac{1}{\mathcal{N}} \int \mathcal{D}\left[\overline{\psi}, \psi, \Phi, A_\mu\right] \exp\left\{i \int dx\left[j_\mu^{ex} A^\mu\right]\right\}$$

$$\times \exp\left\{i \int dx \left[\mathcal{L} + \mathcal{L}_{\text{e.m.}} + j_\mu A^\mu + B_{\mu\nu} A^\mu A^\nu\right]\right\}. \qquad (7.24)$$

As before Z (which provides the photon propagator) will be connected to the response function through the cutting of the external legs. Note that in (7.24) $\mathcal{L}_{\text{e.m.}}$ $\left(= -\frac{1}{4}F_{\mu\nu}F^{\mu\nu}\right)$ embodies (although not explicitly) a gauge–fixing term in order to suitably define the free photon propagator.

Now the e.m. interaction of nucleons and pions does not alter the bilinear structure of the lagrangian with respect to the fermion (as well as to the boson) fields. Accordingly either the boson or the fermion fields can be dropped out. We shall focus

again on the elimination of the fermion degrees of freedom (the alternative option leads to the traditional MEC scheme), which yields

$$Z\left[j_\mu^{\text{ex}}\right] = \frac{1}{\mathcal{N}} \int \mathcal{D}\left[\Phi, A_\mu\right] \exp\left\{i \int dx \left[\frac{1}{2}(\partial_\mu \Phi)^2 - \frac{1}{2}m_\pi^2 \Phi^2 + \mathcal{L}_{\text{e.m.}}\right]\right\}$$

$$\times \exp\left\{i \int dx \left[e(\Phi \times \partial_\mu \Phi)_3 A^\mu + B_{\mu\nu} A^\mu A^\nu\right]\right\}$$

$$\times \left[\det \tilde{S}^{-1}\right] \exp\left\{i \int dx \left[j_\mu^{\text{ex}}(x) A^\mu(x)\right]\right\}, \qquad (7.25)$$

where

$$\tilde{S}^{-1}(x - y)$$
$$= \left\{(i\partial\!\!\!/_x - M) - ig\gamma_5 \boldsymbol{\tau} \cdot \boldsymbol{\Phi}(x) + e\frac{1 + \tau_3}{2} A\!\!\!/(x)\right\} \delta(x - y) \qquad (7.26)$$

describes the propagation of a fermion under the action of the pionic and e.m. field. Its determinant can be cast into the form

$$\det \tilde{S}^{-1} = \exp\left\{-i\Sigma(A, \Phi)\right\}, \qquad (7.27)$$

where

$$\Sigma(A, \Phi) = -i \operatorname{tr} \sum_{n=1}^{\infty} \frac{1}{n} \left[\left(ig\gamma_5 \boldsymbol{\tau} \cdot \boldsymbol{\Phi} - eA\!\!\!/\frac{1 + \tau_3}{2}\right) S_0\right]^n \qquad (7.28)$$

describes a fermion loop with any number of vertices, both of bosonic and of electromagnetic nature.

The response function entailed by (7.25) reads

$$i\Pi_{\mu\nu}^{tot}(x, y) = -\frac{\delta^2 \mathbf{Z}_c}{\delta a_\mu(x) \delta a_\nu(y)}\bigg|_{a_\mu = 0}, \qquad (7.29)$$

where the (classical) external e.m. field has been redefined by including the photon propagator, i.e.

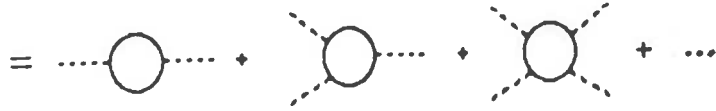$$a_\mu(x) = \int dy\, D_{\mu\nu}^0(x - y) j_{\text{ex}}^\nu(y). \qquad (7.30)$$

To get rid of the e.m. field we keep the coupling with the latter up to the order e^2, retaining only those fermion loops with 0, 1 or 2 external e.m. vertices. Accordingly we write

$$\Sigma[A] \simeq V_\pi[\Phi] + e\alpha_\mu(\Phi|x) A^\mu(x) + \frac{e^2}{2} \beta_{\mu\nu}(\Phi|xy) A^\mu(x) A^\nu(y), \qquad (7.31)$$
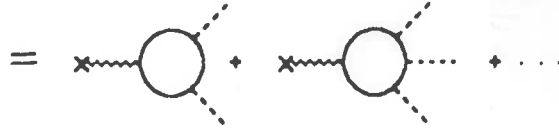
with

$$iV_\pi[\Phi] = \text{tr} \sum_{n=1}^{\infty} \frac{1}{n} [ig\gamma_5 \boldsymbol{\tau} \cdot \Phi S_0]^n$$

$$= \frac{1}{2!} \int dy\,dz\, \Pi^{kl}(z,y) \Phi_k(z) \Phi_l(y)$$

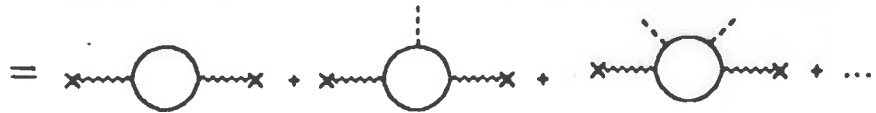$$+ \frac{1}{3!} \int dz\,du\,dy\, \Pi^{klm}(z,u,y) \Phi_k(z) \Phi_l(u) \Phi_m(y) + \mathcal{O}(\Phi^4), \quad (7.32a)$$

$$e\alpha_\mu(\Phi|x) = \left. \frac{\delta \Sigma[A]}{\delta A_\mu(x)} \right|_{A_\mu=0}$$

$$= \frac{1}{2!} \int dy\,du\, \Pi^{kl}_\mu(x,y,u) \Phi_k(y) \Phi_l(u)$$

$$+ \frac{1}{3!} \int dy\,du\,dt\, \Pi^{klm}_\mu(x,y,u,t) \Phi_k(y) \Phi_l(u) \Phi_m(t) + \mathcal{O}(\Phi^4), \quad (7.32b)$$

and

$$e^2 \beta_{\mu\nu}(\Phi|xy) = \left. \frac{\delta^2 \Sigma[A]}{\delta A_\mu(x) \delta A_\nu(y)} \right|_{A_\mu=0}$$

$$= \Pi_{\mu\nu}(x,y) + \int dz\, \Pi^k_{\mu\nu}(x,y,z) \Phi_k(z)$$

$$+ \frac{1}{2!} \int dz\,du\, \Pi^{kl}_{\mu\nu}(x,y,z,u) \Phi_k(z) \Phi_l(u) + \mathcal{O}(\Phi^3). \quad (7.32c)$$

In the above, the quantities $\Pi^{j_1,j_2,\ldots,j_n}_{\mu_1,\mu_2,\ldots,\mu_k}$, which correspond to the set of all the closed fermion loop with n pionic vertices (hence the isospin indices $j_1 \ldots j_n$) and k e.m. vertices (associated with the tensor indices $\mu_1 \ldots \mu_k$) have been introduced. They are just the coefficients of the Volterra series for V_π, α_μ, $\beta_{\mu\nu}$.

Then the generating functional simplifies to:

$$
Z[a_\mu] = \frac{1}{\mathcal{N}} \int \mathcal{D}\left[\Phi, A_\mu\right] \exp\left\{ i \int dx \left[\frac{1}{2}\left(\partial_\mu \Phi\right)^2 - \frac{1}{2}m_\pi^2 \Phi^2 + \mathcal{L}_{\text{e.m.}} \right.\right.
$$
$$
\left.+ e\left(\Phi \times \partial_\mu \Phi\right)_3 A^\mu + e^2 A_\mu^2 \Phi^+ \Phi^- \right] - iV_\pi[\Phi] \bigg\}
$$
$$
\times \exp\left\{ -ie \int dx\, \alpha_\mu(\Phi|x)A^\mu(x) - \frac{i}{2}e^2 \int dx\, dy\, \beta_{\mu\nu}(\Phi|xy)A^\mu(x)A^\nu(y) \right.
$$
$$
\left.+ i \int dx\, dy\, a^\nu(x)D^{0^{-1}}_{\nu\mu}(x-y)A^\mu(y) \right\} \tag{7.33}
$$

and a further gaussian integration eliminates the electromagnetic field, yielding

$$
Z[a_\mu] = \frac{1}{\mathcal{N}} \int \mathcal{D}[\Phi] \exp\left\{ i \int dx \left[\frac{1}{2}\left(\partial_\mu \Phi\right)^2 - \frac{1}{2}m_\pi^2 \Phi^2 \right] - iV_\pi[\Phi] \right\}
$$
$$
\times \exp\left\{ -\frac{i}{2} \int dx\, dy \left[\int dz\, a^\sigma(z)D^{0^{-1}}_{\sigma\mu}(z-x) - e\alpha_\mu(\Phi|x) \right.\right.
$$
$$
\left. + e\left(\Phi \times \partial_\mu^x \Phi\right)_3 (x) \right] D^{\mu\nu}(\Phi|xy) \left[\int dz\, a^\eta(z)D^{0^{-1}}_{\eta\nu}(z-y) \right.
$$
$$
\left.\left. - e\alpha_\nu(\Phi|y) + e\left(\Phi \times \partial_\nu^y \Phi\right)_3 (y) \right] \right\} \{\det D[\Phi]\}^{1/2}. \tag{7.34}
$$

In the above a dressed photon propagator has been defined according to:

$$
\frac{i}{2} \int dx\, dy\, A^\mu(x) \left[D^{0^{-1}}_{\mu\nu}(x-y) \right.
$$
$$
\left. + 2e^2 g_{\mu\nu}\Phi^+(x)\Phi^-(y)\delta(x-y) - e^2 \beta_{\mu\nu}(\Phi|xy) \right] A^\nu(y)
$$
$$
\equiv \frac{i}{2} \int dx\, dy\, A^\mu(x) \left[D_{\mu\nu}(\Phi|xy) \right]^{-1} A^\nu(y), \tag{7.35}
$$

or, equivalently,

$$
D[\Phi] = D^0 - 2e^2 D^0 \Phi^+ \Phi^- D[\Phi] + e^2 D^0 \beta[\Phi]D[\Phi], \tag{7.36}
$$

which is satisfied, to the order e^2, by

$$
D[\Phi] = D^0 - 2e^2 D^0 \Phi^+ \Phi^- D^0 + e^2 D^0 \beta[\Phi]D^0 + \mathcal{O}(e^3). \tag{7.37}
$$

Moreover, with a standard procedure, we get for the determinant in (7.34):

$$\det D[\Phi] \simeq \exp\left\{-\mathrm{tr}(2e^2 D^0 \Phi^+ \Phi^- - e^2 D^0 \beta[\Phi]) + \mathcal{O}(e^3)\right\} \tag{7.38}$$

the first term in the exponent just corresponding to an electromagnetic renormalization of the pion mass (cancelled by the renormalization counterterms) and the second one to a series of fermion loops with $n - 2$ incoming pionic lines and two contracted photon's lines (see Fig. 7.1).
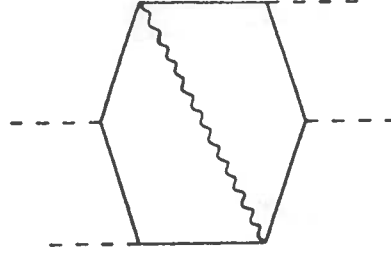

Fig. 7.1 – An example of the diagrams arising from the second term
in the exponent of (7.38).

We thus finally get for the effective action of our system of pions, interacting up to the second order with the e.m. field, the expression

$$
\begin{aligned}
S_{\mathrm{eff}}^B = {} & \frac{1}{2}\int dx\,dy\;\Phi(x)\cdot\Delta_0^{-1}(x-y)\Phi - V_\pi[\Phi] \\
& + e\int dx\, a_\mu(x)\left\{\alpha^\mu(\Phi|x) - e\left[\Phi(x)\times\partial_x^\mu\Phi(x)\right]_3\right\} \\
& + e^2\int dx\, a_\mu(x)\Phi^+(x)\Phi^-(x)a^\mu(x) - \frac{i}{2}\mathrm{tr}(e^2 D^0\beta[\Phi]) \\
& - \frac{1}{2}\int dx\,dy\left\{a^\nu(x)D_{\nu\mu}^{0\,-1}(x-y)a^\mu(y) + e^2\,a^\mu(x)\beta_{\mu\nu}(\Phi|xy)a^\nu(y)\right. \\
& \quad - 2e^2\alpha^\mu(\Phi|x)D_{\mu\nu}^0(x-y)\left[\Phi(y)\times\partial_y^\nu\Phi(y)\right]_3 \\
& \quad + e^2\alpha^\mu(\Phi|x)D_{\mu\nu}^0(x-y)\alpha^\nu(\Phi|y) \\
& \quad \left. + e^2\left[\Phi(x)\times\partial_x^\mu\Phi(x)\right]_3 D_{\mu\nu}^0(x-y)\left[\Phi(y)\times\partial_y^\nu\Phi(y)\right]_3\right\}. \tag{7.39}
\end{aligned}
$$

diagrammatically illustrated in Fig. 7.2. Of course some of the diagrams are irrelevant for our purposes. For example any diagram with an internal photon line will contribute to the order e^4 and should consequently be dropped.
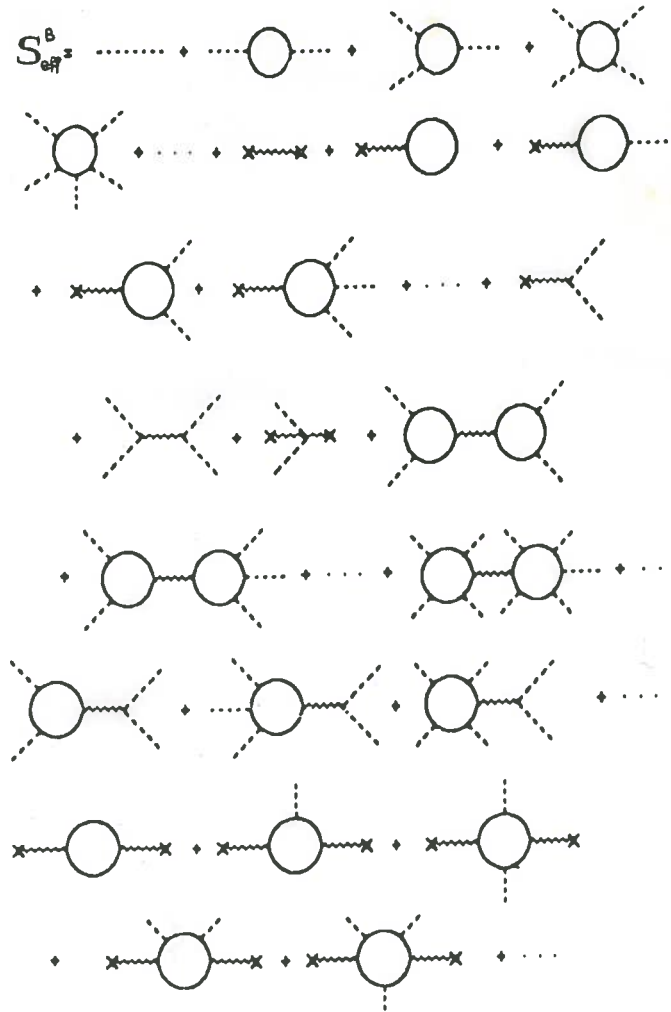
Fig. 7.2 – Diagrammatic representation of the bosonic effective action (7.39).

Let us now deal with the effective action (7.39) in the semiclassical framework. The starting point is again the evaluation of the generating functional

$$Z[a_\mu] = \frac{1}{\mathcal{N}} \int \mathcal{D}[\Phi] e^{iS_{\text{eff}}^B[\Phi]} \tag{7.40}$$

in the Stationary Phase Approximation (SPA). The stationarity condition

$$\frac{\delta S_{\text{eff}}^B[\Phi]}{\delta \Phi^i(x)} = 0 \tag{7.41}$$

(roman indices refer to isospin components) has now the following cumbersome looking

$$(\Box_x + m_\pi^2)\Phi^i(x) + \frac{\delta V_\pi[\Phi]}{\delta \Phi^i(x)} + 2ea_\mu(x)\varepsilon_{3ij}\partial^\mu\Phi^j(x)$$

$$- e\int dz\, a_\mu(z)\frac{\delta\alpha_\mu(\Phi|z)}{\delta\Phi^i(x)} - e^2 a_\mu(x)(1-\delta_{i3})\Phi^i(x)a^\mu(x)$$

$$+ e^2\int dy\, dz\,\frac{\delta\alpha^\mu(\Phi|z)}{\delta\Phi^i(x)}D^0_{\mu\nu}(z-y)\alpha^\nu(\Phi|y) \qquad (7.42)$$

$$+ \frac{e^2}{2}\int dy\, dz\, a^\mu(z)\frac{\delta\beta_{\mu\nu}(\Phi|zy)}{\delta\Phi^i(x)}a^\nu(y)$$

$$+ 2e^2\varepsilon_{3ij}\partial^\mu_x\Phi^j(x)\int dy\, D^0_{\mu\nu}(x-y)\left\{\left[\Phi(y)\times\partial^\nu_y\Phi(y)\right]_3 - \alpha^\nu(\Phi|y)\right\}$$

$$- e^2\int dy\, dz\,\frac{\delta\alpha^\mu(\Phi|z)}{\delta\Phi^i(x)}D^0_{\mu\nu}(z-y)\left[\Phi(y)\times\partial^\nu_y\Phi(y)\right]_3 = 0\,.$$

Yet a solution up to the order e^2 of this equation can be found. For this purpose notice that (7.42) describes the classical pion field in the presence of an external e.m. source. Clearly the vacuum expectation value of the pion field should vanish in the absence of the e.m. field to keep parity and isospin invariance. A non–zero value of the pion field is however induced by the external source. Accordingly we set

$$\Phi_0 = \Phi^{(0)} + e\Phi^{(1)} + e^2\Phi^{(2)} \qquad (7.43)$$

and, by identifying equal powers of e, we obtain for $\Phi^{(0)}$ the equation

$$(\Box_x + m_\pi^2)\Phi_i^{(0)}(x) + \frac{\delta V_\pi[\Phi]}{\delta\Phi^i(x)} = 0 \qquad (7.44)$$

satisfied by $\Phi_i^{(0)} = 0$ since $V_\pi \simeq \Phi^2 + \cdots$. As mentioned in Subsection 7.3, this solution is not unique, other possible ones being associated with the collective modes of the system. Neglecting collective effects, we take again $\Phi_i^{(0)} = 0$ as the starting point for our expansion. Then Φ_0 should be at least of order e and consequently [see eqs. (7.32)] the order of the various terms in the expansion of $\Sigma[A]$ will be

$$V_\pi \sim e^2$$
$$\alpha_\mu \sim e^2 \qquad (7.45)$$
$$\beta_{\mu\nu} \sim 1\,.$$

Therefore $\Phi_i^{(1)}$, in turn, will obey

$$(\Box_x + m_\pi^2)\Phi_i^{(1)}(x) + \int dy\,\Pi^{il}(x,y)\Phi_l^{(1)}(y) = 0 \qquad (7.46)$$

again satisfied by $\Phi^{(1)} = 0$. Thus, at least, $\Phi_0 \sim e^2$, which implies

$$V_\pi \sim e^4, \qquad \alpha_\mu \sim e^4, \qquad \beta_{\mu\nu} \sim 1, \tag{7.47a}$$

$$\frac{\delta V_\pi}{\delta \Phi} \sim e^2, \qquad \frac{\delta \alpha_\mu}{\delta \Phi} \sim e^2, \qquad \frac{\delta \beta_{\mu\nu}}{\delta \Phi} \sim 1. \tag{7.47b}$$

The equation for $\Phi_i^{(2)}(x)$, the first one being non–trivial, reads

$$\int dy [\Delta_0^{-1}(x-y)\delta_{ij} - \Pi^{ij}(x,y)]\Phi_j^{(2)}(y)$$
$$- \frac{1}{2} \int dz\, dy\, a^\mu(z)\Pi_{\mu\nu}^i(z,y;x)a^\nu(y) = 0 \tag{7.48}$$

and its solution

$$\Phi_0(x) = e^2 \Phi^{(2)}(x)$$
$$= \frac{e^2}{2} \delta_{i3} \int dy\, dz\, du\, \Delta_{RPA}(x-u)\Pi_{\mu\nu}^i(y,z;u)a^\mu(y)a^\nu(z) \tag{7.49}$$

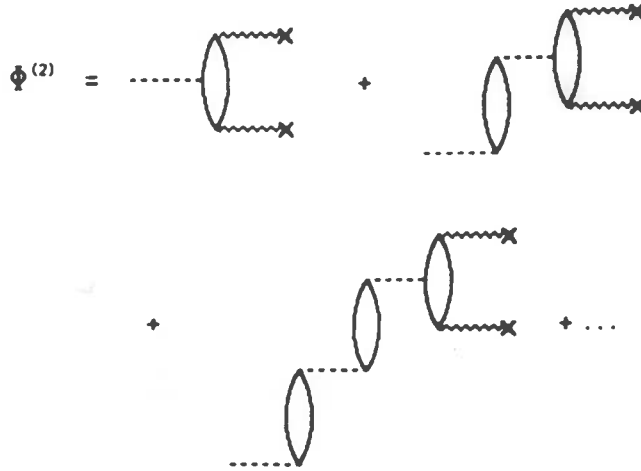is diagrammatically displayed in Fig. 7.3.

Fig. 7.3 – The SPA solution for the pion field.

Therefore the explicit expression for the classical pion field inside the nucleus, coupled to the order e^2 to an external e.m. field, is neutral since the e.m. field and the pion are only coupled through the medium. Note also that the RPA–dressed pion propagator naturally arises from the theory.

Having solved the classical SPA equation, one has for the generating functional

$$Z[a_\mu]_{SPA} = \frac{1}{\mathcal{N}} e^{iS^B_{\text{eff}}[\Phi_0]}. \tag{7.50}$$

and for the associated generator of the connected diagrams

$$Z_c = S^B_{\text{eff}}[\Phi_0]. \tag{7.51}$$

In fact, since $\Phi_i(x) \simeq e^2$, one easily verifies that, to the same order only few terms survive in S^B_{eff} and the second derivative with respect to a_μ leads then to the simple expression

$$\Pi^{tot}_{\mu\nu}(x,y) = e^2 \beta_{\mu\nu}(\Phi_0|xy) = e^2 \Pi_{\mu\nu}(x,y). \tag{7.52}$$

Thus we see that the SPA yields nothing else than *the familiar free particle-hole polarization propagator*, remarkably independent upon the location of the saddle point.

To go beyond this well known result we consider the next order corrections which, in the semiclassical expansion, are the so-called quantum fluctuations around the semiclassical (mean field) solution. The generating functional accounting for the latter, which describes the well-known one-loop corrections, is

$$\begin{aligned}
\mathbf{Z}[a_\mu] &= \frac{1}{\mathcal{N}} e^{iS^B_{\text{eff}}} \left\{ \det \left[\frac{\delta^2 S^B_{\text{eff}}[\Phi]}{\delta \Phi^i(x) \delta \Phi^j(y)} \right]_{\Phi=\Phi_0} \right\}^{-1/2} \\
&= \frac{1}{\mathcal{N}} \exp \left\{ iS^B_{\text{eff}}[\Phi_0] - \frac{1}{2} \text{tr} \ln \left[\frac{\delta^2 S^B_{\text{eff}}[\Phi]}{\delta \Phi^i(x) \delta \Phi^j(y)} \right]_{\Phi=\Phi_0} \right\} \\
&\equiv iS^B_{\text{eff}}[\Phi_0] + iS^{B[1]}_{\text{eff}}[\Phi_0]
\end{aligned} \tag{7.53}$$

and the associated response function reads

$$\Pi^{tot}_{\mu\nu}(x,y) = e^2 \Pi_{\mu\nu}(x,y) - \frac{\delta^2 S^{B[1]}_{\text{eff}}[\Phi_0]}{\delta a_\mu \delta a_\nu} \Big|_{a_\mu=0}, \tag{7.54}$$

with

$$\begin{aligned}
\frac{\delta^2 S^{B[1]}_{\text{eff}}[\Phi_0]}{\delta a_\mu \delta a_\nu} \Big|_{a_\mu=0} &= ie^2 \sum_{i,j} \Big\{ \delta_{ij}(1 - \delta_{i3}) \big[\Delta_{RPA}(x - y) g_{\mu\nu} \delta(x - y) \\
&\quad + \frac{1}{2} \partial^\mu_x \Delta_{RPA}(y - x) \partial^\nu_y \Delta_{RPA}(x - y) \big] \\
&\quad + \int dz\, du \big[\varepsilon_{3il} \partial^\mu_x \Delta_{RPA}(z - x) \Delta_{RPA}(x - u) \Pi^{lj}_\nu(u,z,y) \big]
\end{aligned}$$

$$-\frac{1}{2}\Delta_{RPA}(u-z)\Pi^{ij}_{\mu\nu}(z,u,x,y)]$$

$$-\frac{1}{2}\int dz\,du\,dt\,dw\big[\Delta_{RPA}(u-z)\Pi^{il}_{\mu}(z,t,x)$$

$$\times\,\Delta_{RPA}(t-w)\Pi^{lj}_{\nu}(w,u,y)+\frac{1}{2}\Delta_{RPA}(z-t)\Pi^{ij3}(t,z,u)$$

$$\times\,\Delta_{RPA}(u-w)\Pi^{3}_{\mu\nu}(w,x,y)]\big\}. \tag{7.55}$$

The diagrams accounted for by the above equation are displayed in Fig. 7.4, but for the last term, which is vanishing.
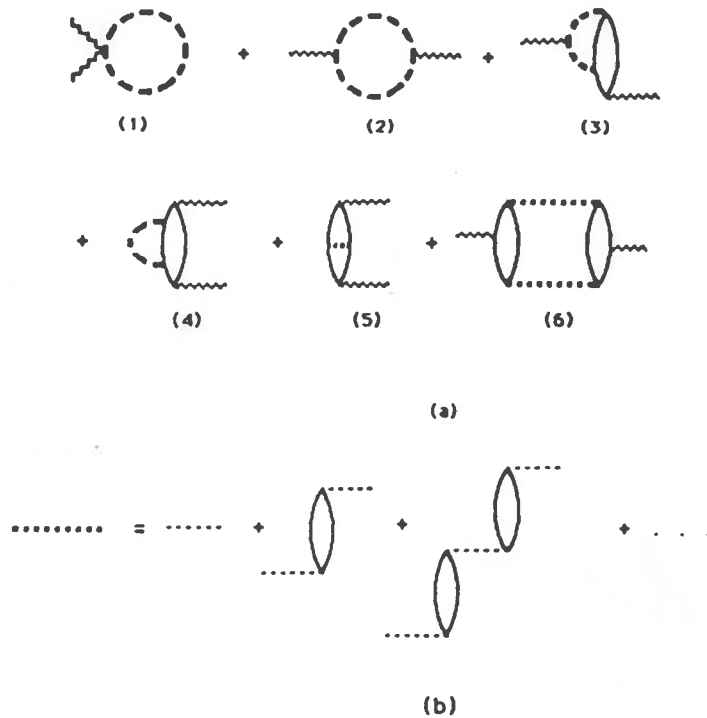

Fig. 7.4 – (a) Quantum fluctuation corrections to the polarization propagator; (b) the RPA dressed pion propagator.

The first two diagrams represent an irrelevant (for the present purposes) renormalization of the photon mass and the hadronic component of the photon wavefunction (see Subsection 6.3). Concerning the second–order (in the exchange of a bare pion) terms of the diagrams (3)→(6), they can be recognized in part of the ones already considered in the Subsection 3.1. However the RPA dressing of the pion propagator extends the diagrams embodied in the quantum fluctuations around the mean field up to the infinite order of perturbation theory.

Final Comment

In conclusion we wish to remind the reader that this presentation of the nuclear responses largely reflects our own experience in the field. Thus many important items have not been addressed: in particular we regret the omission of exclusive processes like $(e, e'p)$, which are disclosing new windows on nuclear structure. Nevertheless the topics embodied here illustrate how much the intermediate and high energy nuclear physics has contributed to our understanding of atomic nuclei, how many unexpected features have come to light in recent years, and how difficult and puzzling are the problems we are still confronting. As far as the general theory is concerned, we believe that in the future the theoretical treatment of the nuclear responses will be developed beyond the linear framework, that the languages adopted at intermediate energy (nucleons and mesons) and high energy (quarks) will be less disconnected from each other (although it is hard to foresee whether a unified description will be ever achieved) and finally that those general requirements like covariance, gauge invariance, etc. will be more and more closely obeyed. All this will entail profound modifications in our conception of atomic nuclei.

REFERENCES

Aculinichev, S.V., S.A. Kulagin, G.M. Vagradov, (1985), *JETP Lett.* **42**, 105; *Phys. Lett.* **158B**, 475.

Adkin, G.S., C.R. Nappi and E. Witten, (1983), Nucl. Phys. **B228**, 552.

Alberico, W.M., R. Cenni, M.B. Johnson and A. Molinari, (1982) *Ann. of Phys.* **138**, 178.

Alberico, W.M., M. Ericson and A. Molinari (1982), *Nucl. Phys.* **A379**, 429.

Alberico, W.M., M. Ericson and A. Molinari (1984), *Ann. Phys.* (N.Y.) **154**, 356.

Alberico, W.M., A. De Pace and A. Molinari (1985), *Phys. Rev.* **C31**, 2007.

Alberico, W.M., A. Molinari, A. De Pace, M. Ericson and M.B. Johnson (1986), *Phys. Rev.* **C34**, 977.

Alberico, W.M., R. Cenni, A. Molinari and P. Saracco, (1987) *Ann. of Phys.* **174**, 131.

Alberico, W.A., P. Czerski, M. Ericson and A. Molinari, (1987) *Nucl. Phys.* **A462**, 269.

Alberico, W.M., A. De Pace, M. Ericson, M.B. Johnson and A. Molinari (1988),

Phys. Rev. **C38**, 109.

Alberico, W.M., R. Cenni, A. Molinari and P. Saracco, (1988) *Phys. Rev.* **38C**, 2389.

Alberico, W.M., A.Molinari, T.W. Donnelly, E.L. Kronenberg and J.W. Van Orden, (1988) *Phys. Rev.* **C38**, 1801.

Alberico, W.M., T.W. Donnelly and A. Molinari, (1989), to be published.

Altemus, R.M., (1980),*thesis*, Department of Physics, University of Virginia.

Anastasio, M.R., A. Faessler, H. Müther, K. Holinde and R. Machleidt, (1979) *Nucl. Phys.* **A322**, 369.

Andronenko, M.N., E.N. Vol'nin, A.A. Vorob'ev, V.T. Grachev, A.A. Lobodenko, I.I. Strakovskii and L.N. Uvarov, (1983) *JETP Lett.* **37**, 530

Arenövel, H. and M.M. Giannini, (1985) *Nucl. Phys.* **A436**, 699.

Barreau, P., *et al.*, (1983) *Nucl. Phys.* **A402**, 515.

Bergqvist, I. *et al.* (1987), *Nucl. Phys.* **A469**, 648.

Blaizot, J.P., D. Gogny and B. Grammaticos, (1976) *Nucl. Phys.* **A265**, 315.

Blaizot, J.P. and G. Ripka, (1986) **Quantum Theory of Finite Fermi Systems**, Cambridge (Mass.).

Blatchey, C.C. *et al.*, (1986) *Phys Rev.* **C34**, 1243.

Bogoliubov, N.N. and O.S. Parasyuk, (1957) *Acta Math.* **97**, 227.

Bogoliubov, N.N. and D.V. Shirkov, (1959) **Introduction to the Theory of Quantized Fields**, Interscience, New York.

Bordalo P., *et al.* (NA10 Collaboration), (1987) *Phys. Lett.* **B193**, 368 and 373.

Brandow, B.H., (1967) *Rev. Mod. Phys.* **4**, 771.

Brown, G.E. and W. Weise, (1975) *Phys. Rep.* **C22**, 279.

Butler, M.N. and S.E. Koonin, (1988) *Phys. Lett.* **B205**, 123.

Carey, T.A., *et al.* (1984), *Phys. Rev. Lett.* **53**, 144.

Cavinato, M., D. Drechsel, H. Fein, M. Marangoni and A.M. Saruis, (1984) *Nucl. Phys.* **A423**, 376.

Cavinato, M., M. Marangoni and A.M. Saruis, (1988) *Phys. Lett.* **213B**, 111.

Celenza, L.S., A. Harindranath, A. Rosenthal and C.M. Shakin, (1980) *Phys. Rev.* **C31**, 946.

Cenni, R. and G. Dillon, (1980) *Nucl. Phys.* **A333**, 413.

Cenni, R., G. Dillon and S. Squarcia, (1981) *Phys. Lett.* **101B**, 294.

Cenni, R. and G. Dillon, (1983) *Nucl. Phys.* **A392**, 438.

Cenni, R., P. Christillin and G. Dillon, (1984) *Phys. Lett.* **139B**, 341.

Cenni, R. and G. Dillon, (1984) *Nucl. Phys.* **A422**, 527.

Cenni, R., P. Christillin and G. Dillon, (1985) *Phys. Lett.* **151B**, 5.

Cenni, R. and P. Saracco, (1988) in: *Proceedings of the fifth Int. Conf. on Nuclear Reaction Mechanisms* ed. by E. Gadioli, Varenna, p.551.

Cenni, R., F. Conte and U. Lorenzini, (1989), submitted to *Phys. Rev.* **C**

Chanfray, G., O. Nachtmann and H.J. Pirner, (1984) *Phys. Lett.* **147B**, 249

Chollet, C. *et al.*, (1983) *Phys. Lett.* **127B**, 331.

Clark, J.W., L.R. Mead, E. Krotscheck, K.E. Kurten and M.L.Ristig, (1979) *Nucl. Phys.* **A328**, 45.

Clark, J.W. and E. Krotscheck, (1983) *Lecture Notes in Phys.* **198**, 127.

Cleymans, J. and R.L. Thews, (1985) *Phys. Rev.* **D31**, 1014.

Close, F.G., R.G. Roberts and G.G. Ross, (1983) *Phys. Lett.* **129B**, 346.

Close, F.G., R.L. Jaffe, R.G. Roberts and G.G. Gross, (1985) *Phys. Rev.* **D31**, 1004.

Co', G., K.F. Quader, R.D. Smith and J. Wambach, (1988) *Nucl. Phys.* **A485**, 61.

De Pace, A. and A. Drago, (1989), submitted for publication.

De Pace, A., S. Rosati and M. Viviani (1989), work in progress.

Dickhoff, W.H., A. Faessler, J. Meyer–ter–Vehn and H. Müther, (1981) *Phys. Rev.* **C24**, 1154; *Nucl. Phys.* **A368**, 445.

Donnelly, T.W., E.L. Kronenberg and J.W. Van Orden, (1988), *Nucl. Phys..*

Dow, K., (1987) *PhD. Thesis*, MIT.

Ericson, M. and M. Rosa–Clot, (1986) *Z. für Phys.* **A324**, 373.

Ericson, M., W. Leidemann and G. Orlandini, (1988) *preprint* CERN–TH 5111/88

Ericson, M. and A.W. Thomas, (1983) Phys. Lett. **128B**, 112

Esbensen, H., H. Toki and G.F. Bertsch (1985) *Phys. Rev.* **C31**, 1816.

Faessler, A., F. Fernandez, G. Lübeck and K. Shimizu, (1982) *Phys. Lett.* **112B**, 201.

Fantoni, S., (1984) *Phys. Rev.* **B32**, 2544.

Fantoni, S. and V.R. Pandharipande, (1986), in: *Proceed. of the CEBAF 1986 Summer Workshop*, June 86.

Fantoni, S., (1988), in: *Proceed. of the Workshop on Heavy–Quark Factory and Nuclear–Physics Facility with Superconducting Linacs*, Courmayeur 1987, ed. by E. De Sanctis, M. Greco, M. Piccolo and S. Tazzari, Bologna.

Feenberg, E., (1969) **Theory of Quantum Fluids**, New York (N. Y.).

Feshbach, H., (1962) *Ann. Phys.* **19**, 287.

Fetter, A.L. and J.D. Walecka, (1971) **Quantum Theory of Many–Particle Systems**, McGraw–Hill, New York (N. Y.).

Gaarde, C., J.S. Larsen and J. Rapaport (1982) in *Spin Excitations in Nuclei*, Proceed. of the Intern. Conf., Telluride (Colorado), March 1982, Plenum Press, p.65.

Galitzkii, V. and A. Migdal, (1958) *Sov. Phys. JEPT* **7**, 96.

Gari, M. and H. Hyuga, (1976) *Z. für Phys.* **A277**, 291; *Nucl. Phys.* **A 274**, 333.

Glauber, R.J., (1959), in: *Lectures in theoretical Physics*, vol.1, eds. W. Brittin *et al.* (Interscience, New York)

Horowitz, C., E. Moniz and J.W. Negele, (1985), Phys. Rev. **D31**, 1689.

Hosaka, A. and H. Toki (1986), *Progr. Theor. Phys.* **76**, 1306.

Hugenholtz, N.M. and L. Van Hove, (1958) *Physica* **23**, 363.

Koch, I.H. and E.J. Moniz, (1979) *Phys. Rev.* **C20**, 235.

Ichimura, M., K. Kawahigashi, T.S. Jorgensen and C. Gaarde, (1988) *Proceed. of the Int. Conf. on Spin Observables of Nuclear Probes*, Telluride.

Ichimura, M., K. Kawahigashi, T.S. Jorgensen, and C. Gaarde (1989) Preprint.

Jackson, A.D., A. Lande and R.A. Smith, (1982) *Phys. Rep.* **C86**, 55.

Jones, H.P. and M.D. Scadron, (1973) *Ann. of Phys.* **81**, 1.

Lenz, F. and E.J. Moniz, (1975) *Phys. Rev.* **C12**, 909.

Lenz, F., (1975) *Ann. of Phys.* **95**, 348.

McCarthy, J.S., (1980) *Nucl. Phys.* **A335**, 27.

Manousakis, E. and V.R. Pandharipande, (1986) *Phys. Rev.* **B33**, 150.

Marchand, C. *et al.*, (1985) *Phys. Lett.* **B153**, 29.

Meziani, Z.E. *et al.* (1984), *Phys. Rev. Lett.* **52**, 2130; (1985) **54**, 1233.

Migdal, A.B., (1967) **Theory of Finite Systems and Applications to Atomic Nuclei**, Wiley Interscience.

Molinari, A. and G.M. Vagradov, (1989) *Z. für Physik* **A**, 332.

Moniz, E.J., (1969) *Phys. Rev.* **184**, 1155.

Moniz, E.J., (1975) in: *Meson–Nuclear Physics, AIP Conf. Proceed. No. 33*, ed. P.D. Barnes, R.A. Eisenstein and L.S. Kisslinger (New York 1976), p.105.

Moniz, E.J. and A. Sevgen, (1981) *Phys. Rev.* **C24**, 224.

Noble, J., (1981) *Phys. Rev. Lett.* **46**, 412.

O'Connel *et al.*, (1984) *Phys. Rev. Lett.* **53**, 1627.

Orlandini, G., M. Traini and M. Ericson (1986), *Phys. Lett.* **B179**, 201.

Oset, E. and S.S. Salcedo, (1987) *Nucl. Phys.* **A468**, 631.

Peccei, R.D., (1968) *Phys. Rev.* **176**, 1812.

Peccei, R.D., (1969) *Phys. Rev.* **181**, 1902.

Pines, D., (1962) **The Many–Body Problem**, New York (N.Y.).

Pines, D. and P. Nozières, (1966) **The Theory of Quantum Liquids**, New York (N.Y.).

Quinn, B.P. *et al.*, (1988) *Phys. Rev.* **C37**, 1609.

Rees, L.B., *et al.* (1986), *Phys. Rev.* **C34**, 627.

Rosati, S., (1981), in: *Proceed. of the International School of Physics "Enrico Fermi", course LXXIX "From Nuclei to Particles"*, ed. by A. Molinari, Bologna.

Schuck, P., (1984) *Lecture Notes on The Random Phase Approximation* (Trieste, february 84).

Serot, B.D. and J.D. Walecka, (1986) in: *Advances in Nuclear Physics*, vol. **16**, Plenum Press (New York).

Siemens, P.J., (1970) *Nucl. Phys.* **A141**, 225.

Skyrme, T.H.R., (1961), Proc. Roy. Soc. **262**, 237.

Skyrme, T.H.R., (1962), Nucl. Phys. **31**, 556.

Speth, J., E. Werner and W. Wild, (1976) *Phys. Rep.* **33C**, 127.

Stroth, U., R.W. Hasse and P. Schuck, (1984) *Journal de Physique coll.* **C6**, 343.

Stroth, U., R.W. Hasse, P. Schuck, W.M. Alberico, A. Molinari and M. Ericson, (1985) *Phys. Lett.* **156B**, 291.

Thomas, A.W., (1983), in: *Advances in Nuclear Physics*, vol. **13**, Plenum Press (New York), 1.

Toki, H. and W. Weise (1979), *Phys. Rev. Lett.* **42**, 42; *Z. für Phys.* **A292**, 389.

Van Hove, L., (1987) Proceed. of the *International Union of Pure and Applied Physics*, Washington, DC (2 October 1987).

Van Orden, J.W., W. Truex and M.K. Banerjee, (1980) *Phys. Rev.* **C21**, 2628.

Van Orden, J.W. and T.W. Donnelly, (1981) *Ann. Phys.* **131**, 451.

Weber, H.J. and H. Arenövel, (1978) *Phys. Rep.* **C36**, 277.

West, G.B., (1975) *Phys. Rep.* **18**, 263.

Williams, A.G. and A.W. Thomas, (1986) *Phys. Rev.* **C33**, 1070.

Zimmermann, W., (1970) *Lectures on Elementary Particles and Quantum Field Theory*, Brandeis Summer Institute 1970, ed. S. Deser, M. Grisaru and H. Pendleton, MIT Press.